Recent Developments and Challenges in Chromatographic Lipidomics

Master's Thesis/ Pro Gradu
BSc Henri Avela
Helsinki University
Analysis and Synthesis

Tiedekunta/Osasto Fakultet/Sektion – Faculty	Laitos/Institution– Department
Faculty of Sciences	Department of chemistry

Tekijä/Författare – Author

Henri Fredrik Avela

Työn nimi / Arbetets titel – Title

Recent Developments and Challenges in Chromatographic Lipidomics

Oppiaine /Läroämne – Subject

Analytical Chemistry

Työn laji/Arbetets art – Level	Aika/Datum – Month and year	Sivumäärä/ Sidoantal – Number of pages
MSc. Thesis	20.08.2019	111 **(+20)**

Tiivistelmä/Referat – Abstract

Lipidomics is a quickly growing trend in metabolomics research: not only seen as passive cell membrane building blocks, lipids contribute actively to cell signaling and identification, thus seen as potential biomarkers (e.g. for early stage cancer diagnostics).

The literature part includes a review of 63 articles on UHPLC/MS-methods in the time frame of 2017-05/2019. The following literature is focused especially on glycerophospholipids (GPs). In addition, an overview to basic glycerolipids (GLs) and sphingolipids (SPs) is established, which evidently affects the emphasis and narration of lipid class representations in this review. Chromatographic methods in lipidomics are used to achieve either very selective or all-encompassing analyses for lipid classes. Since HPLC/MS is an insufficient method for fully encompassing low-abundance lipids, UHPLC/MS was mostly used for metabolic profiling where its large analyte range due to high sensitivity, separation efficiency and resolution excels in performance compared to other methods. Imaging techniques have further diverted towards DIMS and other novel non-chromatographic methods, e.g. Raman techniques with single cell resolution. The field of mass-spectral lipidomics is divided between studies using isotope-labeled standards or fully standardless algorithm-based analyses, furthermore, machine learning and statistical analysis has increased.

The experimental part focused on LC-IMS-MS and plasma-based in-house database method development for targeted analysis of ascites. Method development included optimization of the chromatography, adduct species selection and data-independent/-dependent fragmentation. Totally, 130 potential species from the LIPID MAPS database were used for the identification at the minimum score of 79% for identification in the Qualitative Workflows with retention times (RTs) and Mass Profiler-program with collision cross-sections (CCSs). Plasma sample analyses resulted in the documentation of 70 RTs and 36 CCS values. Two lipid extraction methods (Folch and BUME) with pre-sampling surrogates and post-sampling internal standards were compared with each other. The process resulted in confirming the BUME method in lipidomics to be superior in ecology-, workload-, health- and extraction-related properties. The lipidome of ascites has rarely been studied due to its availability only in diseased patients. Also, limiting factors for these studies are the logistics to realise such a representative analysis.

Avainsanat – Nyckelord – Keywords

Lipidomics, UHPLC/MS, nanoLC, IM-QTOF, biological materials, chemometry, statistical analysis, data-analysis, ascites

Säilytyspaikka – Förvaringställe – Where deposited

University of Helsinki, Department of Chemistry

Muita tietoja – Övriga uppgifter – Additional information

The experimental part was done at the Institute of Analytical Chemistry of the Johannes-Kepler University Linz, 10/2018-03/2019. Local supervisors: Prof. Christian Klampfl, MSc Bernd Reichl)

Contents

Abbreviations

AcCA	acyl carnitine
ACP	acyl carrier protein
AF4	asymmetric flow field flow fractionation
ANOVA	analysis of variance
AUC	area under curve
BEH	ethylene bridged hybrid
BFF	blank feature filtering
BUME	butanol-methanol [extraction]
CARS	coherent anti-Stokes Raman scattering
CCS	collision cross-section
(-/2-/3Hex)Cer	(mono-/di-/trihexosyl) ceramide
CID	collision-induced dissociation
CL	cardiolipin
CM	conditioned (cell culture) medium
CRM	charged residue model
CRS	coherent Raman scattering
CSF	cerebrospinal fluid
CSH	charged surface hybrid
DB	double bond
DDA	data dependent acquisition
(MG/DG/SQ)DG	(monogalacto/digalacto/sulfoquinovosyl) diacylglycerol
DIA	data independent acquisition
DIMS	direct infusion MS (i.e. shotgun MS)
DiffIMS	differentiated IMS
DLF	Douglas lavage fluid
EIC	extracted ion chromatogram
EOC	epithelial ovarian cancer
(H)ESI	(heated) electrospray ionization
FA	fatty acid
FDR	false discovery rate
FT-ICR	Fourier-transform ion cyclotron resonance mass analyzer
GC	gas chromatography
GLs	glycerolipids
GPs	glycerophospholipids
HCA	hierarchical cluster analysis
HGP	human genome project
HPLC	high performance liquid chromatography
IEM	ion evaporation model
IM-MS	ion mobility – mass spectrometry
IMS	ion-mobility spectrometry
ISTD	internal standard [added after sample preparation]
LESA	liquid extraction surface analysis
LOD	limit of detection
LOQ	limit of quantitation
LPLs	lyso-phospholipids
LPA	lysophosphatidic acid
LPC	lysophosphatidylcholine
LPE	lysophosphatidylethanolamine
LPG	lysophosphatidylglycine
LPI	lysophosphatidylinositol
LPS	lysophosphatidylserine

LVTA	lethal ventricular tachyarrythmia
MeOH	methanol
MG	monoacylglycerol
m/z	mass-to-charge [ratio]
(HR/LR)MS	(high/low resolution) mass spectrometry
MS^E	all ions scan
MSI	mass spectrometric imaging
MTBE	Matyash extraction, methyl tert-butylether
NL	neutral loss
NLS	neutral loss scan
NP	normal phase
NSI	nano-electrospray ionization
OC	ovarial cancer
OPLS-DA	orthogonal projections to latent structures discriminant analysis
PA	phosphatidic acid/lyso-
PCA	principal components analysis
PCB-	polychlorinated biphenyl
PC	phosphatidylcholine/lyso-
PCDL	personal compound database library
PCVG	principal component variable grouping
PE	phosphatidylethanolamine/lyso-
PG	phosphatidylglycine
PI	phosphatidylinositole
PIS	precursor ion scan
PKs	polyketides
PL	plasmalogen
PLS-DA	partial least squares discriminant analysis
PRs	prenol lipids
PRM	parallel reaction monitoring
PS	phosphatidylserine
QC	quality control [sample]
QqQ	triple quadrupole mass analyzer
QTOF	quadrupole time of flight
ROC	receiver operating characteristics
RP	reversed phase
RT	retention time
S1P	sphingosine-1-phosphate
SA1P	sphinganine-1-phosphate
SFC	supercritical fluid chromatography
SLs	saccharolipids
SM	sphingomyelin
sn[1;2;3]	stereospecifically numbered carbon
SPs	sphingolipids
SPE	solid-phase extraction
SRS	stimulated Raman scattering
SWATH	sequential window acquisition of all theoretical fragment ion mass spectra
TG	triacylglycerol
TIC	total ion chromatogram
TOF	time of flight mass analyzer
UHPLC	ultra-HPLC
VIP	variable importance projection
ZMF	Linz Center of Medical Research

I Literature part: Recent Developments in Chromatographic Lipidomics - Ultra-high performance liquid chromatography 2017-2019

Master's Thesis/ Pro Gradu
BSc Henri Avela
Helsinki University
chemistry Dept.
Supervisors:
MSc Heli Sirén
03/2019-07/2019

1 Introduction

Lipids are organic biomolecules synthesized in a defined way, barely or non-dissolvable in water.[1] They contribute to energy storing, cellular and subcellular membrane assembly and functionality,[2] signaling[3] and surfactant formation in animals.[4] Lipidomics, a subgroup of metabolome analyses in the -omics cascade that has emerged in 2003,[5] comprises of the identification and quantitation of organic lipids and their derivative variants. The suffix "-omics", derived from the words "genome" and "genomics", indicates a form of totality. It is mostly associated with the Human Genome Project (HGP), which mapped out the entire genome (i.e. all deoxy-ribonucleic acid-sequences of all chromosomes) of the human species from both a physical and functional standpoint. HGP was proposed in 1984 and funded in the years 1988-2003.[6]

Though found surprisingly complex, the idea of obtaining a total map of biomolecules and their metabolic interactions remained. Globally since then, -omics research of biomolecules other than DNA have become an ever-increasing interest of biomolecular and biochemical laboratories. Lipidomics can give an insight to inner workings of an organism. It can explain the physiology of multiple interlinked organs, a single organ, biological tissue, individual cells, or biofluids. Furthermore, reliable information can be obtained from the lipidome's metabolic expression which can be changed due to a disease and detectable biomarker lipids.[4, 7]

The following literature is focused especially on glycerophospholipids (GPs). In addition, an overview to basic glycerolipids (GLs) and sphingolipids (SPs) is established, which evidently affects the emphasis and narration of lipid class representations in this review. Thus, elaborate exposition of the following lipids and lipid-derived sub- and main classes were left out: polyketides (PKs), cholesterol-based sterols (ST) such as cholesteric esters (CEs), prenol lipids (PR), saccharolipids (SLs) and high/low density lipoproteins (HDL/LDL). Lesser attention is focused to sphingosine-1-phosphate (S1P) and sphinganine-1-phosphate (SA1P).

Particularly, the abbreviation for fatty acids is noted as FA, though strictly speaking Fahy et al.[4] defines the abbreviation FA for fatty acyls. As a lipid class, fatty acyls extend to lipid sub-classes such as fatty esters, fatty acyl thioester derivatives with the coenzymes A or ACP, fatty amides and eicosanoids.[4] Anyhow, throughout the thesis FA is used as the general symbol for fatty acids.

2 Lipids

2.1 Classification and nomenclature of lipids

According to the definition by Fahy et al.,[1] lipids are "hydrophobic or amphipathic small molecules that may originate entirely or in part by carbanion-based condensations of thioesters and/or by carbocation-based condensations of isoprene units". The classification for lipids was published in 2009. For example, the glycerophospholipid abbreviations were changed, replacing complex abbreviations like GPCho/GPEtn/GPSer/GPA/GPI with PC/PE/PS/PA/PI.[8] The current classification system with the newest recorded updates was reported by the lipidomics gateway LIPID MAPS® consortium on March 20th 2017.

Lipids are characterized according the backbone structure. Many lipids belong to esterified fatty acids due to chains bound to one or more hydroxyl groups of the glycerol headgroup (glycerolipids, glycerophospholipids), a sphingosine headgroup (sphingolipids) or a sugar backbone (saccharolipids). Furthermore, the three carbons of the glycerol molecule can be stereospecifically numbered (sn), and thus indicating the carbon to which a specific fatty acid is esterified. Other groups are specifically defined by their characteristic hydrocarbon structure (fatty acyls, prenol lipids, sterols and polyketides).[9]

2.2 Lipid types

Fatty acids (FA) are fundamental elements of more complex lipids (e.g. for triacylglycerols). These rather simple building blocks include fatty acids and their modifications (e.g. heteroatom-substituted FAs and esterified conjugates, e.g. acyl carnitines [AcCA] or bis(monomyristoylglycero)phosphate [BMP]), which may include branched or cyclic functionalities.[4] Their name is determined by the amount of carbon in its hydrocarbon chain including the number of double bonds (e.g. dodecane-2,4-dienoic acid: FA[12:2]).

In detail, lipids are primarily based on the fatty acid (FA) synthesis of excess acetyl coenzyme A and assisted by NADPH[10] in the cell's cytoplasm.[11] In a model proposed by Nelson and Cox,[10] the synthesis is a six-step process that involves most notably the derivatives of acetyl coenzyme A with the acyl carrier protein (ACP). The ACP is a part of a larger enzyme complex which holds the metabolite backbone. As for the reactants, an initial thioester carbon chain is modified into a malonyl body, which is further lengthened through a catalysed loop of acetyl group addition. The loop includes catalysed reduction steps of the thioesters keto-groups (and

their leftover double bonds) with NADPH and concludes with the freeing of the synthesized FA conjugate base from the ACP (either fully saturated or unsaturated).[12] According to Dennis,[10] the formed FAs are typically esterified further near other biomolecule's hydroxyl bonds (e.g. glycerol), this to stabilize the otherwise reactive FA.[10] This FA synthesis is the biological basis for the more complex lipids.

Most of the other lipids are either synthesized in the endoplasmatic reticulum, Golgi apparatus or the mitochondria.[13] Glycerolipids (GL) are mono- (MG), di- (DG) or trisubstituted (TG) glycerols, the substituents being commonly esterified fatty acid chains.[10] In literature, mono- di- and triacylglycerides may also be used as the alias. *Figure 1* illustrates the naming of any lipid with FA chains, with a TG as an example. Specific identification of FA chains is usually done with tandem mass spectrometric methods.

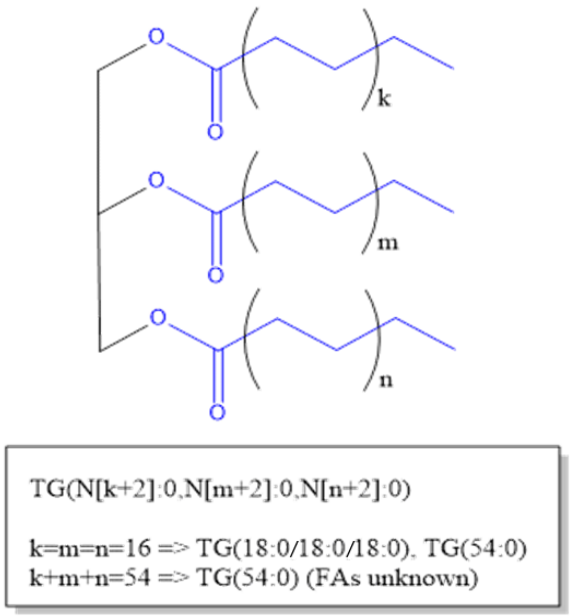

Figure 1. Simple triglyceride (TG) structure. The FA chain length. The positions of a fatty acid on a glycerol-molecule are named sn1 (upper carbon of the glycerol body, if k>n), sn2 (middle carbon of the glycerol body) and sn3 (lower carbon of the glycerol body, if k>n) respectively, when the analyte can be stereoisomerically determined (i.e. on the stereo-molecular species level). If individual chain lengths (and their positions) cannot be determined, the number of the carbon atoms and double bonds are expressed as separate sums.

Glycerophospholipids (GPs) are derived from glycerolipids by adding a phosphate-linked "head group" (typically) to the sn3-carbon of the glycerol. GPs have both passive roles as the lipid bilayer cell membrane components, and active roles as key components in metabolic pathways and cell signaling. The most abundant lipid in eukaryotic cells is phosphatidylcholines (PC) followed by phosphatidylethanolamine (PE) and their derivatives.[4] Other GP sub-groups include phosphatidic acid (PA), phosphatidylserine (PS), phosphatidylinositol (PI), phosphatidylglycerols (PG) and PG-derived cardiolipins (CL).[4]

A sum-up of possible GLs and GPs is illustrated in *Figure 2*. Lyso-phosphatidyl lipids (LPLs) are termed separately due to their lack of a radyl group in a glycerophospholipid structure. This means that one sn-site is reduced to a hydroxyl group from the GP initial structure to a hydroxyl group, e.g. lysoPC (LPC).[9]

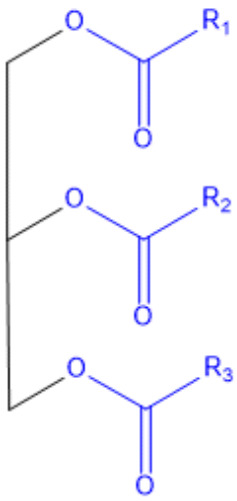

MG: R_1=FA,R_2=OH,R_3=OH *or* R_1=OH,R_2=FA,R_3=OH
DG: R_1=FA,R_2=FA,R_3=OH *or* R_1=FA,R_2=OH,R_3=FA
TG: R_1=FA,R_2=FA,R_3=FA

PC: e.g. R_1=$OPO_3^-CH_2CH_2N(CH_3)_3^+$,$R_2$=FA,$R_3$=FA
PE: e.g. R_1=$OPO_3^-CH_2CH_2NH_3^+$,R_2=FA,R_3=FA
PG: e.g. R_1=$OPO_3^-CH_2CH(OH)CH_2OH$,R_2=FA,R_3=FA
PI: e.g. R_1=$OPO_3^-CH_2CH_2NH_3^+$,R_2=FA,R_3=FA
PS: e.g. R_1=$OPO_3^-CH_2CH(COO^-)NH_2$,R_2=FA,R_3=FA

LPC: e.g. R_1=$OPO_3^-CH_2CH_2N(CH_3)_3^+$,$R_2$=FA,$R_3$=OH
LPE: e.g. R_1=$OPO_3CH_2CH_2NH_3^+$,R_2=FA,R_3=OH

FA: fatty acid residue

Figure 2. Glycerophospholipid structure variations according to sub-class, where the glycerol head group is depicted as black, and the characteristic molecules bound to it as blue. The characteristic molecules other than FA chains are mostly esterified to the sn1 position in organism. Structures derived from ref. **14**

GPs may appear with FAs both bound with ester or ether groups, the latter being defined as plasmalogens (PLs). They cover approximately one fifth of the glycerophospholipids in eukaryotic organisms.[4] PLs are divided into two categories: plasmanyls and plasmenyls. Plasmanyls are noted due to an oxygen bridge with an "O-" at the fatty acid chain (e.g. PI[O-18:0/17:0]) or due to a phosphorus bridge with a "P-" in a case of a plasmenyl group with an ester bond conjugated to a double bond of the FA (e.g. PI[P-18:0, 17:0]).[4]

Sphingolipids (SP), characteristic for eukaryotic cells,[15] have a sphingosine base as the basic backbone (*Figure 3*), but they contain various kinds of lipids in their structures. The backbone "is […] synthesized *de novo* from serine and a long-chain fatty acyl coenzyme A [in mammals]" and from there modified into a specific subclasses.[4] One of these sub-classes are ceramides (Cer), which are sphingoid bases having amine-bonds with FA molecules. Furthermore, a sphingomyelin (SM) is an interrelated[15] phospho-SP that combines a ceramide with phosphatidylcholine (Cer-PC) or with ethanolamine (Cer-PE). SPs are demonstrated visually in *Figure 3*.

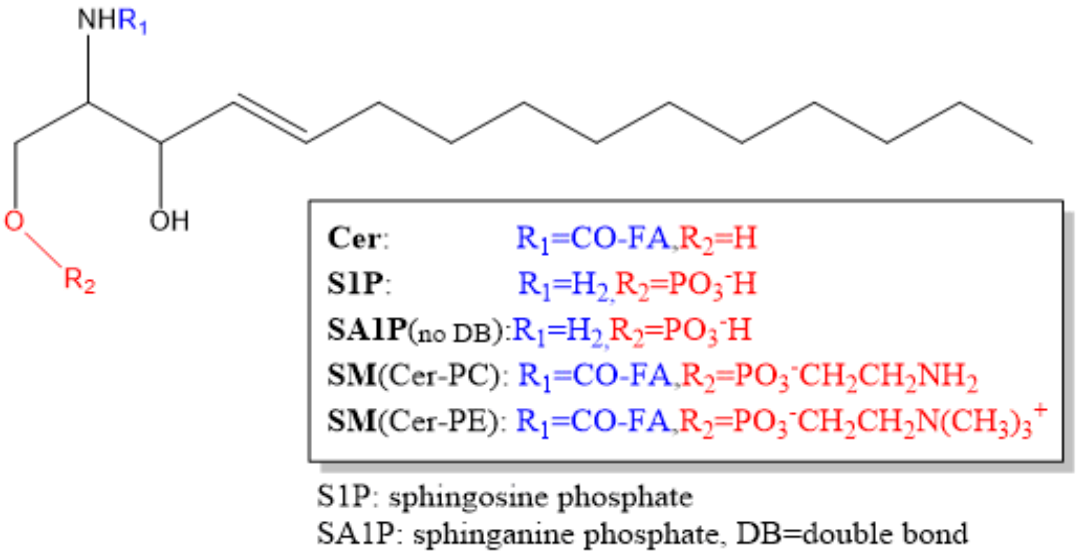

Figure 3. Typical sphingolipid structures. R_1 is an amine that usually has a fatty acid linked to it with an amide bond (blue). R_2 on the other hand is either a free hydroxyl group as in ceramides but occupied with a characteristic phosporylated molecule in SMs (red). Structures derived from ref. **14**

3 Chromatographic lipidomics

Not all lipids are visible when directly analyzing biological organisms or materials. Therefore, extraction and separation techniques have been developed to isolate only the analytes the research is interested in. As some techniques are specifically better or worse for certain lipid classes and sample types, prior knowledge must be considered before choosing a method. For identification, lipid species are usually reported by their adduct m/z ratio.

3.1 Sample preparation

In lipidomics, sample preparation primarily aims for reproducible and representative biochemical analyses. Analysis of structure and concentration- in assistance need to be in correlation with proper storage conditions such as low temperature and other measures against degradation or other alteration in the sample's lipidome. All this may be achieved through delaying of several decomposition processes, optimization of lipid recovery, concentration enhancement of the sample or analyte modification through derivatization. Additionally, costs, availability of resources, time constraints, method complexity, and environmental issues are important factors affecting the execution of sample preparation.[16]

The decomposition of the relatively chemically stable group of lipids is considered mainly in the biological way. Directly after isolation from an organism, self-degradation of analytes initiates via enzyme activation at room temperature. To avoid this, proteins must be precipitated, usually by introducing a degradation agent like methanol (MeOH) or isopropanol (IPA)[48], alternatively, by snap freezing the sample for storage. Protein precipitation includes simplified liquid matrix and thus allows improved sensitivity in detection.[17]

Considering chemical degradation, double bonds of unsaturated fatty acids are susceptible to peroxidation, hydrolytic degradation, and oxidation. Especially after isolation and extraction, antioxidative properties of biological compounds are disposed of or lost when the sample is stored in an improper manner. Apart from oxidation, major factors contributing to degradation are formation of ice crystals combined with osmotic shock when freezing the sample. Osmotic shock occurs when freezing of water decreases the volume of liquid water. Thus, the process assists in the breaking of structures (e.g. membranes) between lipids and enzymes that may act on them.[18]

As to biological matrices, extraction and analysis should be done as soon as possible after sampling. Jurowski et al.[18] reported drastic changes in the lipid composition of plasma, when the sample was stored for 1-3 years in -20 ˚C. Furthermore, Jurowski et al.[18] observed an increase in concentration saturated FAs and decrease of unsaturated polyFAs, which distorted the results. They proposed this to be due to enzymes and antioxidants' activity, which eventually degraded the amounts of stored lipids.[18] Furthermore, the recent review by Hyötyläinen and Orešič[19] inform a drop in LPC-concentrations which can be detected in less than two hours (storage temperature 4 ˚C). However, an increase was seen during 24 hours, potentially due to activity of the phospholipid-splicing phospholipase A_2. On the other hand, most PCs and sphingolipids seemed to stay stable for this time even at room temperature.[19] According to the study, erythrocyte FAs in plasma already degraded within one week at storage temperatures between 4 ˚C and -20 ˚C. Jurowski et al.[18] concluded that -60 ˚C was enough for recognizing "virtually no change" within one year of storaging.[18] Hyötyläinen and Orešič[19] agreed the stable storage of -80 ˚C for at least six months, but a change was seen at a time span of five years.[19] As an example of other studies about degradation in living organisms, Lam et al.[5] reviewed an observed phospholipase D conversion of PCs to PAs by Zien et al.[20] in the *Arabidopsis* plant.[5] During negative mode ESI-ionization, Tumanov et al.[21] claimed to observe a bias in LPA quantitation. The concentration of LPAs can be easily overestimated due to typical over-abundance of LPCs combined with their choline moiety loss during ionization.[21]

In the Folch-method[22] about 5% of proteins are left in the organic phase, which may contribute to matrix effects and higher background noise.[17] In comparison to Folch, BUME[23] is an extraction method considered superior from the environmental, economical and preparative standpoints, since extraction needs no chloroform and less solvent. This allows to extract all matrices into milliliter volumes with comparatively lowered safety hazards.[24-27]

For samples with low lipid concentrations, solid phase extraction (SPE)[28, 29] or lyophilization (i.e. freeze-drying)[29] can be considered to concentrate a sample for the analysis of already low abundance lipids. Here, SPE may substitute the extraction procedure entirely. Moreover, Teo et al.[29] introduces the concept of energy-based extraction methods (i.e. pressurized liquid, microwave- or ultrasonic-assisted extraction) alongside polarity-based extraction methods (i.e. single solvent, liquid-liquid, solid phase extraction plus supercritical fluid extraction

[Jurovski et al.][18]), out of which the latter is used more frequently in lipidomics studies.[29] Energy-based techniques heat up the extraction system to achieve a faster and more efficient extraction.[29]

Apparently, even lipid extractions on chips and in tubes to obtain high reproducibility and recovery have been studied: Bang et al.[30] used a SPE-like superabsorbent polymer (SAP) device for small sample sizes to minimize carry-over of aqueous solvent. As the aqueous solvent is gelated into polymer, the organic solvent can be collected with lipid recoveries similar or greater to the Folch extraction.[30]

Further extractions have included variations of methods mentioned before, [18, 22-29] as well as other single solvent or liquid-liquid extractions (e.g. acetonitrile or chloroform/methanol 2:1)[31, 32], QuEChERS,[30] "Bligh and Dyer",[33] and methyl-tert-butylether (MTBE, i.e. Matyash)[19] extraction procedures. All extraction methods have been discussed and compared in a broader manner by Pöhö,[34] Reis et al.,[26] Hyötyläinen et Orešič,[19] Jurowski et al.,[18] Zhang et al.[35] and Ulmer et al.[36] The extraction methods are compiled in *Table 1* below.

Table 1. Extraction and sample purification methods used in lipidomics

Class	Technique	Citation
Polarity-based	Single solvent extractions	31, 32, 37
Polarity-based	Liquid-liquid extractions	31, 32, 37
Polarity-based	Single solvent mixtures	31, 32
Polarity-based	Bligh and Dyer	33
Polarity-based	BUME	23
Polarity-based	Folch	22
Polarity-based	MTBE	19
Polarity-based	QuEChERS	30
Polarity-based	Supercritical fluid extraction (SFE)	18, 29
Polarity-based	Solid phase extraction (SPE)	28, 29
Polarity-based	Superabsorbent polymer extraction (SPE)	30
Energy-based	Microwave-assisted extraction (MAE)	18, 29
Energy-based	Ultrasonic-assisted extraction (UAE)	18, 29
Energy-based	Pressurized liquid extraction	18, 29

3.2 Sample composition

Lipidomics has an important role in the profiling of isolated cell types (e.g. cancer cell lines or bacteria[18]) as well as biological materials directly from a subject (e.g. plasma[38, 39] and human amniotic membrane[40]). The selection of experimental settings consist of *in vitro* cell culture experiments and *in vivo* clinical sample analyses. The aspects of lipidomic profiling in other than biological material (e.g. environmental samples,[41] foodstuffs[42] and nano-tailored products[43]) are not included in the literature review, since the attention is to focus on the experimental settings in determination of lipids.

Another distinction can be made between solid and liquid matrices, which must be homogenized and prepared for maximal representative results. Moreover, food products[42] and synthesized lipid structures,[43] such as nanoscale liposomes have been studied as well. In context, all samples analyzed in the experimental part can be considered biofluids: *in vitro* samples included conditioned cell culture medium (CM, a suspension acquired from cells), and *in vivo* clinical samples targeting to human amniotic fluid, plasma and most of all ascites.

According to Ghosh and Nisala[7] suggested that even human tears include 600 identified lipids.[7] Thus, it can be assumed that a single-cell suspension could be more dilute, less diverse and easier to analyze than an aqueous liquid from a multicelled, complex organism. CMs of cell cultures (e.g. cancer cell lines) are isolated and characterized to understand single lipid components in the context of a multivariate tissue.[7]

Furthermore, Ghosh and Nishala[7] describe plasma as a complicated though easily available matrix with a wide range of GPs, SLs, CEs and TGs to name a few.[7] This is understandable, since the bloodstream of an organism is linked to the most of its individual cells, able to transport nutrition, hormones or cell metabolites of used molecular structures (e.g. dead blood cells). However, Hyötyläinen and Orešič[19] report serum to have a more stable lipid profile than plasma. Hence, a potential alternative for a more reliable analysis. For plasma, their review suggests differences within sample types such as lower lipid content in citric acid containing plasma compared to EDTA modified plasma.[19]

Amniotic fluid was used during method development as an easily obtainable alternative for ascites. Lipids in amniotic fluid were indicators for the stages of pregnancy or pregnancy complications, e.g. total lipid and phospholipid concentration was observed to increase from

24 weeks of gestation until labor. Thus, routine test for fetal development through the lechitin/sphingomyelin -ratio could be used for a longer time. Furthermore, lipidomic profiles of amniotic fluid have been observed to be different between infants born term or pre-term.[7]

The primary ascites sample matrix of the experimental study is abnormal formation of intra-peritoneal fluid in the patient's abdominal cavity.[44] It is divided into two types according to its formation: non-inflammation induced (e.g. hydrostats- or osmosis-produced) transudates and inflammation-accompanied exudates. Transudates are suspect of de-compensation of blood circulation, kidneys, or liver, whereas exudates are formed from the oozing of ruptured or otherwise damaged cell tissue resulting in complications found around cysts of ovarian cancer tumors. In contrast to commonly clear transudates in the intraperitoneal space, exudates are noticed to have higher protein-concentrations due to their less filtrated nature.[44]

3.3 Standards and normalization

A conventional targeted approach needs a lot of calibration standards in lipidomics.[45] It is not feasible to calibrate all lipids individually. Thus, a simpler compromise on class-representative lipid standards with optimally chemical similarities are often applied in lipidomic studies. Ideally, however, standards and analytes should be chemically equivalent.

Normalization of data aims for stabilization of random and systematic errors contributing to the fluctuation of results, effected typically on peak areas. Normalization can be achieved via an internal standard (ISTD) or a surrogate. An ISTD is added to samples before analyses to account for instrumental fluctuations. A surrogate is added before sampling or storage. A chemically similar surrogate simulates chemical modifications of analyte that it mimics.

In state-of-the-art lipidomics, a pool of all samples forming a quality control sample (QC sample) is fancied. The QC sample goes through the same sample preparation as a single sample and is then used to screen matrix effects and possible instrument fluctuation in the method. Thus, it is used as a reference to each individual sample aliquot and their average matrix effects.

Though expensive, the most used ISTDs are deuterated standards, most often by Avanti Polar Lipids (Alabaster, AL, USA). Typically, the protons are deuterated at the FA end of the carbon chain with either 7 or 9 deuterium atoms. For representative standards in analysis, a self-made

or commercial standard mixture is typically used (e.g. a SPLASH mix[37] or well-known organic standard [porcine brain, chicken egg, e. coli][51]). The molecular ion and its fragments that still include the deuterated FA chain experience a noticeable shift in their m/z value compared to their non-deuterated counterparts. Since fragmentation is identical for both variants, this m/z differentiation is ideal for ISTD normalization via EICs.[126]

4 High-performance liquid chromatography in lipidomics

High-performance liquid chromatography (HPLC) is a method for separation of analytes in a liquid mobile phase through partitioning (typically adsorption) of analytes with a stationary phase. As the mobile phase encounters the stationary phase in a column, analytes will pursue an equilibrium. Hence, the analytes are retained depending on the strength of the interaction between the stationary phase and the mobile phase. A modern HPLC-instrument consists of a pump, an autosampler, a column compartment, a detector with a data recording system, appropriate tubing, and bottles for eluents and waste. For high resolution MS, a reference solution for tuning of the mass spectrometer is included.

Though reversed phase (RP) column LC is dominant in chromatographic lipidomics research, since it separates the lipid species by subspecies polarity and FA chain length, studies for normal phase (NP) hydrophilic interaction chromatography (HILIC) separation by polar head groups has increased. According to a Scifinder search (with duplicates removed), an increasing trend on HILIC publications can be observed (*Figure 4*).

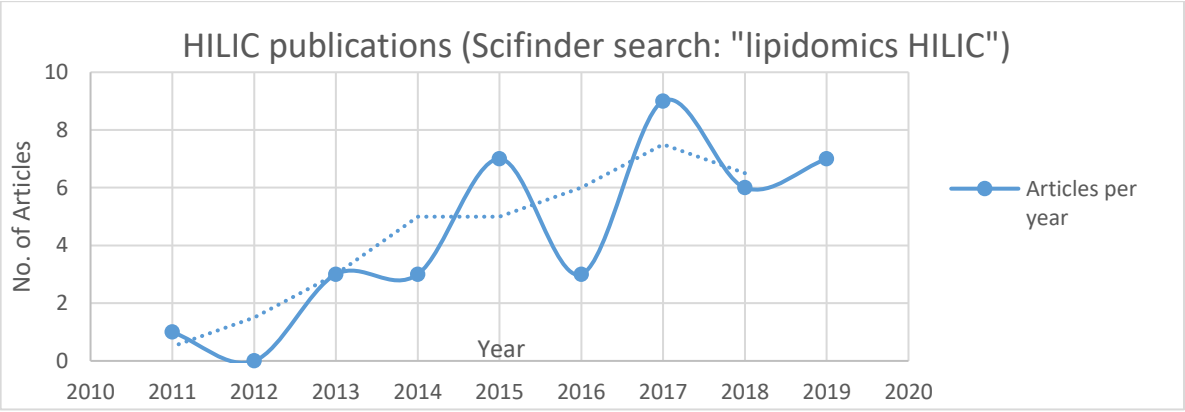

Figure 4. Publication trend on HILIC-articles in lipidomics over the last eight years (Date: 16.07.2019)

Jeucken et al.[46] used an UHPLC HILIC column to separate HeLa-cell lipid metabolites. A 96-well of HeLa cell units was filled and cultivated in the presence and absence of lipid metabolic

pathway inhibitors, to see what changes in the lipidome expression occur in an altered metabolic state. Since there is no separation by the FA chain lengths in NP, the precursors (and their m/z ratio) affecting the RTs and fragmentation patterns can give information on the nonpolar lipid species present in each cell culture. However, the identification of different chain lengths and saturation states calls for high resolution MS for compensation of the separation, as is done by Jeucken et al.[46] A downside of HILIC is the observed retention of inorganic ions, which may lead to distorted adduct formation, decreased quantitation repeatability and co-elution.[47]

Additives (e.g. acids, bases or organic/inorganic salts) are ion ligands used in promille and millimolar amounts for the enhancing of detection parameters, namely increased ionization efficiency and method sensitivity. Increased sensitivity leads to better analyte peak shapes and detected lipid coverage of low-abundance analytes.[48]

Additives are typically dissolved in only the aqueous solvent for convenience or both aqueous and organic solvents to stabilize the adduct concentration throughout a gradient run. An additive ion may form complexes with a neutral species before detection due to forming an adduct. It can also quench and suppress oppositely charged ion species. Furthermore, additives enable the controlling of predictable adduct formation ratios, if weaker ligands are present or if the concentration of considerable ligands is negligible. Moreover, as Erngren et al.[47] has demonstrated with positive mode ionization, inorganic ions are retained in a NP separation column, thus leading to possible co-elution, complex adduct or cluster formation and decreased repeatability in quantitation.[47] This may also be the reason for the usage of post-column additive addition used by Monnin et al.[48]

Monnin et al.[48] compared the performance of the additives acetic acid (AcA) versus AmOH post-column in negative ionization mode, AmAc versus AmOH in the mobile phase and AcA . AmAc versus AmAc/AcA as the mobile phase. Generally, additive ions form pseudo-neutral adducts that also change the interaction between the analyte and the stationary phase via adduct-driven polarity manipulation of a compound. For the gas-phase additive introduction with AcA versus AmOH in negative mode, the importance of proton affinity between additives was inspected. Despite its higher proton affinity, 0.1 AmOH% contributed to more suppression than 0.02% AcA.[48] For the in-solvent experiment with AcA versus AmOH in negative ionization mode, though the GP population was at an optimal degree of ionization with 0.1% AmOH,

severe 4.4-1000 fold suppression was experienced compared to 0.1% AcA despite the 2.3-3.2 fold suppression for PEs.[48] Comparing the adducts with experimentally optimized ratios 0.02% AcA, 10 mM AmAc and their combination in negative ESI mode, AcA turned out to outperform both variants except for the lipid classes PA(<AmAc, included mixed results), PE(<<AmAc/AcA), PC (<<AmAc<AmAc/AcA), LPC(<AmAc/AcA), LSM(no signal<AmAc/AcA<AmAc) and Cer(<<AmAc<AmAc/AcA) in their peak areas. On the flipside, the signal increase caused by the additives remarkably broadened LPA and PA peaks, not to mention a slighter tailing and peak broadening for PS compounds.[48]

For understanding a metabo-lipidomic system, one must first map out the lipidome or -at least- the critical lipid subset. Merrill Jr. et al.[49] designed a workflow for SP analysis of a lyophilized cell culture by using multiple LC-MS/MS protocols. Though these protocols for specific SP subclasses were introduced in 2005,[49] performing a comprehensive lipid polarity range analysis is still sought for until today. However, since these four protocols have distinct target groups to analyze, prior knowledge to whether some SPs are present or not may allow the leaving out of some sample analyses. On another note, Merril Jr. et al.[49] mentions the interconnection between SPs and their derivatives which reminds of the biochemical equilibrium present in a biological system.

When chromatographic methods were developed, the term ultra-high-performance liquid chromatography (UHPLC) was introduced to describe a fast chromatography with “nano-columns” by Jorgenson in 1997.[50] In an article by Fekete et al.,[50] the pressure needed for a reasonable flow rate through less than 2 µm sized particles in columns was made commercially possible in 2004.[50] The UHPLC instrument is left with fields to improve like (1) the upper pressure limit or flow rate, (2) column temperature modulation for stationary and mobile phase heating, (3) dead volume expulsion to avoid peak broadening (e.g. extra-column dispersion), (4) handling of the improper isocratic mixing that leads to dwell volume of a gradient (combatted by additional mixing devices in the instrument), (5) minimization of column frictional heating, and (6) increasing of the sensitivity-defining data acquisition rate of detectors.[50] UHPLC benefitted of better throughput and resolution compared to traditional HPLC. Its success was followed by a near exponential growth of UHPLC and UHPLC-MS publications in the following ten years.[50]

Resolution of a UHPLC method is very high. Therefore, it can combat the spectral interferences of co-elution observed in conventional HPLC. Based on Danne-Rasche et al.[52] a Venn diagram showed only some lipid species to be detectable with more sensitive methods (i.e. UHPLC and nanoLC) than conventional HPLC (Figure 5). Additionally, the illustration introduces a nanoLC-technique where the column material is packed in a narrow-bore capillary, which will be discussed later.

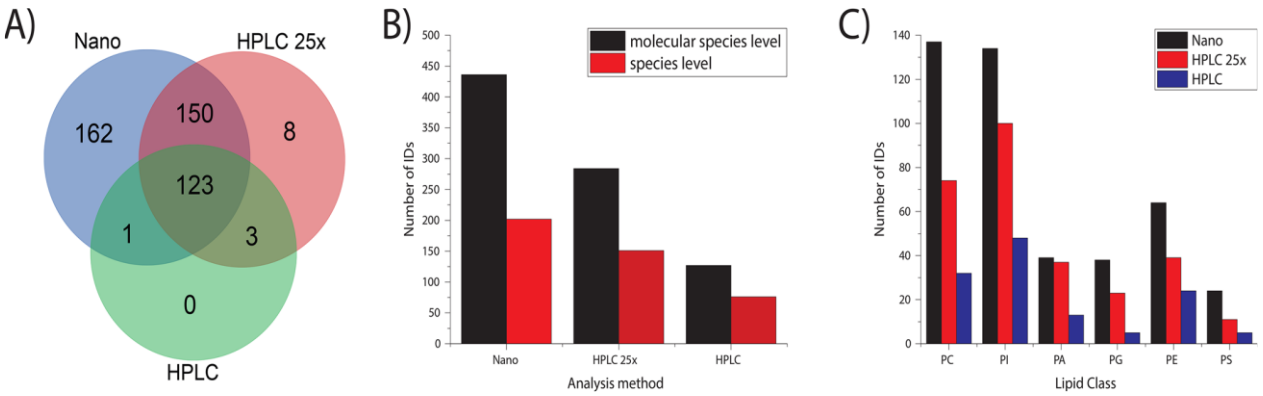

Figure 5. Yeast lipidome coverage with HPLC, UHPLC, and nano-LC. A)Venn diagram for total lipid coverage of different chromatographic techniques, B)molecular species and species level compared to each other and C)Lipid class coverage comparison[52]

This figure was borrowed from Reprinted with permission from ref **52 © 2018 American Chemical Society**

Teo et al.[29] studied various biofluids and tissues analyzed with different chromatographic techniques and their ionization methods until 2015. Primarily, GLs; GPs; SPs and occasional STs of both liquid biological materials (e.g. blood components and secretions) and solid tissues (e.g. eyeball, fibroblasts and skin) have been studied with LC.[29] Jurovski et al.[18] also includes FAs and CEs as major classes studied in clinical samples.

Since the variation even within lipid classes is enormous, it is not surprising that the polarity of their species varies a lot. *Figure 6* demonstrates the lipid-subclass range of four distinct chromatographic approaches, of which they form two pairs (one a RP, one a NP separation strategy in each pair). The subclasses in (a) include lipids of the nonpolar kind, whereas the separations of (b) are modelled for the polar lipid subclasses. Self-evidently, the lyso-forms are more polar than their counterparts with an extra FA chain. Particularly, polar (b) and mid-polar (PS, PG, PI, Cer) lipids seem to be species often analysed with negative mode, though more species are primarily found with positive mode. From the GLs only MG has a FA chain

count small enough to be rather polar. As a thumb rule, SPs are on the mid-polar lipid spectrum if they include amide-bound FA chains.

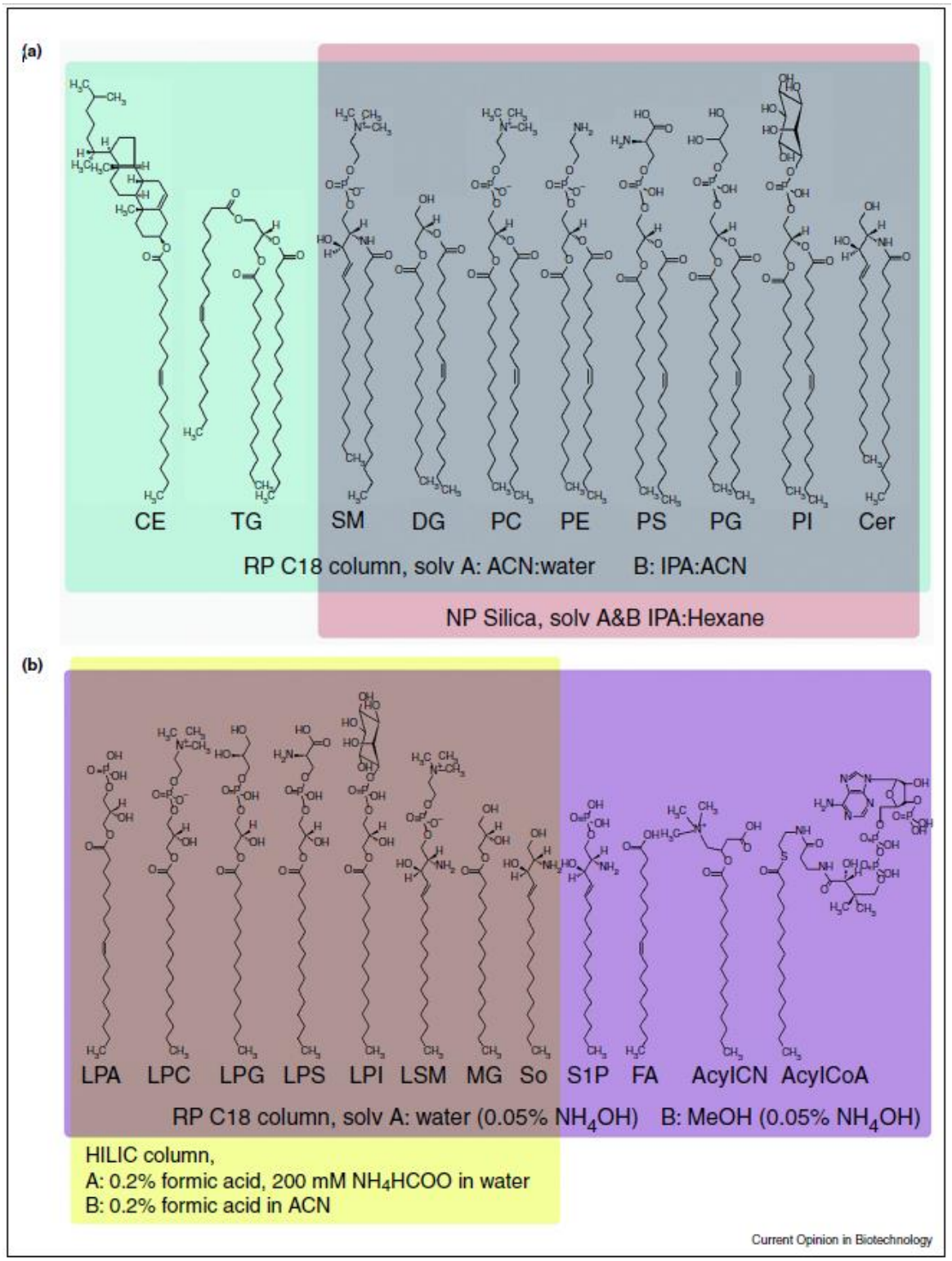

Figure 6. '(a)' Nonpolar and '(b)' polar lipid subclass separation techniques.

Reprinted with permission from ref **21**, **DOI: 0958-1669/© 2016 S. Tumanov and JJ Kamphorst. Published by Elsevier Ltd, an open access article under the CC BY license.**

5 Mass spectrometry of lipids

Modern lipid analyses from simple profiling to complex metabolite interaction mapping are primarily conducted via mass spectrometric (MS) methods and techniques. Holcapek et al.[3] divided mass spectrometry into three major approaches in lipidomics: direct infusion MS (DIMS, i.e. shotgun lipidomics, flow injection MS), chromatographic methods coupled with MS, and desorption techniques in MS.[3, 53]

DIMS is a fast technique that analyzes a homogenous sample throughout runs. Thus, it is a very appealing method for tandem mass spectrometric methods with multiple precursors or fragments to be monitored. However, DIMS needs very high resolving power, proper dilution of samples to avoid instrument contamination or detector saturation. Furthermore, prior knowledge on spectral interference must be available for correcting quantitation data and considering possibility of identical isomer fragmentation behavior.[53] Furthemore, matrix effects (though equally strong throughout runs) can be high depending on a sample's properties.[54]

Chromatographic techniques, meaning gas chromatography-MS (GC-MS), HPLC-MS, ion mobility MS (not a chromatographic method), and supercritical fluid chromatography-MS (SFC-MS)- have the advantage of separation efficiency, which enables improved sensitivity compared to DIMS. GC-MS usually needs derivatization to improve volatility and sensitivity of specific lipid class analyses, which is rarely needed for HPLC. However, a comprehensive time-consuming lipidomic analyses can be achieved with both optimal chromatographic performance (preparative extraction, LC parameters, column, etc.) and high resolution (maximal ionization in an ion source, with a high resolution mass spectrometer).[3] Not only is analytes separation in HPLC-MS slow compared to other methods, equilibration between runs increases run sequence as well.[55] Lísa et al.[55] reported an up-trend for the column domain with particle size less than 2 µm hybrid silica SFC-MS metabolomic experiments in the year 2017. One reason for the trend could be the quickness of separation done in both polar and nonpolar systems.[55] Hyphenated chromatography with mass spectrometry enables two-dimensional MS when using two orthogonal columns, which gave more information about analytes than a corresponding complex and time-consuming chromatographic method.

Desorption techniques are ideal for mass-spectrometric imaging (MSI) techniques of material surfaces, such as tissues or cells.[3] Since locating the origin of the lipids is not possible in conventional LC-MS, desorption techniques offer a fast solution to the task. Holcapek et al.[3] (2018) and Yang et al.[53] (2017) mentioned only matrix-assisted laser desorption-ionization MS (MALDI-MS) as a desorption technique used in metabolomics. Furthermore, Yang regarded proficient properties of MALDI-MS to be easy sample preparation, quickness of measurements, and possibility to re-analyze samples with this barely destructive method. Disadvantages are met at low mass range which is typically distorted by matrix. Low repeatability is an issue when sample spots are analyzed, in-source fragmentation ('post source decay') and formation of multiple adducts.[53]

A mass spectrometer is used to measure charged molecules and their abundances of observed mass-to-charge (m/z) in proportion to the m/z of carbon (molar mass 12.00 Da). Before measuring, in a hyphenated HPLC-MS method dissolved molecules are ionized and the ions are transferred into gas phase as fine spray in an ion source. It couples the HPLC instrument with the mass spectrometer and, hereby, enables dissolved components to ionize and to form ionized gas molecules. This flux of ions is then focused and dispersed with electric and/or magnetic optics, filtered with a mass analyzer, and finally detected with a mass sensitive detector plugged to a data processor.

Efficiency of mass detection is not only determined by the properties of the detector, but also by the converter transferring information to the computer/recorder. Hence, limitations to collect strong analyte signals leads to saturation of a mass detector and unreliable results in quantitation. Other measuring devices such as ion mobility MS, Raman, or even other scanning mass spectrometers such as NMR may be included in the instrumental sequence to enhance identification and acquisition of chemical information.[54]

5.1.1 Ion source and ionization

After the chromatographic separation, the mobile phase is directed from the HPLC totally or partially into an ion source. As to an electrospray ionization source (ESI source), it can be directed orthogonally towards the mass analyzer. Then, the ESI source applies a high voltage on its metal-coated capillary to eject a fraction of the LC mobile phase flow. As a result, a fine spray of ions is produced and charged liquid droplets are transcended into the gas phase. Only a fraction of the mobile phase is directed to the ESI source. It enables reproducible ion flow and transfers a limited amount of the liquid mobile phase.[56]

The composition of the arriving mobile phase into an ion source determines the chemical, electroconductive and rheological (e.g. viscosity, surface tension) properties of the sprayed liquid, thus contributing to possible matrix effects (i.e. signal suppression, signal enhancement) and rate of ionization. These properties can be adjusted with additives, which are commonly used as potential contributors to adduct-formation with analytes.[56]

The voltage applied to the capillary tip in ESI needs to give sufficient electrical potential to eject a proton (H^+) from a molecule or energy to transfer a proton to a molecule. The polarity of the ions produced are reciprocally activated by a steel tip polarity. With increasing voltage, ions with multiple charges are encountered.[57]

Classically, single or multiple charged analyte ions from suitable ionization circumstances appear via radical-assisted deprotonation ($[M-nH]^{n-}$) or protonation ($[M+nH]^{n+}$). However, analyte signals may also be expressed in escort with an additional ion. The resulting combination is called an adduct ion, which may be formed with organic or inorganic ions. The formation of complex adduct variations is claimed as characteristic for ESI, as mentioned by Erngren et al.[47] The discovery of adducts has emphasized the increasing trend of additive buffers for both buffering of the pH during analysis and increasing of analyte sensitivity through increased intensity of the adduct ions. Furthermore, di- or trimers of analyte ions may be formed. In essence, adduct and dimer formation during ionization needs to be controlled for absolute quantification of the analyte.

As additives affect the pH of a solution, the pH affects ionization efficiency of the analytes by regulating the concentration of charge carriers. Furthermore, ion formation occurs both in the solvent and ESI tip. Monnin et al.[48] investigated this pre- and post-column dual jet additive introduction in negative ESI mode, since this enabled the inspection of both the ionization and

adduct formation processes in-solvent and aerosol formation. Effects were mixed according to lipid class (*Figure 7*).

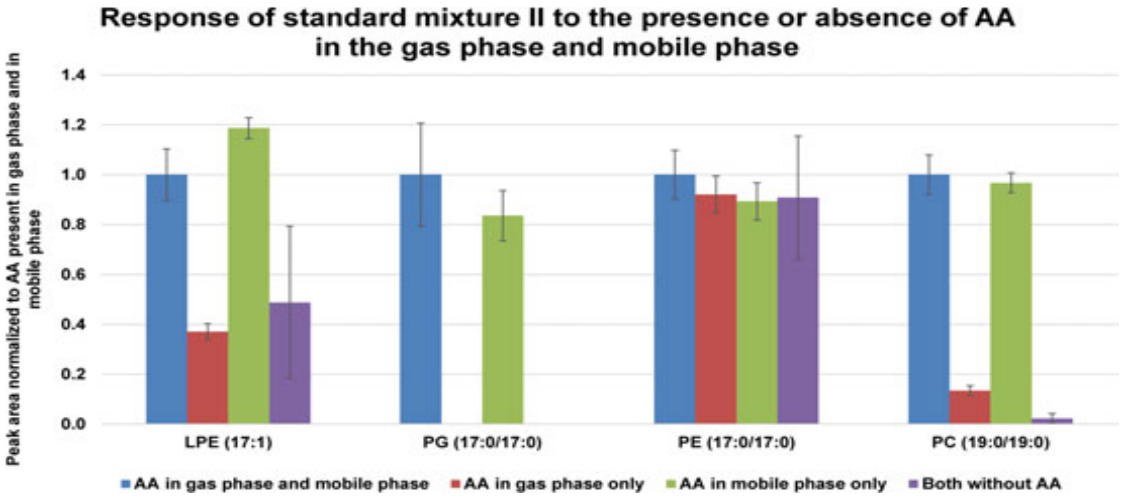

Figure 7. Normalized analyte peak areas in comparison to additive introduction strategy. Reprinted with permission from ref **48 © 2017 John Wiley & Sons, Ltd.**

At the correct potential and pneumatically assisted ejection, the repulsion of same-charge droplets on the capillary tip in a mass interface produces a jet-plume shape called the Taylor-cone. Considered a reproducible and well-documented ejection shape, the Taylor cone includes charged ions that are attracted with an opposite charge (i.e. a counter electrode) and moved as clusters into the mass analyzer, while neutral species are separated and left further away.[56]

Though the behavior of ion formation in the ESI-source is not yet completely understood, three models are used to explain ion formation: the charged residue model (CRM) and ion evaporation model (IEM). A combination of the two, the ion emission model, has been proposed as well.[58] CRM predicts the emergence of a single ion from a small and ever evaporating solvent droplet. On the other hand, IEM describes the ejection of small molecules from solvent droplets in the Taylor cone. The droplets become smaller, when their surface charges increase and surface areas decrease. The surface tension (Rayleigh limit) is overcome by the surface charge for ejecting the small ions.[59, 60]

Rarely, APCI sources (ionization with a corona discharge needle, some LC/MS devices have interchangeable ESI/APCI interfaces) are used instead of ESI sources in UHPLC-lipidomic

studies.[46, 61, 62] This technique has the advantage that it has more similar response factors among the various lipid classes in the positive ionization mode. On the downside, APCI is less sensitive than ESI, and lipid headgroups are lost due the harsher ionization conditions. Furthermore, low resolution and low mass-accuracy instruments such as linear ion traps, cannot discriminate between nominally isobaric diacyl- and ether lipid species by MS1 alone.[46]

5.1.2 Mass analyzer

Mass analyzers aim to modify the stream of ions fed by the ion source. The mass analyzer is chosen to measure the abundances at a specific m/z range or separate species in a definite time frame. This means that the time for a single mass spectrum scan (i.e. the scan rate) increases its acquisition time. The longer a single m/z abundance is screened, the more there are m/z species in detection.

Evidently, when the abundance of one m/z species takes 100 milliseconds to be collected, 10 collected m/z data points of a mass spectrum take one second to be collected. Therefore, scanning instruments may be adjusted in targeted analysis to collect only discrete m/z abundances instead of fully scanning the mass range.

Not only can a scan be cut to small ranges, it may also be limited to discrete m/z ion species. This kind of very specific scanning is known as selected ion monitoring (SIM), which gives a basis to qualitative analyses with high scan rate tandem mass spectrometry. The SIM technique enables longer individual acquisition times and shorter scans, thus, higher sensitivity and throughput. In turn, by decreasing the individual acquisition times more data points (i.e. mass spectra) can be collected, which increases resolution between peaks detected in the chromatogram.

In addition to scanning mass analyzers, there are instruments that can measure at once the full range of m/z with abundances. These analyzers are either based on the mathematical Fourier transform-deconvolution of a single signal into all its basic sine-wave signals (e.g. Orbitrap and ion-cyclotron resonance mass analyzer) or comparison of flight times in a controlled environment (e.g. time of flight instruments). Such instruments have the high throughput-advantage, meaning that more measurements can be made in a much shorter time in contrast to scanning instruments. Furthermore, mass analyzers with indirect

measuring systems, as in the case of Fourier transform mass spectrometers, have the multiplex-advantages. This means that mass spectra can be measured fast and at multiple times, thus increasing the total resolution of such instruments by comparing sequential image currents with each other.

Another class of mass analyzers are ion traps. These instruments collect and store an entity of ions, then analyzing them separately from the continuous flow. The operations possible to conduct (e.g. scanning, SIM) are once again dictated by the mechanism of the mass analyzers.

Since a mass analyzer instrument is very dependent of its vacuum created by an external high-efficiency pump, imperfect vacuum in the TOF may lead to in-source fragmentation, which is frequent in lipidomics. In nanoscale, in-source fragmentation is induced via the impact of analytes and remaining air molecules. For example, DGs lose neutral water from their structure.[19]

Lipidomic studies usually prefer high resolution MS instruments (i.e. instruments reaching a less than 2 ppm mass accuracy) with MS/MS capabilities. For this reason, a good compromise for this has been a QTOF, since it possesses moderate resolution and the possibility of MS/MS experiments for both untargeted and targeted analysis. However, method sensitivity is decreased in exchange of selectivity when conducting a MS/MS analysis instead of a TOF-only scan. *Table 2* sums up the yearly mass analyser profile in UHPLC-MS research.

Table 2. UHPLC-MS mass analyzers. The visual mass analyzer ratio is calculated separately for each year

Instrument	2017 (n=25)	2018 (n=27)	2019 (n=14)
IM-QTOF	1	1	0
LTQ	0	0	1
LTQ-Orbitrap	0	2	0
N/A	0	1	0
Orbitrap	6	2	1
QOrbitrap	5	9	4
QqQ	3	1	0
QTOF	9	9	7
Qtrap	0	2	1
UHR-QTOF	1	0	0

n: amount of articles

As another mass analyzer favorite, the Orbitrap stands out with its exceptional resolution. This makes it an attractive choice for targeted (quantitative) analysis, while the identification of lipids can be conducted with another mass. However, even untargeted approaches can be considered with an Orbitrap since the recent developments in identification softwares. The emergence of a newly commercialized "Q-Orbitrap" can be observed to have increased in usage.

5.1.2.1 Triple quadrupole

A triple quadrupole mass analyzer (QqQ) is a scanning instrument with three quadruple- or multipoles, i.e. two mass filters (Q1 and Q3) and a collision cell (q2). Collision induced dissociation (CID) is conducted in the collision cell by introducing an inert collision gas (e.g. N_2, Ar, He) to ions, leading to collision and potential fragmentation of analyte ions. Q1 may be used to select precursors to collide, Q3 for the scanning of specific m/z fragment ions. QqQs are frequently used for low-resolution mass spectrometric measurements.[62-66] These include both fragment studies with selected ion, selected reaction and multiple reaction monitoring (SIM,[62] SRM[64] and MRM[63, 65, 66]) as well as qualitative and quantitative untargeted methods.[62, 65, 66]

Figure 8 demonstrates the basic structure of a QqQ instrument without the detector following after Q3. Due to extensive research around quadrupole instruments, the quadrupoles may have been substituted by multipoles (e.g. hexa- or octopoles) for improved instrument selectivity.[56] Furthermore, no optics for ion stream focusing were noted as they vary largely among the different instruments made by different companies.

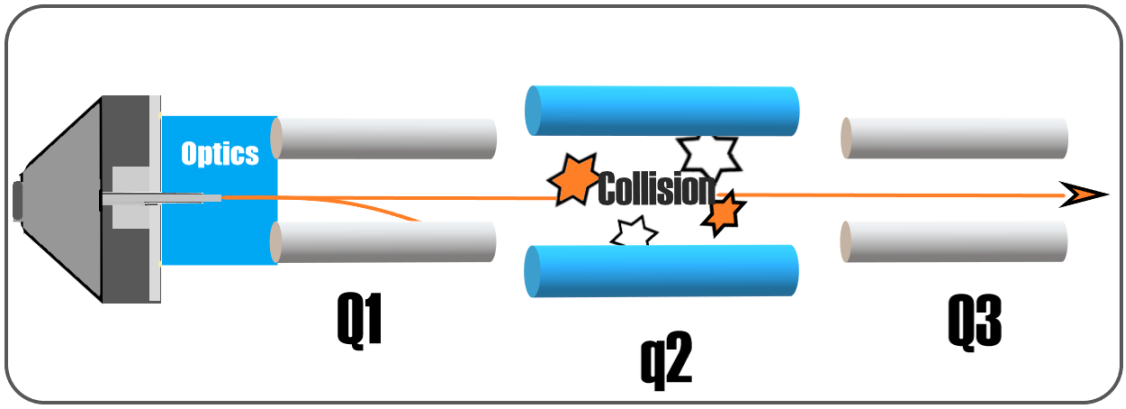

Figure 8. Inner workings of a QqQ performing a precursor ion scan. The orange line represents the ion current that goes through the mass analyzer. Image is inspired by **Ref. 56**

5.1.2.2 Time of flight

The time of flight mass spectrometer (TOF) is a universal mass analyzer, known as an instrument that analyzes ions "all at once". Ions are pulsed into a free drift tube, where their drift time from a laser-pulsing site to the detector is recorded in sequence. Most TOF instruments include an ion mirror to increase the path length of freely drifting ions to improve resolution in exchange of sensitivity. Furthermore, phase-shifts of identical m/z-species but with unequally pulsed kinetic energies are corrected (i.e. time-lag focusing). Modern TOF-instruments of today are regarded as very fast, accurate and sensitive, well resolved and equipped with practically unlimited range.

By substituting Q3 of a QqQ with a TOF mass analyzer, a QTOF is produced. A QTOF instrument enables both high throughput and acquisition of tandem mass spectrometric information in one run, though affecting the sensitivity by exchanging it with more selectivity. In other words, it combines the tandem mass spectrometric capabilities of a triple quadrupole and the TOF.

The ESI-interfaced QTOF is a frequent choice for lipidomic studies alongside the ever so popular Orbitrap. As all m/z abundances can be measured practically simultaneously upon detection in a TOF, it enables the storage of a full m/z-scan for post-analysis irrelevant to the on-going study. As an instrumental example, *Figure 9* describes the inner structure of an ion mobility QTOF (IM-QTOF).

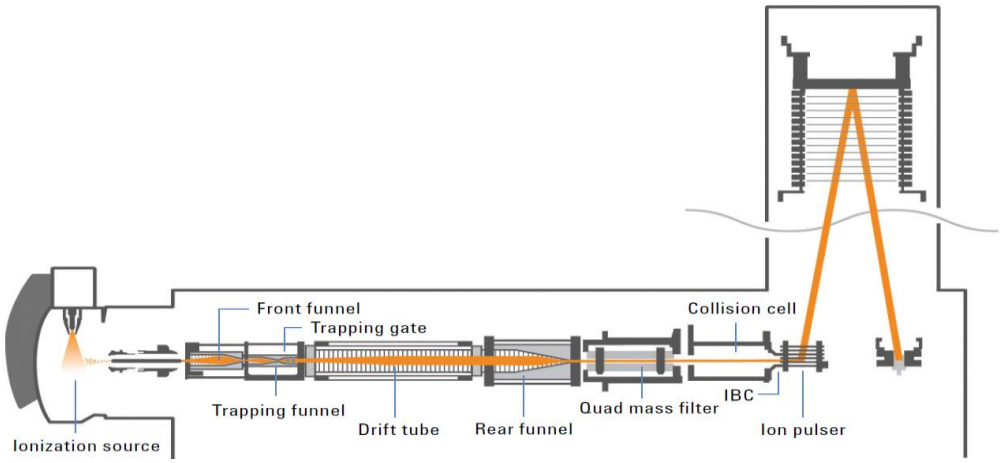

Figure 9. The Agilent IM-QTOF used in the experimental part, an example of a QTOF instrument. Displayed are the ionization source, single bore capillary leading to the ion mobility system: a front funnel, trapping funnel, drift tube and rear funnel; the QTOF part includes a mass filter (Q1), collision cell (q2) and TOF unit (Q3) including an ion pulser, reflectron and detector.

Reprinted from **ref 67 © Agilent Technologies, Inc., 2013**

5.1.3 Tandem mass spectrometry

Tandem mass spectrometry ($MS(/MS)_{n-1}$ or MS^n for *n* scans/selections) is the practice of scanning or selecting a set of ions, fragmenting them in controlled circumstances, scanning or selecting once more, and possibly repeating the process until detection. This can be achieved with either tandem in space, where separate conjoined mass analyzers scan or select m/z ions between fragmentation and detection, or using tandem in time, where the same mass analyzer instrument (so far, only an ion trap device) may scan or select the ions indefinitely. A scan consists of selected m/z ion species is called a precursor, their fragments after collision product ions. Tandem MS enables improved selectivity in targeted analysis as well as more structural information in non-targeted analysis, isomer verification, and though depending on its scan mode.

A common mechanism for controlled fragmentation is analyte ion collision with accelerated inert gas (e.g. Ar, He, or N_2), resulting in controlled CID. CID is commonly achieved in either a QqQ or ion trap mass analyzer. As the collision gas hits the right group or structure in a molecule, the ionized molecule is spliced into smaller parts. The potential used for the collision gas acceleration is commonly between 1-20 keV.[68] Other fragmentation methods such as multistage fragmentation or ozone dissociation[5] were not considered since such technology was neither trending[69] nor observable in the dataset.

Scan modes, i.e. m/z separation operations consecutively combined with collisions and detection, introduce various ways to acquire information on qualitative and quantitative properties of analytes. Lately, metabolomics studies have started to frequently use the definition data-dependent and data independent analyses (DDA and DIA). DDA needs pre-selected data to conduct a MSMS-experiment, whereas DIA only needs the collision energy used.[70]

DDA scan modes include a product ion scan, a precursor ion scan (PIS), a neutral loss scan (NLS), and a selected reaction monitoring (SRM) scan. In a product ion scan, precursors are selected and collided to fully scan the profile of the product ions. In a precursor ion scan (PIS) a m/z range is first scanned, only to monitor specific fragments after CID. In a neutral loss scan (NLS) both initial analytes and their CID fragments are scanned to find a molar mass shift of m/z species abundances. In selected reaction monitoring (SRM) both precursors and product ions are selected to prove the presence of a specific analyte in a sample.

The Agilent MassHunter Workstation for data acquisition of a QTOF proposes two DIA scans (all ions scan and autoMS) and a DDA (targeted MS) scan. In an all ions scan, both a full scan and universal fragmentation is done in turns In an autoMS-scan, computer-assisted fragmentation of the most abundant or most preferred ions takes place and in targeted MS a targeted precursor ion scan only commences at a defined RT for defined m/z ions.[71]

6 Ion-mobility spectrometry

As a charged particle is moving against an inert gas with known velocity, its movement can be rotationally averaged. Ion mobility spectrometry (IMS) observes this by recording the drift time of an ion species in an electric field.[71]

As the Mason-Schamp equation[71] (*equation* 1.1) states (exclusively for uniform drift tubes), the buffer-gas specific drift time (Ω) is directly proportional to the collisional cross-section (CCS) -the averaged effective area of the analyte that collides with the inert buffer gas.

$$\Omega = t_{drift} * \frac{z}{\beta * \sqrt{\left(\frac{m_I}{m_B + m_I}\right)}} = \left(t_{tot} - t_{fix}\right) * \frac{z}{\beta * \sqrt{\left[\frac{m_I}{m_B + m_I}\right]}} \quad (1.1)$$

$$\beta = \frac{\sqrt{18\pi} * e * E * 760 * T_{instr}}{16 * \sqrt{k_B T_{instr}} * L * P * 273.2 * N} = 1.3074 * \frac{e * E * T_{instr}}{\sqrt{k_B T_{instr}} * L * P * N} \quad (1.2)$$

$$\beta = 5.6369E - 8 * \frac{E * T_{instr}}{\sqrt{T_{instr}} * L * P * N} \quad (1.3)$$

, where *z* is the charge of an analyte, t_{drift} the drift time acquired by subtracting the fixed time not included in the drift tube (t_{fix}) from the total time spent in the ion mobility section of the instrument (t_{tot}), m_I the mass of an analyte ion and m_B the mass of the buffer gas molecule. The constants in the equations of β include the elementary charge e (1.602 x 10^{-19} C), the Boltzmann constant k_B (1.3806 x 10^{-23} $m^2kgs^{-2}K^{-1}$), and the instrumental parameters of the drift cell: the electric field E, temperature T_{instr}, the length L of the drift tube, the pressure P and the number density N. Hence the theoretical CCS value of the analytes can be measured via their drift times, no calibration standards are necessarily needed.[71]

Some QTOF-instruments are equipped with an IMS module, enabling further identification tactics with another molecular property dimension. However, identifying CCS values of molecules in ion mobility-mass spectrometry mode (IM-MS mode) decreases the amount of ions ending up at the TOF, which in turn decreases sensitivity in the analyzer.

7 Data-analysis and processing

Pre-processing softwares have been developed to convert experimental data, correct baselines, refine chromatograms by filtering out background noise and even discarding noisy data entirely.[72] For both identification and quantitation, the supply of commercial, open-source and home-made tools for primary processing have exploded as already reviewed by Pöhö[34] as well as Sethi and Brietzke.[54] This can also be said for statistical tools, analysis softwares and algorithms, which enable visualization and perceiving of patterns for large datasets.[71, 72]

For pre-processing and extracting of information, data was typically analyzed via a specifically tailored automatic data-processing software e.g. Markerlynx, MZmine, Qualitative Workflows or XCMS. Metabolic profiling of data was done with similar programs, e.g. Metaboanalyst or MeV.[72] Another popular solution were manually crafted solutions self-programmed in a coding language. Popular software environment languages for data processing included MatLab, Python, R (base for XCMS and MeV) and SPSS. Self-evidently, manual programming from the ground up or with borrowed code demands more computational expertise from the researcher. However, Koelmel et al.'s[73] article, which compared available identification algorithms with the commercial R-based LipidMatch-tool, mentions most lipid identification softwares to be written with "middle level languages […] such as C++".[73]

Metabolic correlation and significance analysis of lipids is typically conducted with a set of visual chemometric analyses and statistical methods. Chemometric methods include a typical overview on analyte clusters, the principal component analysis (PCA);[72] regression analysis of partial least-squares data-analysis (PLS-DA) and/or orthogonal projections to latent structures data-analysis (OPLS-DA);[137] a (relative or actual) concentration boxplot or heatmap;[34] analyte interaction study via hierarchical cluster analysis (HCA) or pathway analysis; importance testing of PLS-DA variables with variable importance projection (VIP);[72] visualizations such as the Bland-Altman or volcano plot for significant outlier detection; and/or method or sample comparisons with Venn diagrams.

Principal component analysis pursues to flatten a large dataset with multiple variables to find the most important two sources of variation, i.e. principal components. This is done by comparing the variation between all variables and flattening these into only two dimensions with matrix operations. This way, most important information of the multivariate data is

found. e.g. to divide analytes into different groups and characterizing them.[74] PLS-DA, on the other hand, approaches the flattening of multivariate data parallel (whereas OPLS-DA orthogonal) to the partial least square plateau of the dataset.[75] Moreover, HCA displays clusters of sample components that correlate with each other. The recognition of this correlation is derived from information often visualized in heatmaps,[76] which include a matrix including the analyzed samples sorted with found lipid species in them, color-scaled in the concentration or change of concentration the analyte has experienced.

Typical statistical methods include a null hypothesis to test dataset similarity. With the p-value parametric Student t- or with the non-parametric Mann Whitney U-test; and analysis of variance (ANOVA) for more than two variables. Additionally, statistical tests have correction methods such as Benjamini-Hochberg[77] to calculate the false discovery rate (FDR) for minimizing false positives in a dataset.

The Mann-Whitney U-test[78] (also known as the Wilcoxon rank-sum test) is used to non-parametrically evaluate the similarity of two independent dataset medians with a null hypothesis. For two sets with same or different sample sizes, the values of both datasets are sorted from smallest to largest. The ranking value is divided among identical values (e.g. for values 2 and 2: 1.5 & 1.5). Then, the separately ranked sample value sets are summed individually, and if one of the sums is critical value range of a u-test table, the null hypothesis can be rejected. [78] Akin to the Student t-test, the u-test with large sample sizes is evaluated by determining the z-score of a normal distribution.[78]

In the Benjamini-Hochberg method[77] p-values of two sample sets (i.e. control and test group) are inflated mathematically to reveal possible false positives. Since affected and unaffected lipids represent two distinct normal distributions, false positives can be ideally seen as a separate normal distribution at big sample sizes. In the method, (lipid species') p-values are put into "bins" adjusted as big as the significance that is desired for the p-values (e.g. P=0.1, 10% significance). The bins are then ranked from smallest to largest p-value, after which individual p-values are "modified" from largest-to-smallest. The largest p-value keeps its value, but the second largest p-value is determined as the smaller value of two options: either it is the value preceding it, or the value calculated with a separate equation.[79]

For instance, Tietz-Bogert et al.[80] calculated the FDR for a lipido-metabolomic study researching significant biomarkers of primary sclerosing cholangitis,[80] a disorder in the bile duct of unknown origin. The lipid species' concentration between control samples to the clinical samples of diseased patients in both portal blood and bile were compared to exclude FDR-values under 0.01 from the dataset.[80]

Since targeted and untargeted methods are two distinctively different approaches, so are their means of data processing. Gorrochategui et al.[72] describes the targeted processing of metabolites in five phases (for more detailed flowcharts, I recommend to read the full article): at first, raw data is acquired via conduct analysis and a referential database is picked by either using a predefined local, open-source or commercial database. Alternatively, an in-house database can be created via standard compound analysis. Next, metabolites are isolated via pre-processing of data, which is followed by identification of the metabolites, quantification and chemometric/statistical evaluation. The evaluation may be conducted manually or with the help of a program. Finally, the processed data and its results are interpreted considering the initial hypothesis proposed. Despite the high sensitivity and accuracy, a targeted approach is only limited to the predefined database. Thus, Gorrochategui[72] predicts future methods with not only targeted, but also untargeted elements.[72]

Untargeted lipid metabolomics analysis follows a similar, though 9-stepped path. Raw data is *acquired*, the *stored* data file *converted* and *exported* via a tool compatible with the acquisition software, and the file is *imported* into a specifically tailored or universal interface for pre-processing. For lipid metabolome analysis, *biomarkers* and *metabolites* can be *screened* with either statistical tests or chemometric analyses and then identified, both of which are irrelevant for profiling of the sample's lipidome. Identification proceeds through either commercial, open-source or self-acquired data libraries. Finally, the data is interpreted through prior knowledge or a proposed hypothesis.[72]

8 Development of ultra-high performance chromatography

8.1 Emerging trends in lipidomics

The use of unconventional non-chromatographic methods has increased during the time frame of 2017-05/2019. For example, mass spectrometric imaging (MSI), once synonymous with desorption techniques like desorption ESI (DESI) and matrix-assisted laser desorption ionization MS (MALDI-MS) has expanded to other strategies. Methods not discussed in this review include secondary ion MS (SIMS),[2] nanostructure initiator MS (NIMS),[2] laser ablation ESI (LAESI)[81] and direct analysis in real time (DART).

Li et al.[82] conducted MALDI-MS imaging experiments with a FT-ICR mass spectrometer to analyze liver cancer *in situ* on human patients. The scarcely studied metabolic lipid profiling of hepatocellular carcinoma revealed down-regulation of TGs with less than two double-bonds and ceramides, and conversely, up-regulation in only GPs and SM. Particularly, new information on TG, PC, PE and PI trends was uncovered in the study.[82]

As a side note, the decline of chip analysis in UHPLC research done in 2014-2017 can be observed: only a limited amount of articles including that technology, such as on-chip analysis or microchip NSI.[83-85] Thus, the study field was excluded from this literature review.

A biocompatible surface probe (BCSP) was used as a solid phase microextraction (SPME) device, which is directly immersed on the precise position of the probe surface to be analyzed.[81] However, this introduces an additional step to the analysis procedure since the analytes are desorbed from the adsorbent into a solvent-prefilled nanospray tip after loading of the material.[81]

In addition, liquid extraction surface analysis (LESA) has shown promises as an alternative surface analysis method. In LESA a liquid solvent is temporarily applied on the sample's surface, is aspired back into the injection pipette and analyzed. In practice, Zong et al.[85] conducted such an analysis with an LTQ mass spectrometer hyphenated with an NSI source to a microchip nozzle array. Then, the equilibrated liquid was transferred from a single-use pipette to the single-use chip. LESA is an *in situ* qualitative analysis method apparently capable of lipidomic profiling (at least *in vivo*) and metabolic differentiation (e.g. increased anti-oxidant activity in multidrug-resistant MCF-7/ADR in comparison to the baseline cells).[85]

A potent complementary method, nondestructive imaging achieved with Coherent Raman scattering (CRS) has been tested by Kim et al.[86] and reviewed by Gupta et al.[87] For CRS imaging to work, a material must either be active at the anti-Stokes frequency (for coherent anti-Stokes Raman scattering, CARS, which follows a quadratic signal) or else must be stimulated (for stimulated Raman scattering, SRS, which follows a linear signal).Two types of intensity measurements can be made in SRS: signal capture of stimulated frequencies or the loss of signal intensity, both at specific Raman wavelengths.

The resolution of MALDI-MS (~10 µm)[2] can be compared with that of CRS (~0.1 µm)[87] by analyzing single cells (single cell size: ~8 µm x 12 µm)[82]. For example, Kim et al.[86] encapsulated water-oil emulsified microalgae cell solution carried with PDMS that splits the cell solution with a T-junction into droplet culture chambers. After isolation into the chambers, cell solution taken from a cell culture plate could be analyzed *in vivo* with a CRS technique. Microalgae are speculated to be potential renewable biofuels in the future.[86]

Nanospray ionization (NSI) lipidomics was heavily dominated by shotgun lipidomics between 2017-05/2019. As DIMS injections reach equilibrium before 30 seconds,[81] a rapid analysis time of 1 minute allows very high throughput compared to separation techniques. NSI increased the sensitivity of the method substantially, which was important considering that DIMS needs high signal strength for the deconvolution of data and identification of analytes with very similar RTs. However, DIMS is inherently prone to low abundance analytes and spectral overlap of isomer or stereo-chemical species, because the method includes no separation (e.g. PCs and PEs with same m/z ratios[21]). This also explains the trend of more derivatization in DIMS compared to HPLC. DIMS is considered a method for moderate lipid abundances, as extensive abundances of lipids lead to the need for higher resolution.[2]

Looking back on the 35 year long (1982-2017) MS development harnessed in lipidomics, Gross[2] defines the present problem of lipid analysis as the lack of specifity. Apparently, unidentified contaminants in multiple reaction monitoring (MRM) experiments lead to a high false discovery rate and deviation in quantitation results.[2] Moreover, as the average identification accuracy of UHPLC-ESI-MS in both mass spectrometric modes lies around 89-105% (±10%, n=5, *Attachment 1*), [28, 64, 65, 88, 89] false positives remain at estimated values of 57% for positive and 27% for negative ionization mode.[51] With an algorithm-assisted nanoLC-

NSI-method, the RSD of the mass spectrometer's response was <10% (positive and negative)[52].

In 2017, Lam et al.[5] reviewed accurate quantitation practices including identification. Though qualitative analysis plays an integral role, quantification is also dependent on other parameters which can be roughly divided into pre-, post- and analytical factors. By my interpretation, pre-analytical factors include matrix- and analyte-altering inter-batch effects[5] caused by a typically extended time of clinical sample acquisition and storage, and intra-batch[5] effects caused by sample preparation, i.e. alterations between storage and analysis. Analytical factors for optimal quantification include instrumental properties and calibration, method settings, circumstances of analysis and method performance, whereas post-analytical factors affecting quantitative representativeness include data pre-processing, prior data processing and validation steps.

Knowledge of molecular properties in addition to the usage of supporting standards and samples are key elements to proper quantification. Molecular properties include polarity and chemical structure, both of which lead to characteristic ionization and fragmentation behavior. Furthermore, ideal internal calibration standards with the same head groups and similar but not identical FAs (e.g. odd-numbered [<1% abundant in higher organisms] or isotope-labeled FAs) are preferred for normalization.[5] External calibration standards such as the QC sample may account for the post-calibration of systematic errors.[5] Also, mathematical model-based *in silico* algorithms can be applied to correct systematically biased data, diminishing the need for qualitative standards.[5]

Deuterated standards as surrogates, ISTDs and representative standards are needed in lipodomics. In spite of those targeted standards, the progress in the power and speed of computers have allowed algorithm-based library identifications[72, 73.] Therefore, analyses[5] *in silico* can be conducted independently without lipid standards. The *Attachment 3 shows* that in cases of 26 out of 58 analyses included no standards. Most probably it will be the trend to use validated commercial and/or in-house accumulated libraries for identification. As another alternative for single or representative standards, they may be substituted with (mostly biological) standard reference materials (e.g. porcine brain, egg) that include a known set of lipids.

Without even mentioning the false negatives, the search for a sufficiently reliable though nimble method is still on-going. Identification of analytes can be improved by increasing the "dimensions" with which they are evaluated, i.e. by analyzing more of their independent properties (RT, m/z, CCS, MS/MS, Raman). *Table 3* gives insight to the strategies used for identification, starting from interface-driven one-dimensional to multi-dimensional identification (1D-3D), or alternatively via a routine software. Approximately half of the 56 nanoLC/UHPLC lipid articles were automated identification analyses.[30, 35-37, 41, 46, 51, 55, 61, 63, 91, 94-99, 105-111, 117-119]

Table 3. Dimensions (1D-3D) and specific means of identification (*Matching*) with UHPLC-MS.

Citation	Approach	Identification	Matching details	Year
90	UT	1D manual	m/z spectra	2017
39	UT	2D manual	molecular ion	2017
62	UT	2D manual	APCI fragmentation pattern	2017
45	T/UT	3D manual	molecular ion, C isotope pattern	2017
91	UT	3D manual	POS: data-dependent CID	2017
82	UT	3D manual	MSE	2017
42	T	3D manual	MSE, PRM	2017
92	UT	3D manual	MS/MS fragment spectra	2017
65	UT	3D manual	MRM	2017
66	UT	3D manual	RT, m/z, MRM	2017
93	UT	3D manual	PIS?	2017
30	T/UT	Routine software	iLipid 1.2 (homemade)	2017
91	UT	Routine software	NEG: LiPilot	2017
94	UT	Routine software	SIMLIPID c6.01	2017
95	UT	Routine software	GeneData	2017
96	UT	Routine software	LipidSearch	2017
51	relT	Routine software	Lipidfrag	2017
97	UT	Routine software	MetaboAnalyst	2017
55	T/UT	Routine software	MassLynx	2017
98	UT	Routine software	Mzmine, LipidMatch	2017
99	UT	Routine software	Lipidsearch 4.0	2017
35	UT	Routine software	Lipidsearch	2017
41	UT	Routine software	Progenesis QI 2.2	2017

Citation	Approach	Identification	Matching details	Year
100	UT	2D manual	SRM	2018
79	UT	2D manual	Molecular ion	2018
15	T	2D manual	RT, m/z	2018
101	UT	3D manual	MS/MS spectra	2018
80	UT	3D manual	MS/MS spectra	2018
102	T/UT	3D manual	C-isotope profile (relative to ISTD)	2018
52	UT	3D manual	PRM, MS/MS fragment spectra	2018
103	UT	3D manual	SRM	2018
104	UT	3D manual	Product ion scan	2018
88	UT	3D manual	MS spectra match, CCS	2018
28	T	3D manual	MRM transition, 1-2 qualitative ions	2018
64	T	3D manual	precursor ion, product ion	2018
105	UT	Routine software	SIMLIPID	2018
106	UT	Routine software	LipidSearch	2018
107	UT	Routine software	LipidView	2018
108	T/UT	Routine software	XCMS: RT, m/z, I, MS/MS	2018
109	UT	Routine software	Lipidmaps	2018
36	T	Routine software	LipidSearch	2018
110	UT	Routine software	MS-DIAL (spectra matching)	2018
111	UT	Routine software	MassLynx	2018
63	PT	Routine software	LipidSearch: RT, m/z, MS/MS	2018
61	UT	Routine software	MS-DIAL	2018
112	T/UT	2D manual	RT, m/z	2019
113	UT	2D manual	RT, m/z	2019
114	UT	3D manual	MRM (GPs) or product ion mode (FAs)	2019
115	UT	3D manual	MSE	2019
89	relT/T	3D manual	MRM or PIS	2019
116	T	3D manual	MRM	2019
117	UT	Routine software	LipidMatch	2019
46	UT	Routine software	R: XCMS	2019
118	UT	Routine software	MetaboAnalyst	2019
37	UT	Routine software	MS-DIAL	2019
119	UT	Routine software	MS-DIAL, MS-FINDER	2019

relT: relatively targeted analysis approach**, i.e.** analysis with computer-generated data library
T: targeted analysis approach**, UT**: untargeted analysis approach

8.2 Samples in lipidomic studies

Conventional (i.e. classical) biological materials are materials that are commonly investigated medical routine analysis matrices such as urine, faecal matter and the separate components of blood, and unconventional biological materials samples that are often acquired through procedures requiring more effort (e.g. surgery): hence, used for supplementary diagnostics. Just like Jurovski et al.[18] reviewed lipidomics studies between 2014-2016, the UHPLC-research located on the time frame of 2017-05/2019 also trended towards classical biological materials. Indeed, the samples of *Table 4* and *Table 5* leaned overwhelmingly towards methods encompassing blood components (e.g. plasma and exosomes), mostly TGs for GLs, PCs; PEs; LPCs and LPEs for GPs (GPs are included in 87% of the studies between 2017-05/2019), and SMs for SPs. In contrast, urine samples were exceptionally represented 2014-2016, whereas liver tissue was the next frequent matrix between 2017-05/2019.

Table 4. Classical biological material types. Extension to Jurovski et al.'s[18] Supplementary Table.

Biological samples		**Lipid classes**	**Reference(s)**
classical biological materials (conventional)	Urine	AcCa, MG, DG, TG, PC, PE, LPC, Cer, SM, CEs	**7**, 91
	faecal matter	FA, GPs, STs, SPs, PRs, PKs	45, 102
	blood derivatives:		
	x plasma	FA, MG, DG, TG, PA, PC(+PLs), PE(+PLs), PI, PS, LPA, LPC, LPE, Cer(+Hex/Hex2/sulfoHex), SM, S, SA, cholesterol, CEs, SLs, STs	**7**, 28, 79, 36*, 55, 61-63, 79, 89, 93, 94, 97, 100, 110, 111, 113, 115, 120
	x serum	MG, DG, TG, PA, PC(+PLs), PE(+PLs), PG, PI, PS, LPA, LPC, LPE, Cer(+HexCer/Hex2Cer), SM, S, CEs, STs, PRs	**7**, **15**, 96, 104, 106, 108, 115
	x erytrocytes	PC(+PLs), PE(+PLs), LPC, LPE, Hex2Cer, SM	55
	x blood platelets	AcCa, FA, DG, TG, PA, PC, PE, PG, PI, PS, LPA, LPC, LPE, Cer, SM	119

*NIST SRM 1950 plasma

Hex: for hexosyl, **Hex2**: dihexosyl, **S**: sphingosine, **SA:** sphinganine

bolded articles: reviews,

Table 5. Alternative bioloical materials. Extension to Supplementary Table 1 by Jurovski et al.[18] Hex is an abbreviation for hexosyl, Hex2 for dihexosyl

Biological samples		**Lipid classes**	**Reference(s)**
alternative biological materials (unconventional)	aqueous humor		**7**, 30
	Bile		80
	cerebrospinal fluid (CSF)		**7**
	colon derived suspension		112
	Milk	DG, TG, PC, SM	88
	tear drops		**7**
	cells and cell lines:		
	x exosomes	FA, GLs	**7**, 91, 105
	x liposomes	FA	121
	x alveolar cells	PC, PE(+PLs), PS, LPC, LPE, SM, Cer, HexCer	92
	x lipid droplets		87
	tissues:		
	x adipose tissue	Cer, SM	**15**
	x lung tissue	AcCa, FA, TG, PC(+PLS), PE(+PLs), PG, PI, PS, LPC, LPE, LPI, LPS, Cer, SLs	110, 113
	x renal tissue	FA, GLs, GPs, SLs, STs, PRs	104
	x myocardial tissue	FA, CL, DG, TG, PA, PC, PE, PG, PI, PS LPC, LPE, Cer, cholesterol	90, 96
	x brain tissue	Cer, SM, thromboxane, prostaglandins	**15**, 63, 64
	x liver tissue	DG, TG, PA, PC(+PLs), PE(+PLs), PG, PI, PS, LPA, LPC, LPE, LPG, LPI, LPS, Cer(+HexCer), SM, STs	**15**, 30, 63, 82, 92, 98
	x colonic tissue		112
	x tumor tissue	PC(+PLs), PE(+PLs), LPC, LPE, Hex2Cer, SM	55

bolded articles: reviews

The range of unconventional biological extracts and tissues was, as described by Jurovski et al.,[18]: very broad. Furthermore, *in vitro* biological cell culture analyses reached a high variation

of studies among themselves, which lead to include them separately in *Table 6*. Finally, even more exotic sample types hard to categorize were listed in *Table 7*. The multi-matrix approach was a pool of plasma, urine and faecal matter of the same patient.[63] Other details can be purchased from the references in *Tables 6* and *7*

Table 6. Cell culture matrices analyzed with UHPLC-MS techniques.
Hex is an abbreviation for hexosyl, Hex2 for dihexosyl

Biological samples		**Lipid classes**	**Reference(s)**
Cell cultures	HC1*	DG, CL, BMP, PE(+OxPE), PG, PS, LPE, PRs	117
	HCC827 (+HCC827-GR)		65
	HeLa	CL, DG, TG, PC, PE, PG, PI, PS, LPC, LPE, Cer(+HexCer), SM	46, 37
	Huh7	LPC, LPE	101
	HTC-116		65
	Huh7	LPC, LPE	101
	MDCK (+MDCK-GR)		65, 15
	OVCAR-3		65
	OxWR*	CL, DG, BMP, PE, PG, PS, LPE, PRs	117
	PANC-1	CE, DG, TG, PC, PE, PI, PS, LPC, Cer, SM	35
	PC-9 (+PC-9-GR)		65
	PC12	PC, PE, PI, PS	116
	RAW 264.7 (macrophages)**	GLs, PA, PC, PE, PG, PI, PS, LPLs, SPs, CEs, cholesterol	99, 66
	SKOV-3		65
	Bladder cancer cell		63
	Melanoma B16***	Cer, SM	15
	Primary CD4+T lymphocytes***	Cer, SM	15
	Yeast	PA, PC, PE, PG, PI, PS	52

*anaerobic, *oxalobacter formigenes* ; **widest lipid range ; ***mouse

Table 7. Special matrices analyzed with UHPLC-MS techniques

Biological samples		Lipid classes	Reference(s)
Botany (plants)	leaves, new shoots[A]	DG, TG, PC, PE, PG, PI, PS, CEs, SLs	95
	Berries[B]	TG, PC, STs	118
	bee pollen	DG, TG, LPC, Cer	99
Simple organism	C.Elegans	DG, TG, PC(+PLs), PE(+PLs), PS, LPC, LPE, Cer, SM	51, 92
	Earthworm	LPC, LPE, LPI, LPS	107
	larvae (*lysphlebia japonica)*	TG, PA, PC(+PLs), PE(+PLs), PG, PI, PS, LPC, LPE, PG, PI, SPs, SLs	109
Special matrix	multi-matrix analysis		63
	Buttermilk (foodstuff)	TG, PC, PE, PI, PS, LPC, LPE, SM	42

**Camellia sinensis L.* ; ***Sambucus nigra*

8.3 High resolution chromatographic techniques in lipidomics

Table 8 includes both the stationary and mobile phase properties used in analysis, including the gradient (e.g. curved gradient following an exponential or logarithmic function, stepped gradient, linear gradients etc.). More detailed column information was included separately in *Attachment 2*.

The methods within LC separation techniques (HPLC, UHPLC or nanoLC) differ in their different stationary (i.e. column packing, type and dimensions) and mobile phases (i.e. solvent(s), gradient, additives) used for analyte interaction optimization. Considering the column and solvent choices made by various researches, the most popular column (n=52) for comprehensive lipidomics were variations of C18, the most popular solvent combination (n=27) being variations of 60:40 ACN:H_2O and 90:10 IPA:ACN with the most typical additive combination (n=25) of 5-10 mM ammonium formiate (AmFo) and 0.1-0.05% of formic acid (FoA). Sometimes, only AmFo (n=6) or FoA (n=7) was used. Other used additives (n<6) included ammonium acetate (AmAc), acetic acid (AcA), ammonium hydroxide and ammonium carbonate.

In the time frame of 2017-05/2019, occasional polar BEH produced amide[80] and HILIC[46, 55] column method analyses were conducted along with C8[63, 95, 119] and phenyl[112] methods. The trend towards nonpolar stationary phases is probably due to the easy identification between lipid classes according to their retention time and head group product ions, after the lipids have been separated according to their nonpolar structure (but not vice versa). Other solvent combinations included water and MeOH, water:ACN and IPA:MeOH:ACN, water:ACN and ACN:acetone, and their dilutions with an extra proportion of water or ACN in either the polar A- or organic B-solvent.

Table 8. Stationary phase (column) and mobile phase (gradient, solvent+additive) information (detailed column and additive information in *Attachment 2*)

Precolumn	Gradient	Column	Solvent A (v/v ratios)	Solvent B (v/v ratios)	Solvent C	Additives	Year	Citation
yes	step-pit-step	T3 C18	1:1 MeOH:H_2O (pH 7.5) (PG;PS)	6:4 MeOH:ACN (GP;PS)		AmFo, FoA	2017	42
	exp curved	C18 GOLD	19:19:2 ACN:MeOH:H_2O	IPA		AmFo, FoA	2017	66
		T3 C18	3:4:3 ACN:acetone:IPA (DG;TG)	3:7 ACN:IPA (DG;TG)		AmOH	2017	42
	Curved	C18 BEH	40:60 ACN:H_2O	90:10 IPA:ACN		AmAc, AcA	2017	121
	Linear	N/A	40:60 ACN:H_2O	90:10 IPA:ACN		AmAc	2017	93
	s-curve	C18	50:50 ACN:H_2O	95:5 IPA:ACN		AmFo, FoA	2017	35
	reversed, log curved	C18 CSH	50:50 IPA:ACN	H_2O		AmFo, FoA	2017	97
	abrupt change + smooth s-curve	C18	60:40 MeOH/H_2O	60:40 MeOH:IPA		AmAc, AcA	2017	65
	Linear	C18	60:40 ACN:H_2O	90:10 IPA:ACN		AmAc	2017	99
	two-stepped	C18	60:40 ACN:H_2O	90:10 IPA:ACN		AmFo, FoA	2017	51
	3-stepped, inclined	C18 CSH	60:40 ACN:H_2O	90:10 IPA:ACN		-	2017	90
	4linear-3ramp	C18 CSH	60:40 ACN:H_2O	90:10 IPA:ACN		AmAc, FoA	2017	39
	Linear	C18 CSH	60:40 ACN:H_2O	90:10 IPA:ACN		AmAc	2017	99
	N/A	C18 CSH	60:40 ACN:H_2O	90:10 IPA:ACN		AmFo, FoA	2017	30
	Linear	C18 GOLD	60:40 ACN:H_2O	90:10 IPA:ACN		AmFo	2017	96
	Linear	C18 BEH	90:10 ACN:H_2O	90:80:1 IPA:ACN:H_2O		AmFo, FoA	2017	98
	log curved	C18 BEH*	90:10 H_2O:ACN	20:20:60 MeOH:ACN:IPA		AmFo, FoA	2017	91
	Linear	T3 C18	90:10 IPA:ACN	30:70 H_2O:ACN		AmFo	2017	82
	Linear	HILIC BEH	96:4 ACN:H_2O	H_2O		AmAc	2017	55
	Linear	C8 BEH	H_2O	2:5 IPA:ACN		AmFo, FoA	2017	92
	linear;isocratic	C18 BEH	H_2O	50:50 IPA:ACN		-	2017	121
	linear, isocratic	C18	H_2O	60:36:4 IPA:ACN:H_2O		AmFo	2017	62
	log curved	C8	H_2O	70:30 ACN:IPA		AmAc, FoA	2017	95
	log curved A->B->C	C18 BEH	H_2O	ACN	90:10 IPA:ACN	FoA	2017	94
	Linear	C18 T3	H_2O	ACN		FoA	2017	41
	s-curve, plateau	C18 BEH	H_2O	MeOH		AmAc	2017	45

Precolumn	Gradient	Column	Solvent A (v/v ratios)	Solvent B (v/v ratios)	Solvent C	Additives	Year	Citation
	N/A	C18 CSH	40:60 ACN:H_2O	90:10 IPA:ACN		AmFo, FoA	2018	110
	Isocratic	C18	45:55 ACN:H_2O			AcA	2018	64
	2-stepped, exp curved	C18 BEH	60:40 ACN:H_2O	81:10:9 IPA:ACN:H_2O		AmFo, FoA	2018	104
	3-stepped, inclined	C18 CSH	60:40 ACN:H_2O	90:10 ACN:IPA		AmFo, FoA	2018	79
	Linear	C18	60:40 ACN:H_2O	90:10 IPA:ACN		AmFo	2018	108
	three-stepped	C18	60:40 ACN:H_2O	90:10 IPA:ACN		AmAc	2018	107
yes	three-stepped	C18 CSH	60:40 ACN:H_2O	90:10 IPA:ACN		AmFo, FoA	2018	88
	Linear	C18 GOLD	60:40 ACN:H_2O	90:10 IPA:ACN		AmFo	2018	106
yes	exp curved, drop	C18*	60:40 ACN:H_2O	90:10 IPA:ACN		AmFo, FoA	2018	52
yes	s-curve, drop	C18*	60:40 ACN:H_2O	90:10 IPA:ACN		AmFo, FoA	2018	52
	Stepped	C8 BEH	60:40 ACN:H_2O	90:10 IPA:ACN		AmAc	2018	63
	Stepped	C8 BEH	60:40 ACN:H_2O	90:10 IPA:ACN		AmAc	2018	63
	Linear	C18 BEH	60:40 ACN:H_2O	90:10 IPA:ACN?		AmFo	2018	15
		C18 BEH	60:40 ACN:H_2O	90:8:2 IPA:ACN:H_2O		AmFo, FoA	2018	36
yes	log curved	C18 BEH*	90:10 H_2O:ACN	20:20:60 MeOH:ACN:IPA		AmFo, FoA	2018	100
yes	log curved	C18 BEH*	90:10 H_2O:ACN	20:20:60 MeOH:ACN:IPA		AmFo, FoA	2018	103
	3-stepped curve	C18 RRHD	H_2O	90:10 ACN:H_2O		AmAc, AcA	2018	28
	invert s-curve	C18	H_2O	ACN		FoA	2018	61
	curved A->B->C	C18 BEH	H_2O	ACN	90:10 IPA:ACN	FoA	2018	105
	exp curved	C18 BEH	H_2O	ACN		AcA	2018	101
	s-curve	C18 HSS	H_2O	ACN		FoA	2018	102
	N/A	Amide	H_2O	MeOH		AmHCO3	2018	80
	N/A	Amide	H_2O	MeOH		AmFo	2018	80
	N/A	C18 BEH	H_2O	MeOH		PFPA, FoA	2018	80
	N/A	C18 BEH	H_2O	MeOH		PFPA, FoA	2018	80
	Linear	C18 CSH	H_2O	MeOH		FoA	2018	111
	s-curve	C18 HSS	H_2O	MeOH		FoA	2018	79

Precolumn	Gradient	Column	Solvent A (v/v ratios)	Solvent B (v/v ratios)	Solvent C	Additives	Year	Citation
	log curved	C18 BEH*	10:90 H_2O:ACN	20:20:60 MeOH:ACN:IPA		AmFo, NH3	2019	38
	left-skewed pyramid	C18 CSH	40:60 ACN:H_2O	90:10 IPA:CAN		AmFo, FoA	2019	113
	Linear	C18	50:50 ACN:H_2O	20:80 IPA:MeOH		AmAc	2019	116
yes	N/A	C18 CSH	60:40 ACN:H_2O	90:10 ACN:H_2O		AmFo, FoA	2019	115
yes	s-curve	C18 CSH	60:40 ACN:H_2O	90:10 IPA:ACN		AmFo, FoA	2019	37
yes	s-curve	C18 BEH	60:40 ACN:H_2O	90:8:2 IPA:ACN:H_2O		AmFo, FoA	2019	117
	N/A (linear? A->B)	HILIC	90:10 ACN:acetone	70:30 ACN:H_2O		AmFo, FoA	2019	46
	N/A (linear? A->B)	HILIC	90:10 ACN:acetone	70:30 ACN:H_2O		AmFo, FoA	2019	46
yes	linear (j-curve)	C8	H_2O	55:40:5 ACN:IPA:H_2O		AmAc	2019	119
	s-curve	C18	H_2O	75:25 IPA:ACN		AmFo	2019	118
	s-curve	C18	H_2O	75:25 IPA:ACN		AmAc	2019	118
	Linear	C18	H_2O	MeOH		AmAc, FoA	2019	114
	Linear	C18	H_2O	MeOH		AmAc, FoA	2019	114
yes	s-curve	Phenyl	H_2O	MeOH		AmAc	2019	112
	Linear	C18 BEH	MeOH	2:5 ACN:IPA		AmAc, FoA	2019	89

*nano-LC

BEH: ethylene bridged hybrid, **CSH**: charged surface hybrid, **HSS:** high strength silica**,**

Exp: exponentially (curved gradient), **log**: logarithmically (curved gradient)

However, because of the wide range of similar methods, *Table 9* includes an averaged value on all for the RT, flow rate, column compartment temperature and particle size. *Attachment 4* gives more detailed information on the individual methods (both UHPLC/MS and nanoLC). In 2018, an outlier runtime of 110 minutes was excluded from the average.[52]

Table 9. Average experimental conditions. For explicit details to the UHPLC-MS settings, see *Attachment 4*.

	t (min)		Flow (ml/min)		T[column] (˚C)		Ø (um)	
Parameter	**Average**	**SD**	**Average2**	**SD2**	**Average3**	**SD3**	**Average4**	**SD4**
2017 (n=25)	22	8.9	0.3	0.09	42	12.3	1.8	0.3
2018 (n=26+1) *	21	6.8	0.4	0.12	49	12.1	2.0	0.4
2019 (n=14)	18	8.3	0.5	0.22	44	12.3	2.0	0.5
TOTAL	**22**	**14**	**0.38**	**0.13**	**48**	**11**	**1.9**	**0.4**

Ø: particle size of the column packing that is used**, *:** +1 is an outlier excluded from the calculation

The usage of pre-columns in UHPLC has increased within the time frame as majority of the total 10 articles[37, 42, 52, 88, 100, 103, 112, 115, 117, 119] are centered around 2019,[37, 112, 115, 117, 119] though overall pre-columns were still neglected by the majority of the UHPLC studies. Indeed, it could be speculated that researches in the lipidomics field preferred reproducibility (i.e. most studies are without a pre-column), lower backpressure and/or smaller risk of increased void volume over column safety and matrix filtering.

Nano-LC is the rather new practice of using packed capillary columns with conventional column packing material. All experimenters (Lee[100], Yang[91], Danne-Rasche[52] and Kim[103]) created a capillary column by unpacking a commercial column and repacking it into a nano- or narrowbore capillary. *Table 10* includes analysis parameters for used in nanoLC-studies: the mass analyzer, runtime *t*, flow rate, column compartment temperature *T[column]* and particle size Ø.

Table 10. Experimental conditions for nanoLC experiments.

Mass analyser (nanoLC)	t (min)	Flow (µl/min)	T[column] (˚C)	Ø (um)	Year	Citation
LTQ Velos ion trap, Velos TSQ vantage QqQ	46	0.35	-	1.7	2017	100
LTQ Velos ion trap, Velos TSQ vantage QqQ	51	0.30	-	1.7	2018	91
LTQ Velos ion trap, Velos TSQ vantage QqQ	49	0.30	-	1.7	2018	103
LTQ Velos ion trap, Velos TSQ vantage QqQ	40	0.30	-	1.7	2018	103
LTQ Velos ion trap, Velos TSQ vantage QqQ	54	0.30	-	1.7	2019	38

Ø: particle size of the column packing that is used

In contrast to a faster UHPLC separation compared to HPLC, the "loading time" preceeding the sample elution is extended due to the low flow rate in the µl/min range.[38] Recalling the yeast lipidome analysis by Danne-Rasche,[52] nano-LC showed to have even more capacity for analyte identification than UHPLC, with both an extremely broad identification range and a sensitivity in the low fmol scale. The study compared the sensitivities of HPLC- and nanoLC diameter columns, reaching the low fmol range with almost every GL, GP, SP and their lipid derivatives they analyzed in positive mode (*Figure 10*). For example, the calibration curve for PE 17:0/14:1 demonstrates a linear relationship for up to 10 fmol in positive and <1 fmol in negative mode. By contrast, positive mode HPLC reached for the same analyte around 100 fmol in positive and 10 fmol in negative mode. The exact lipid species are found in detail from the original source.[52] Similarly, Kim et al.[103] achieved a LOD-range from 59 fmol (LPC(17:0)) to 507 fmol (LPG(14:0)).

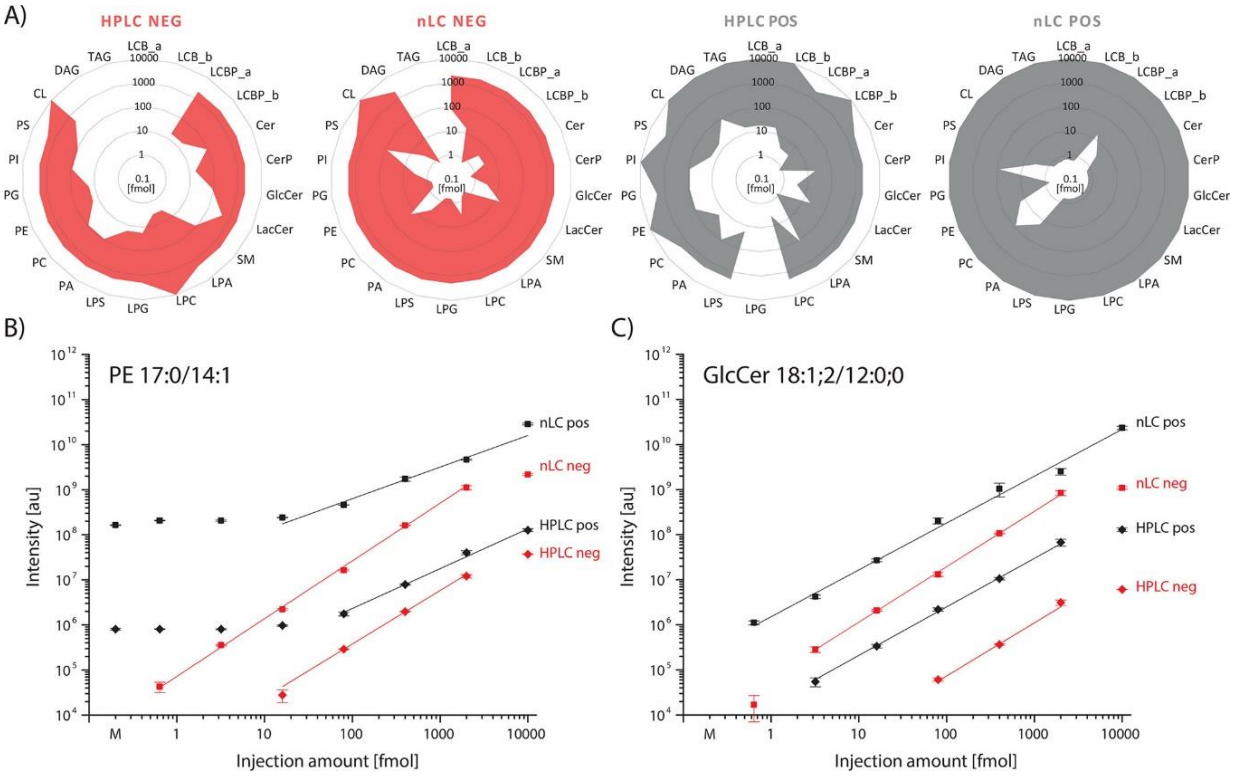

Figure 10. A) Sensitivity comparison of HPLC and nanoLC modes with ray diagrams, furthermore, demonstrations of calibration curves for **B)** PE(17:0/14:1) and **C)** GlcCer(18:1;2/12:0;0). **CerP**: ceramide 1-phosphate, **GlcCer**: glukosylceramide, **LacCer**: lactosylceramide, **LCB**: long-chained sphingoid base, **LCBP**: long-chained sphingoid base 1-phosphate. Reprinted with permission from **Ref 52**, **© 2018 American Chemical Society**

An accurate mass is an exact mass with instrument resolution high enough to be determined 2 µg/ml level or lower. *Table 11* includes a variety of instrument approaches, their chosen mass accuracies and reported resolution. Indeed, the emergence of the Q-Orbitrap and NSI has increased the resolution capabilities extremely (>35 000 /m) for lipidomic studies. The emphasis on mass accuracy or resolution is usually chosen depending on whether identification or quantitation is preferred. Also, when looking at analytes of low concentration, higher mass accuracy is often preferred in exchange for lower resolution to increase sensitivity. Usually, some sensitivity is sacrificed for the sake of improved comprehensive identification, which in turn is usually compensated by increased injection volume and a bigger analyte mass window for more features.[52] QTOF experiments have typically a mass accuracy of less than 3-30 µg/ml, whereas Orbitrap-experiments had a range of 0.01-15 µg/ml.

A slight trend of multiple studies on bigger lipid structures (e.g. cell cultures, exosomes,[91, 105] lipid droplets[87] and liposomes[121]) can be observed. This can be partly explained with the newly trending asymmetric flow field flow fractionation (AF4)[91, 100, 103] instruments with their ability to rather precisely separate biomolecules by mass into smaller fractions before primary analysis.

Table 11 shows the LC- (e.g. UHPLC, nanoLC), ionization (e.g. APCI, ESI or heated ESI [HESI]) and supporting approaches (e.g. AF4) with the mass spectrometer that was used, not to mention the reported mass accuracy/isolation window and resolution. Discussed in *chapter 8.5*, the new MS/MS method, sequential window acquisition of all theoretical fragment ion mass spectra (SWATH), has emerged lately.[37, 61, 119]

In UHPLC-MS lipidomics, the concept of using a pooled QC sample between analysis runs has been standardized in the ranks of lipidome researchers: in the years 2017 (11/25), 2018 (14/22) and 2019 (8/10) published papers showed a trend of increased pooled sample usage (even in qualitative analysis). The QC-sample is used to control possible instrument fluctuation and works as a reference point to each individual sample aliquot and their matrix effects.

Table 11. Mass accuracies and instrument resolutions for various lipidomic approaches. *K*=**1000*

Approach	Mass accuracy (ppm)	Resolution	Citation
UHPLC-QTOF-MS/MS	≤10		79
AF4, nanoLC-ESI-MS/MS	≤3		100
AF4, nanoLC-ESI-MS/MS	≤3		91
AF4, nanoLC-ESI-MS/MS	≤3		103
nanoLC-NSI-QTOF	≤3	70K	52
nanoLC-NSI-QTOF-MS/MS	≤3	17.5K	52
UHPLC-ESI/APCI-QTOF		20K	61
UHPLC-ESI/APCI-QTOF-MS/MS (SWATH)		15K	61
UHPLC-ESI-IMS-QTOF-MS/MS	≤0.01		55
UHPLC-ESI-LTQ-Orbitrap	≤0.01	20K	111
UHPLC-ESI-LTQ-Orbitrap-MS/MS	≤0.01	18K	111
UHPLC-ESI-MS/MS	≤6		28
UHPLC-ESI-Orbitrap	≤10	10K	95
UHPLC-ESI-QOrbitrap	≤1	70K	117
UHPLC-ESI-QOrbitrap-MS/MS	≤3, ≤10	LPL(>110K), GP(>90K), TG(>80K), CL(>70K)	92
UHPLC-ESI-QOrbitrap-MS/MS	<1		115
UHPLC-ESI-Qorbitrap-MS/MS	≤1	35K	117
UHPLC-ESI-QOrbitrap-MS/MS	≤2.5	35K	98
UHPLC-ESI-QOrbitrap-MS/MS	≤5	100K	93
UHPLC-ESI-QTOF	≤3	12K	15
UHPLC-ESI-QTOF-MS/MS	≤10		51
UHPLC-ESI-QTOF-MS/MS	<5		107
UHPLC-ESI-QTOF-MS/MS	≤5		82
UHPLC-ESI-QTOF-MS/MS	≤10	35K	30
UHPLC-ESI-QTOF-MS/MS	≤15		89
UHPLC-ESI-QTOF-MS/MS	≤8		118
UHPLC-ESI-QTOF-MS/MS	≤30		108
UHPLC-ESI-QTOF-MS/MS	≤30		109
UHPLC-ESI-QTOF-MS/MS (SWATH)	≤2	>15K	119
UHPLC-ESI-QTOF-MS/MS?	≤10		41
UHPLC-HESI-LTQ-Orbitrap-MS/MS	≤10	60K	121
UHPLC-HESI-Orbitrap	≤3		45
UHPLC-HESI-QOrbitrap	≤6		112
UHPLC-HESI-QOrbitrap	≤6	140K	102
UHPLC-HESI-QOrbitrap	≤10		110
UHPLC-HESI-QOrbitrap	≤5	70K	99
UHPLC-HESI-QOrbitrap-MS/MS	≤10	35K	80
UHPLC-HESI-QOrbitrap-MS/MS	≤5	60K	113
UHPLC-HESI-QOrbitrap-MS/MS	≤0.35		36
UHPLC-HESI-QOrbitrap-MS/MS	≤5	15K	99
UHPLC-HESI-QOrbitrap-MS/MS	≤5		35
UHPLC-Zspray-IMS-QTOF	≤10	25K	39

8.4 Overview on research topics

Research articles could be roughly divided into four topics: (1) method development of analytical methods and techniques, (2) physiological or metabolomic profiling of organism's lipids or their output via specific lipid group analysis, (3) disease profiling of living organisms, their expressed biomarkers or tumor tissue as is often the case in cancer research, (4) and product analysis (e.g. nano-tailored liposome drugs). In *Figure 11,* a quick analysis on the major categories was done to compare the ratio of publication in each category. Biomarker analysis of diseases is a subcategory of metabolic profiling. UHPLC-MS has established itself as a method specialized in lipid metabolome research.

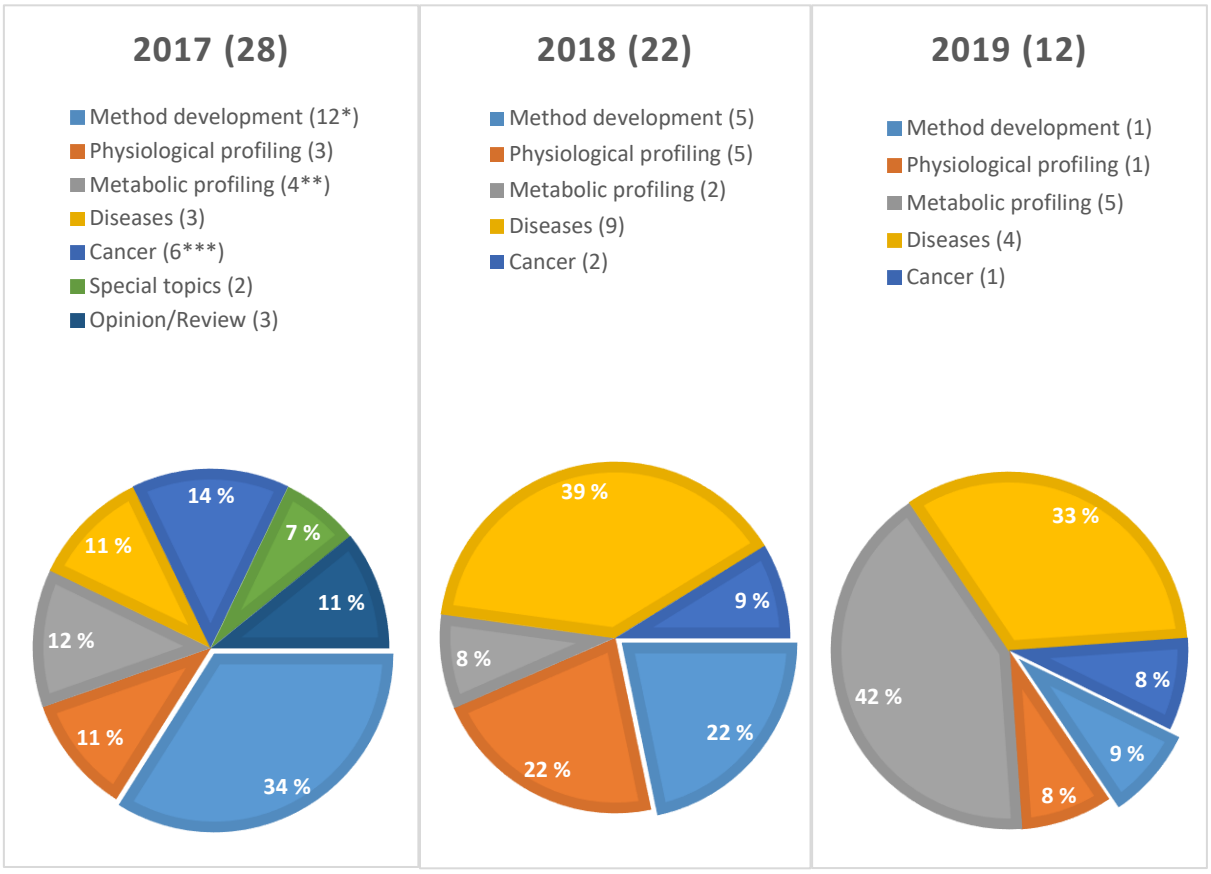

Figure 11. Research topics with UHPLC-MS techniques between 2017-05/2019.
Out of these 63 articles, 7.94% (5 articles) were nanoLC, and 1.59% (1 article) included a SFC study. *5, **4 and ***1 article(s) had another distinct topic alongside them.
(number of articles per topic in parentheses).

Like Taylor et al.[69] observed, environmental analysis was still scarce in lipidomic research. This is backed up by the fact that, according to the article search of my review, only Ribeiro et al.[41] concluded an environmental UHPLC-study between 2017-05/2019, namely a lipidomic analysis of tap and mineral water.[41]

In *Table 12,* all lipid groups discussed in the articles are displayed. Also, sub-groups, the totality of identified lipids, and biomarker lipids were included. In total, a range of 5-700 total lipids and 5-87 proposed biomarkers were discussed in the articles. Typical GLs in articles included DGs and TGs, with MGs or BMP.[117]

Lipid groups not discussed in this study can be found in *Attachment 5*. In addition to extensive fatty acyl research in physiological profiling,[28, 45, 64, 99] lipido-metabolomic[46, 79, 117] and disease biomarker studies [7, 89, 104, 105, 110, 111, 119] (including BMPs and CLs) CEs were frequently found in both method development[35, 37, 55, 62, 63] and cancer research.[35, 55, 91, 108]

Table 12. Common lipids according to research topic and identification approach. If "Identified lipids" are indicated as a sum without any explanation, it means that the first number is the amount of lipids found in positive and the second in negative mode (positive+negative).

Citation	Theme	T/relT/UT	GLs	GPs	PLs	Ox	LPLs	SPs	Hex	Identified lipids	Bio-markers
88	Method development	UT	2	1				1		429	
51	Method development	relT	1	4				1			
92	Method development	UT	2	3	1		2	1	1		
92	Method development	UT	2	4	2		2	2			
92	Method development	UT		3	1		2	2	1		
52	Method development	UT		6	6					436	
30	Method development	T/UT	2	6			5	2		207	
37	Method development	UT	2	4			2	*		292+206	
36	Method development	T	1	4			2	1		22	
63	Method development	PT	2	2	2		2	2	2	515+630+640 [D]	
62	Method development	UT	2	3			1	2		104	
121	Method development	UT								403	
35	Method development / cancer research	UT	2	4			2	2		226-414	
98	Method development / Metabolomics	UT	*	*						83	8
55	Method development / cancer research	T/UT	3	5			3	2	1	132	
91	Cancer research	UT	2	1	1			2	1	286	34
82	Cancer research	UT	2	2							50
108	Cancer research	T/UT	3	5	3			3	2	493	14+10+2 [B]

Citation	Theme	T/relT/UT	GLs	GPs	PLs	Ox	LPLs	SPs	Hex	Identified lipids	Bio-markers
101	Diseases and Biomarkers	UT					2			24	
114	Diseases and Biomarkers	UT		4			2	1		129	
106	Diseases and Biomarkers	UT	3	6			3	3		749	16
90	Diseases and Biomarkers	UT	1	2						12	9
104	Diseases and Biomarkers	UT	*	*				*		179	
104	Diseases and Biomarkers		*	*				*		196	
96	Diseases and Biomarkers	UT	1	2			1	1		746	11
96	Diseases and Biomarkers		2	2			1	1			
97	Diseases and Biomarkers	UT	3	5				4		261+39	7
100	Diseases and Biomarkers	UT	1	2	1		2	2		365	19
103	Diseases and Biomarkers	UT	2	2	1		2	2	3	363	28
105	Diseases and Biomarkers	UT	1	1						Features	Features
7	Diseases and Biomarkers		2	4				1			>25
89	Diseases and Biomarkers	relT/T								81 [A]	17 [A]
113	Diseases and Biomarkers	UT									77
119	Diseases and Biomarkers	UT	2	5			3	2			77
110	Diseases and Biomarkers	UT	1	5	2		3	1		188+62	87
111	Diseases and Biomarkers		2	1			1	1			
39	Drug-testing	UT	1	1			1	1		155	
42	Foodstuff profiling	T	1	4			2	1		81	
79	Metabolomics	UT	1	5			1	*		61	
107	Metabolomics	UT					4				
115	Metabolomics	UT	2	4			*				
95	Metabolomics	UT	2	5				1		178	
117	Metabolomics	UT	1	4	1	1	1			97	
117	Metabolomics		1	3	1		1				
120	Metabolomics	UT	1	2			2	1		226	
46	Metabolomics	UT		5				1		249+451	
118	Metabolomics	UT	1	1						7	
116	Metabolomics	T		4						22	5
66	Metabolomics	UT	3	6			6	7		523	
45	Physiological profiling	T/UT		*				*		Features	
28	Physiological profiling	T									
15	Physiological profiling	T						2		45	
109	Physiological profiling	UT	1	6	2		2	2		283	
61	Physiological profiling	UT								12	
64	Physiological profiling	T								5	
99	Physiological profiling	UT			1			1		184+150	
93	Physiological profiling	UT	2	1							35

*: Lipid subgroups could not be determined

T/relT/UT: targeted/relatively targeted/untargeted

[A] for hyperlipidemia: plasma(74, 57 biomarkers), VLDL(74, 52 biomarkers), LDL(76, 42 biomarkers), HDL(73, 41 biomarkers)

[B] non-small cell lung cancer+lung benign disease+healthy controls

[C] metabolites

[D] in plasma+tissue+cell

Moving on, *Table 13* sums up the lipid group ratios within all 58 articles that mentioned the lipid groups they were investigating. GPs constituted the majority of lipids studied (86%), mentioning basic GPs at 46, LPLs at 29 and PLs at 12 occasions. Next come the GLs with 42 articles (72%) and SPs with 39 articles (67%), out of which 7 reports with SPs (mostly for method development) included various hexosyl ceramides ("Hex").

When the research topics are concerned, a slight majority of the articles in the dataset were disease biomarker studies (33%). No substantial amount of variation could be observed in the average (between 1-5) or standard deviation of lipid groups discussed in one paper per topic. However, the range of how many of the eight lipid classes were discussed did differ: disease biomarker studies had the broadest range for having biomarkers searched from 1-7 lipid classes. Conversely, cancer research had the most focused range by analysing lipids from 2-4 groups per paper.

Table 13. Percentages of lipid groups discussed in all articles (**Article%=N/N_{TOTAL}, N_{TOTAL}**=58). Also, the average (**AVE**), standard deviation (**SD**) and **Range** of lipid groups in each category.

FAcyls	GL	GP	SP	CE	SL	ST	PR	PK	Lipoprotein
33 %	**72 %**	**86 %**	**67 %**	**19 %**	**16 %**	**14 %**	**9 %**	**2 %**	**2 %**

	N	Article%	AVE (group)	SD (group)	Range
Method development	13	**26 %**	3.2	1.1	1-5
Cancer	5	**9 %**	3.6	0.8	2-4
Diseases	16	**28%**	3.4	1.5	1-7
Metabolism	13	**22 %**	3.3	1.1	1-4
Physiology	9	**16 %**	2.4	1.6	1-6

The next five chapters include analyses on each five themes of research: comparison or introduction to new applications and methods, physiological profiling of biological and synthetic materials, analyses on metabolic pathways, lipidomic characterization of diseases and their biomarkers and studies on cancer in a lipidomic context.

8.4.1 Method development

The wide range of articles introducing a new or improved lipidomic UHPLC/MS or nanoLC/MS method (*Table 14*) can be further categorized into sub-groups based on different phases of an analytical method. Though many of these studies concentrate on either sample preparation,[30, 35-37] development of the chromatography[52, 92, 99, 102, 121] or MS(/MS)[55, 62, 65, 102] approaches, occasional computational methods for the improvement of measurement performance[98] and data analysis[51, 73, 88] appear every now and then.

Xuan et al.[63] conducted a multimatrix analysis in negative and positive ESI-mode. Three conventional biological materials (plasma, tissue and cells) of the same patient were pooled to increase repeatability and lipid coverage. Apparently, this improved the identification of diabetes patients via biomarkers.

Table 14. New analytic method development ("Method Dev.") and application enhancements in lipidomics (18 articles)

Year	Citation	Theme	Subtheme
2017	51	Method Dev.	Improvement to in-silico fragmentation prediction
2017	92	Method Dev.	Ultrahigh preformance chromatography lipidomics
2017	30	Method Dev.	Super absorbent polymer extraction chip testing
2017	86	Method Dev.	Single-cell resolution, PDMS microfluid droplet chip Raman method
2017	73	Method Dev.	LipidMatch comparison to other software
2017	62	Method Dev.	Method development, low resolution MS identification
2017	121	Method Dev.	*in vitro* method, excessive adipocyte lipolysis
2017	55	Method Dev. / Cancer research	Comparison of LC/MS, SCF/MS and DIMS, kidney cancer patient analysis
2017	99	Method Dev. / Cancer research	Bee pollen analysis, method validation
2017	35	Method Dev. / Cancer research	Lipid extraction comparison with pancreatic cancer cell line
2017	65	Method Dev. / Cancer research	Quantitative analysis PIS 184 optimization for PC and SM, cancer cell lines
2017	98	Method Dev. / Metabolomics	Data processing improvements, nonalcoholic fatty liver disease analysis
2018	88	Method Dev.	Machine learning algorithms for CCS values
2018	52	Method Dev.	Reproducible nano-LC NSI method
2018	102	Method Dev.	Multi-matrix platform validation
2018	36	Method Dev.	Optimization of established extraction techniques
2018	63	Method Dev.	Multimatrix method development, a mixture of untargeted/targeted
2019	37	Method Dev.	Extraction comparison ("IPA-75", "IPA-90" vs. B&D), MS-DIAL, SWATH

8.4.2 Physiological profiling

Determining an organism's lipidome may both act as a fingerprint to the species in question, a distribution of traits in a population as well as a baseline or reference for possible changes of the organism's state. All articles concerning this type of research were listed in *Table 15*.

As an example, Meulebroek et al.[45] developed a method which may cover all eight lipid classes via faecal matter, using a polarity-switching UHPLC-interfaced Orbitrap. With this, healthy controls and type 2 diabetes patients were monitored, their lipidomic profiles compared with each other.[45]

Instead of trying to analyze as many lipids as possible, Manni et al.[15] focused selectively on multiple tissue's and cell culture's 12 Cer:s and 31 SMs in positive mode. Tissue types in this targeted approach included adipose tissue (human, rat), liver (dog, human, rat, mouse), brain (rat, mouse) and serum (human, rat, mouse)[15] For more exotic lipid classes, Drotleff et al.[61] identified and quantified ST hormones from plasma, and, similarly, Gobo et al.[64] cerebral prostaglandins from brain tissue.

Table 15. Research on physiological profiling (9 articles)

Year	Citation	Theme	Subject
2017	45	Physiological profiling	Human gut phenotype profiling
2017	42	Physiological profiling	Buttermilk profiling
2017	93	Physiological profiling	Distinguishing between canine breeds
2018	28	Physiological profiling	Oxylipin analysis in human patients
2018	15	Physiological profiling	SM and Cer in multiple tissues/cell cultures of humans, dogs, mice and rats
2018	109	Physiological profiling	Larvae profiling (*Lysphlebia japonica*)
2018	61	Physiological profiling	Steroid hormone quantification in human plasma
2018	64	Physiological profiling	*In vivo* prostaglandin identification and quantitation in human brain tissue
2019	87	Physiological profiling	Coherent Raman scattering (CRS), non-destructive lipid/metabolite profiling

8.4.3 Metabolic lipid profiling and pathway analysis

Metabolic lipidomix included a discrete comparison of two different diets or other similar analyses between controlled base and altered states of an organism's lipidome (*Table 16*). Though like physiological profiling, metabolic lipid profiling takes the analysis a step further by investigating not only the lipid compounds but also the dependence/correlation between lipid species.

Equilibria between lipids in a lipidome may give insight to an organism's metabolism either in a system or between systems under certain conditions. For instance, Cheema et al.[94] studied rhesus monkeys' (*Macaca Mulatta*) metabolomic response to a potential radiation countermeasure agent: gamma-tocotrienol (GT3).[94] GT3-dysregulated biomarker lipids in serum after radiation included stearic acid, PC(20:5/20:5), PI(20:4) and PS(16:0/21:0). Moreover, antioxidants and anti-inflammatory metabolites, including docosahexaenoic acid (DHA, i.e. FA(22:6)), showed an increase in the nonhuman primates within 1-3 days. Thus, Cheema et al.[94] argues GT3 to be a potential anti-radiation agent when taken 24 hours prior to radiation exposure.

As another example, Zalloua et al.[115] noted a correlation between serum SMs and plasma cholesterol (i.e. LDL, HDL and total cholesterol). 34 metabolite features (m/z 750-810, associated with SMs) expressed a strong correlation to cholesterols.

Table 16. Metabolomics research topics (11 articles)

Year	Citation	Theme	Subject
2017	98	Applications / Metabolomics	Nonalcoholic fatty liver disease profiling, improved data-analysis
2017	94	Metabolomics	Radiation countermeasure mechanism, GT3 inhibitor test
2017	95	Metabolomics	Fertilization of plants
2017	66	Metabolomics	Inflammatory macrophage characterization
2018	79	Metabolomics	Ketogenic diet, consequent metabolic perturbations, odd carbon lipids
2018	107	Metabolomics	Bioaccumulation & metabolomic response to chiral PCB 91
2019	115	Metabolomics	Correlation between serum SMs and plasma cholesterol
2019	117	Metabolomics	Oxalobacter profiling for oxalate-based disease research
2019	46	Metabolomics	High-throughput 96-well cell culture assay
2019	118	Metabolomics	Elevated CO2 concentration, leaves & berries of the black elder plant
2019	116	Metabolomics	Metabolism changes upon PCB153/PC12 exposure

8.4.4 Diseases and biomarker analysis

Hyötyläinen and Orešič[122] describe a model for the development of a complex disorder in an organism: an accumulation of environmental triggers (e.g. changes in one's lifestyle or exposure to a stressor) lead the organism to initiate allostatic adaptation, i.e. the organism's countermeasure to maintain homeostasis. When triggers concerning a specific lipidomic pathway achieve an extended time to stress the organism, an allostatic load will accumulate (early phase of a clinical condition) until the organism either recovers from the load or fails in the process. Upon failure, a breakdown of the allostatic adaptation can be observed as an over- or decompensation of the metabolic pathway biomarkers; a time/concentration threshold essential for clinical diagnostics.[122] Biomarkers studied between 2017-05/2019 and in the fashion of this disease model were listed in *Table 17*.

Table 17. UHPLC-research (16 Articles) on lipidomic pathway-based diseases and potential biomarkers

Year	Citation	Theme	Subject
2017	90	Diseases and Biomarkers	**Diabetic cardiomyopathy**
2017	96	Diseases and Biomarkers	**Lethal ventricular tachyarrhytmia** induced by **myocardial ion channel diseases** & **infarction**
2017	97	Diseases and Biomarkers	**Atheroslerotic dyslipidemia** via a high-fat diet on mice
2018	101	Diseases and Biomarkers	*In vitro* **Coronavirus-infection** of cell cultures
2018	80	Diseases and Biomarkers	**Primary sclerosing cholangitis**
2018	106	Diseases and Biomarkers	**Lethal ventricular tachyarrhytmia** induced by **myocardial ion channel diseases**
2018	104	Diseases and Biomarkers	Glyoxylate-induced **nephrolithiasis**
2018	100	Diseases and Biomarkers	**Acute coronary syndrome**
2018	103	Diseases and Biomarkers	**Alzheimer's disease** and amnestic **mild cognitive impairment**
2018	105	Diseases and Biomarkers	Plasma derived exosomal biomarkers, **radiation exposure**
2018	110	Diseases and Biomarkers	Dysregulation in **respiratory syncytial virus pneumonia** (mouse)
2018	111	Diseases and Biomarkers	Regulation of rosuvastatin in **lipidemia** patients
2019	114	Diseases and Biomarkers	**Obesity** biomarkers (rhesus monkey)
2019	89	Diseases and Biomarkers	VLDL, LDL and HDL CEs during **lipidemia** (golden hamster), unsaturation correlation with logarithmic mathematical model
2019	113	Diseases and Biomarkers	GL-induced **acute lung injury** (lipopolysaccharides, mouse)
2019	119	Diseases and Biomarkers	Blood platelets in **coronary artery disease**

8.4.5 Cancer lipidomics

As a subclass for metabolic lipid profiling, lipidomic cancer research pursues a better understanding of the unknown pathways, mechanisms and pathological characteristics (e.g. metastasis) of different cancer types. It encompasses both *in vitro* cancer cell line research and *in vivo* animal/clinical experiments concerning cancer lipidomics. Lee et al.[38] studied 5 different cancer types in human patients (n=84) and profiled their plasma-lipidomic changes in contrast to a control group (n=20). A total of 50 biomarkers were found among the typical set of DGs, TGs, GPs and SPs. In greater detail, an over two-fold change (typically a decrease) with a significance of 95% or 99% was found for 32 biomarkers for liver, 16 for gastric, 25 for lung, 23 for colorectal and 14 for thyroid cancer.[38]

Articles on lipidomic cancer research were listed in *Table 18*. As another example, Li et al.[99] proposed bee pollen to have anti-inflammatory properties suitable for the soothing of cancer patient's inflammation of tumors. As observed, bee pollen inhibits nitrous monoxide (NO) production and restrains several messenger-ribonucleic acids (mRNAs) associated with inflammatory response proteins (cytokines) in LPS-stimulated RAW 264.7 cancer cells. Furthermore, bee pollen has an abundance of phospholipids, unsaturated FAs, and cytokine inhibition properties as fish oil. This suggests bee pollen to have similar benefits, though it would be cheaper to produce.[99]

Table 18. Lipidomic UHPLC-research (9 articles) focusing on cancer

Year	Citation	Theme	Subject
2017	55	Applications / Cancer research	Kidney cancer, human patients; Comparison of LC/MS;SCF/MS;DIMS
2017	99	Applications / Cancer research	Bee pollen anti-inflammatory properties on cancer cells
2017	35	Applications / Cancer research	Lipid extraction comparison with pancreatic cancer cell line
2017	65	Applications / Cancer research	Cancer cell lines, Quantitative analysis, PC/SM PIS-184 optimization
2017	91	Cancer research	Urinary exosomes in prostate cancer patients
2017	82	Cancer research	Hepatocellular carcinoma in cancer patients
2018	38	Cancer research	Review comparing plasmalipid profiles of liver, lung, gastric, colorectal and thyroid cancer, nanoflow UHPLC
2018	108	Cancer research	Non-small cell lung cancer serum biomarker identification
2019	112	Cancer research	Colorectal cancer, Validation of colon cell/tissue analysis

8.5 Tandem mass spectrometry

All tandem mass spectrometric information was listed in *Table 19*. At rare occasions, a DDA method was noted as a "Top10 ddMS2" analysis[52, 70, 113, 36] instead as a conventional product ion scan, PIS, or SRM. Also, MRM analyses were plenty. Interestingly, parallel reaction monitoring (PRM) constitutes a new type of tandem MS for the popular DDA and MRM methods that have been used for decades.[52, 70, 61] Since high resolution mass spectrometers combined with high computing capacity enable high processing and acquisition capacity of data, PRM aims to measure all fragments of the pre-defined ions instead than a mere subset, as in MRM. Consequently, PRM techniques enhance the selectivity of metabolic or lipidomic identification.[70]

MS^E- or all ions scans constituted a majority of the DIA methods. As such, only SWATH was reported as an alternative to this DIA method in the dataset, though other DIA methods exist (e.g. autoMSMS). SWATH operates on a defined mass range by consequtively fragmenting all precursors in a given time frame. Compared to DDA methods, it has a better detection rate, broader analyte range and higher specifity.[119]

Table 19. MS and MS/MS chromatographic methods

Approach	ESI mode	MS/MS?	Tandem mode	Year	Citation
UHPLC-ESI-IMS-QTOF	Positive	No	-	2018	88
UHPLC-ESI-QTOF-MS/MS	positive, negative	Yes	PIS?	2017	51
UHPLC-ESI-QOrbitrap-MS/MS	positive, negative	Yes	MSE	2017	92
nLC-NSI-QTOF-MS/MS	positive, negative	Yes	Top10 ddMS2, PRM	2018	52
UHPLC-HESI-Orbitrap	polarity switching	No	-	2017	45
UHPLC-ESI-MS/MS	Negative	Yes	enh. product ion scan, MRM	2018	28
UHPLC-ESI-QTOF-MS/MS	positive, negative	yes	MSE, PRM	2017	42
UHPLC-ESI-QTOF-MS/MS	positive, negative	Yes	MSE	2017	94
UHPLC-QTOF-MS/MS	positive, negative	Yes	PIS?	2018	79
UHPLC-ESI-QTOF-MS/MS	positive, negative	Yes	PIS?	2018	107
UHPLC-ESI-QOrbitrap-MS/MS	positive, negative	Yes	MSE	2019	115
UHPLC-Zspray-IMS-QTOF	positive, negative	No	-	2017	39
UHPLC-QTOF-MS/MS	positive, negative	yes	PIS	2018	101
UHPLC-ESI-QTOF-MS/MS	positive, negative	yes	MRM (GPs), product ion mode (FAs)	2019	114
UHPLC-HESI-QOrbitrap-MS/MS	positive, negative	yes	MRM	2018	80
UHPLC-ESI-QOrbitrap	positive, negative	No	-	2018	106
UHPLC-ESI-QTOF	Positive	No	-	2017	90
nLC-NSI-QTOF-MS/MS	Positive, negative	yes	SRM	2019	38
UHPLC-ESI-MS/MS-TOF	positive, negative	yes	product ion scan	2018	104
UHPLC-ESI-QOrbitrap	positive, negative	no	-	2017	96

Approach	ESI mode	MS/MS?	Tandem mode	Year	Citation
UHPLC-ESI-QTOF-MS/MS	positive, negative	yes	MSE	2017	97
AF4, nLC-ESI-MS/MS	polarity switching	yes	SRM	2018	100
AF4, nLC-ESI-MS/MS	positive, negative	yes	SRM, PIS	2017	91
AF4, nLC-ESI-MS/MS	positive, negative	yes	SRM	2018	103
UHPLC-HESI-QOrbitrap	Polarity switching	no	-	2019	112
UHPLC-ESI-QTOF-MS/MS	positive, negative	yes	MSE	2017	82
UHPLC-ESI-Orbitrap	positive, negative	no	-	2017	95
UHPLC-ESI-QTOF-MS/MS	positive, negative	yes	MSE	2018	105
UHPLC-ESI-QOrbitrap-MS/MS	positive, negative	yes	N/A	2019	117
UHPLC-HESI-QOrbitrap	polarity switching	no	-	2018	102
UHPLC-ESI-QTOF-MSMS	positive, negative	yes	MSE	2017	30
nLC-ESI-MS/MS	positive, negative	yes	SRM	2019	87
UHPLC-APCI-QLIT-MS/MS or	Positive	no		2019	46
UHPLC-HESI-OrbiFusion-MS/MS	Negative	no		2019	46
UHPLC-ESI-QTOF-MS/MS	Positive	yes	dMRM, PIS	2019	89
UHPLC-ESI-QTOF-MS/MS	positive, negative	yes	MSE	2019	118
UHPLC-ESI-QTOF-MS/MS	positive, negative	yes	MSE	2018	108
UHPLC-ESI-Qtrap-MS/MS	positive, negative	yes	MRM	2019	116
UHPLC-ESI-QTOF	Positive	no?		2018	15
UHPLC-ESI-QTOF-MS/MS	positive, negative	yes	SWATH	2019	37
UHPLC-HESI-QOrbitrap-MS/MS	positive, negative	yes	Top10-ddMS2	2019	113
UHPLC-ESI-QTOF-MS/MS	positive, negative	yes	PIS	2018	109
UHPLC-ESI-QTOF-MS/MS	positive, negative	yes	SWATH	2019	119
UHPLC-HESI-QOrbitrap-MS/MS	positive, negative	yes	top10-ddMS2	2018	36
UHPLC-HESI-QOrbitrap	positive, negative	yes	N/A	2018	110
UHPLC-ESI-LTQ-Orbitrap-MS/MS	positive, negative	yes	MSE, MRM	2018	111
UHPLC-ESI-QQQ-MS/MS	positive, negative	yes	MRM	2018	63
UHPLC-ESI(neg: APCI)-QTOF-MS/MS	positive, negative	yes	SWATH, PRM	2018	61
UHPLC-ESI-QQQ	Negative	yes	SRM	2018	64
UHPLC-ESI-IMS-QTOF-MS/MS	Positive	yes	N/A	2017	55
UHPLC-ESI-QOrbitrap-MS/MS	polarity switching	yes	N/A	2017	98
UHPLC-HESI-QOrbitrap-MS/MS	positive, negative	yes	product ion scan	2017	99
UHPLC-HESI-QOrbitrap-MS/MS	positive, negative	yes	PIS	2017	35
UHPLC-ESI-QTOF-MS/MS?	Positive	yes	MSE	2017	41
UHPLC-ESI(/APCI)-QQQ-MS/MS	polarity switching	yes	SIM	2017	62
UHPLC-ESI-QqQ-MS/MS	positive (SPs), negative (SM)	yes	MRM	2017	65
UHPLC-ESI-QqQ-MS/MS	positive, negative	yes	MRM	2017	66
UHPLC-ESI-QOrbitrap-MS/MS	positive, negative	yes	N/A	2017	93
UHPLC-HESI-LTQ-Orbitrap-MS/MS	positive, negative	yes	PIS	2017	121

Enh.=enhanced

8.6 Analysis tools and statistical methods

Apart from the arithmetic average, (relative) standard deviation, linear regression and p-value calculations, statistical methods of lipidomic research has broadened into a far broader variety of numeric tests and visualization techniques. Classical analysis of variance (ANOVA)[95, 105] for multiple[36, 95, 105] and Student t-tests for two variables[116] were occasionally used.

A t-test designed for comparing two independent variables (e.g. patient versus control group lipidome, the lipidome before versus after drug ingestion) may be unreliable, if the sample size is small (n<30) and other than normal distributions arise through the data.[117] This is the case in most of the sample sizes in the experiments of the 39 articles (for 21 articles, sample size was not available), since the average was around n=11±11 when the outliers n=283[109] and n=10,115[9] were removed (for 10 control samples: 7-16 or ~30[63, 111]). Instead, a Mann-Whitney U test fitted for non-Gaussian distribution data combined with a Benjamini-Hochberg (or Bonferroni-Holm[117]) false discovery rate (FDR) estimate. These have been applied in multiple studies to limit uncertainty. Furthermore, Paepe et al.[102] used cross-validated ANOVA (CV-ANOVA) to improve reliability. In *Figure 12*, all statistical tools used in the articles were listed by the relative frequency each year.

Briefly, combined studies of machine learning/software evaluation and UHPLC-MS lipidomic analysis were met in a set of articles.[51, 88, 93, 96, 108] As machine learning knowledge has boomed, an increasing supply of automated lipidomic analysis, ROC/AUC cross-validation analysis,[96] random forest, neural network,[73,] *in silico* spectra[51] and CCS value[88] generation algorithms have emerged.

In addition to home-made databases,[63, 89, 105, 108, 109] commercial and open-source libraries have gained popularity and variety in both lipid range and search tools. These libraries included CEU Mass Mediator,[105, 117] ChemSpider,[41, 54] Foodb,[118] Greazy,[73] HMDB,[54, 79, 82, 90, 104, 105, 111, 117, 118, 121] KEGG,[108, 111] LipidBlast,[39, 51, 88, 110] LipidMatch,[73] LIPID MAPS/Lipidomics Gateway,[39, 54, 55 79, 82, 89, 90, 92, 104, 106, 111, 121] MassBank,[51] MetaboAnalyst,[108] MetLin,[79, 104, 111, 117] Program R's MeV package (version 4.5.1),[96] MS-DIAL,[73] MZmine,[73] NIST (e.g. NIST14),[88] PubChem[41] and Reactome.[106]

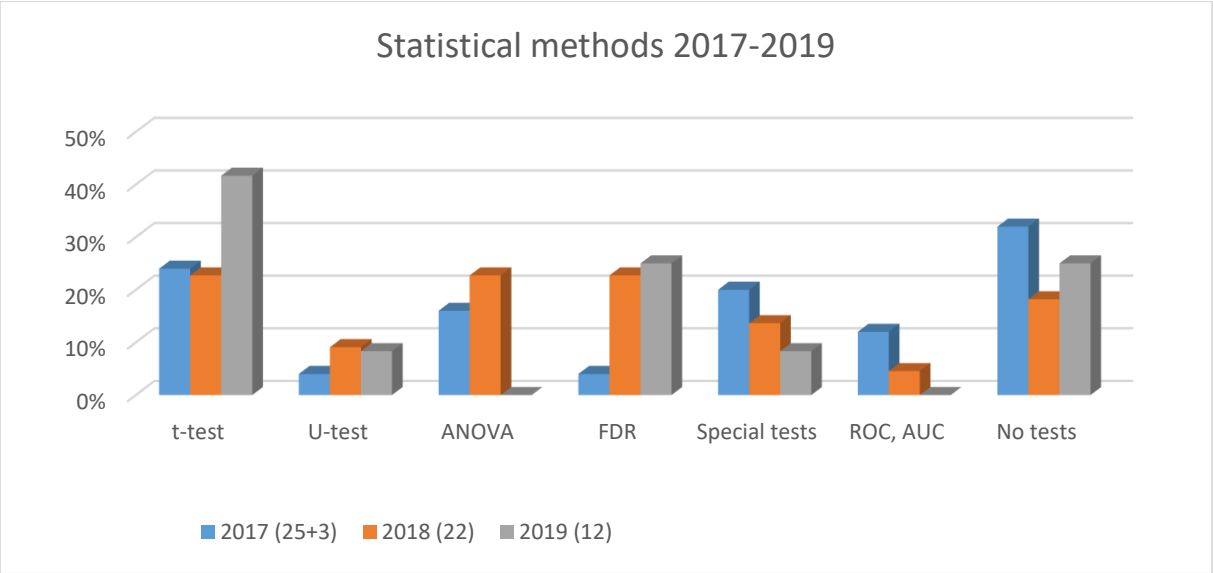

Figure 12. Percentages of statistical methods found in the defined three years. Special statistical tests and techniques not discussed included foreground class probablilities,[51] a neural network pattern; radial basis function/linear basis function (RBF/LBF),[88] ingenuity pathway analysis (IPA),[94] paired t-test,[94] over-representation analysis,[80] cross-validated ANOVA,[45] Turkey test,[104] , relative frequency analysis,[118] random forest generation,[93, 94, 118] Hodges-Lehmann estimator,[109] principal component variable grouping,[119] principal component linear discriminant analysis,[93] root mean squared error cross validation[121] and Shapiro-Wilk normal distribution testing.[115]

Established chemometric methods such as PCA (principal component analysis, multivariate technique) and PLS-DA (Partial least squares regression - Discriminant Analysis) have kept their position as most common tools for visualizing analyte groupings (PCA) and metabolic changes (PLS-DA). Moreover, the importance of orthogonal projections to latent structures discriminant analysis (OPLS-DA, orthogonal partial least squares discriminant analysis) has increased since Pöhö's review in 2013.[34] Also, VIP (Verification and Identification Protective data handling) has emerged as an emphasis estimator of PLS-DA variables. [66, 96, 101, 105, 106, 111] In contrast, boxplot usage has declined in the face of volcano plots alongside heat maps with included or separate hierarchical cluster analysis (HCA) figures. Just like with the statistical tools, chemometric methods and plot types were listed in *Figure 13*.

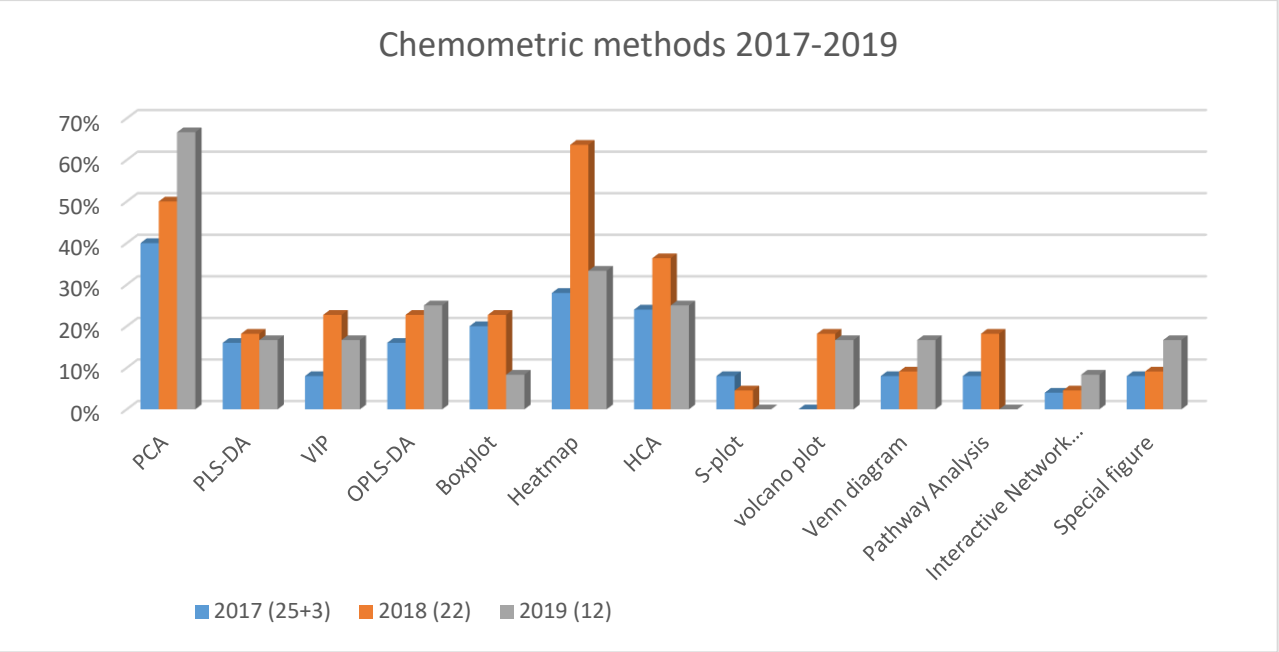

Figure 13. Chemometric method ratios and figure/plot types found in the defined three years. **Interactive Network…**: interactive network analysis. Special tests included a spider web diagram,[52] a clustered image map,[97] a chord diagram,[46] cross-validated PCA,[45, 112] three-dimensional PLS-DA[111] and two-way PLS (O2PLS)[121]

8.7 Quantitative and qualitative lipid analysis

Identification "dimensions" (e.g. CCS [collision cross-section], MS/MS, Raman) are often added to the RT and m/z aspects of species, up to the point where the identification process is automated with softwares often written with "middle level languages".[73] These identification platforms usually work by either measured parameter, spectral library or mixed comparisons (open-source, commercial or self-acquired).

Statistical tools and chemometric softwares have been developed to enable false positive analysis and pattern recognition for large datasets for an abundance of lipid analytes.[71, 72] This combination of identification and statistical tools enhances the specifity of a method, making it possible to quantify an analyte more reliably.

Interference due to analyte degradation before analysis (i.e. inter- and intra-batch effects),[5] for instrumental reasons, in the data or spectra all affect the representativeness of the species' quantitation. Especially during method development and data-analysis, knowledge of

molecular properties in addition to supporting standard and sample analyses are essential for executing proper quantification. For example, alterations take place due to biological or instrumental reasons, as is the case with phospholipase D conversion of PCs to PAs as is the case in the *Arabidopsis* plant,[5] or a bias in LPA quantitation due to LPA-increase via in-source fragmentation of lyso-phospholipids (LPCs).[21]

Ideally for surrogates and internal calibration, near to identical lipid species with odd-numbered FAs, which are <1% abundant in higher organisms,[5] or isotope-labeled FAs (e.g. deuterated or C-13 labeled) are often used. As retention times for interferents differ, an internal standard should be as equally retained as possible to representatively mimic the matrix effects experienced by the analyte. However, usually only one internal standard is used to normalize analyte data (e.g. peak areas) and correct experimental and instrumental fluctuations, as is the case for calibration standards as well.

If standard addition is neglected,[64] a typical and effective quantitative analysis in lipidomics is achieved with a single point calibration (e.g. with a deuterated standard) or calibration curve, of which the former takes less effort but the latter is more precise. Moreover, prior knowledge to an analyte's chemical properties can help to predict unwanted analyte/analyte population manipulations that distort the estimations for, say, measured analyte concentration. These properties include the polarity and chemical structure of an analyte, both of which lead to characteristic ionization and fragmentation behavior. For example, if fragmentation takes place where it cannot be observed (e.g. in-source) or if decomposition of another analyte affects concentrations of other analytes, measures must be taken to account for this in the quantitative calculations. In-source fragmentation correction may be solved with a fitting representative calibration standard that has the same experimental conditions (including matrix and sample preparation) and, thus, same modifications as the analyte. Saturation and peak broadening may also distort the quantitation result, as the peak shape is compromised.

For chromatographic lipid analyses in our UHPLC-dataset, 57 out of 61 studies used RP columns. In contrast, 4 NP analyses were conducted. The trend towards NP stationary phases may stem from the easier identification between nonpolar structure separation and MS/MS identification by lipid class product ions. Examples of RP-UHPLC separation zones can be observed in *Figure 14*.

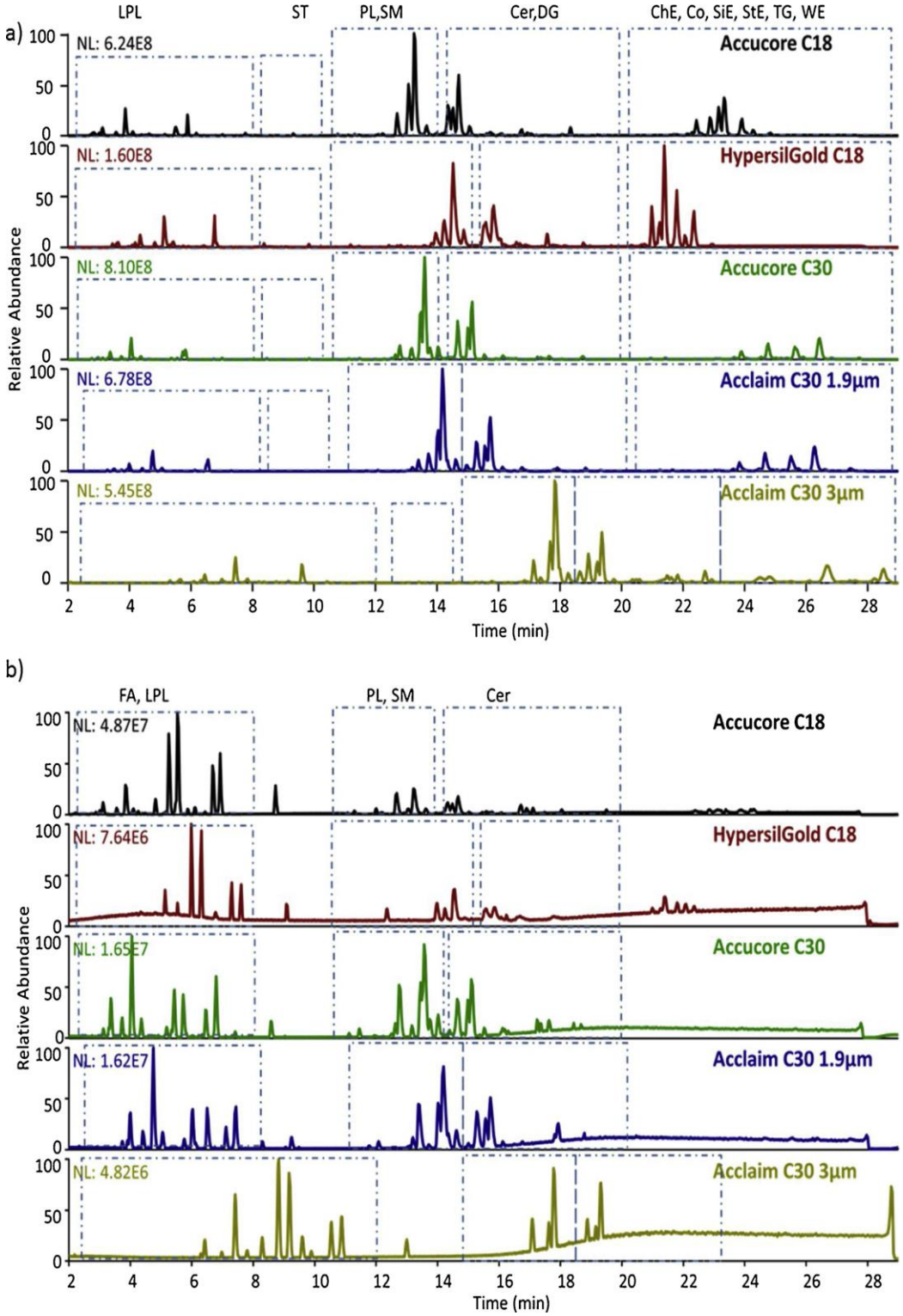

Figure 14. C18 and C30 columns used for plasma HPLC/MS in **a)**positive and **b)**negative ESI mode, with the solvents 50:50 ACN:H_2O and 85:10:5 IPA:ACN:H_2O (5 mM AmFo). The columns used were Accuore C18 (solid core, 2.6 µm), HypersilGold C18 (fully porous, 1.9 µm), Accuore C30 (solid core, 2.6 µm), Acclaim C30 (fully porous, 1.9 µm) and Acclaim C30 (fully porous, 3.0 µm)

ChE: cholesteryl ester, **Co**: coenzyme, **SiE**: sitosterol ester, **StE**: sterol ester, **WE**: wax ester

In the UHPLC/MS article dataset, chromatograms were shown surprisingly rarely which may be linked to the high frequency of automation (about half of these articles used automated identification via a database library platform).

As seen by a standard separation by Pham et al.[124] (*Figure 15*), HILIC separates all lipid classes neatly from each other compared to C30. In my experience, the C30-produced chromatogram is very representative for other RP-column separation chromatograms such as C8 or C18, both of which have at least one bulk where multiple GPs are retained. Nevertheless, a large quantity of lipid species may be identified more easily with RPLC, since separation to nonpolar qualities of analytes (i.e. FA chains) occurs as opposed to HILIC. Furthermore, HILIC is susceptible to distorted adduct formation, decreased quantitation repeatability and co-elution due to the stationary phase's capacity to retain inorganic ions.[47] Alternatively, resolution may compensate up to a point for the separation efficiency.[46]

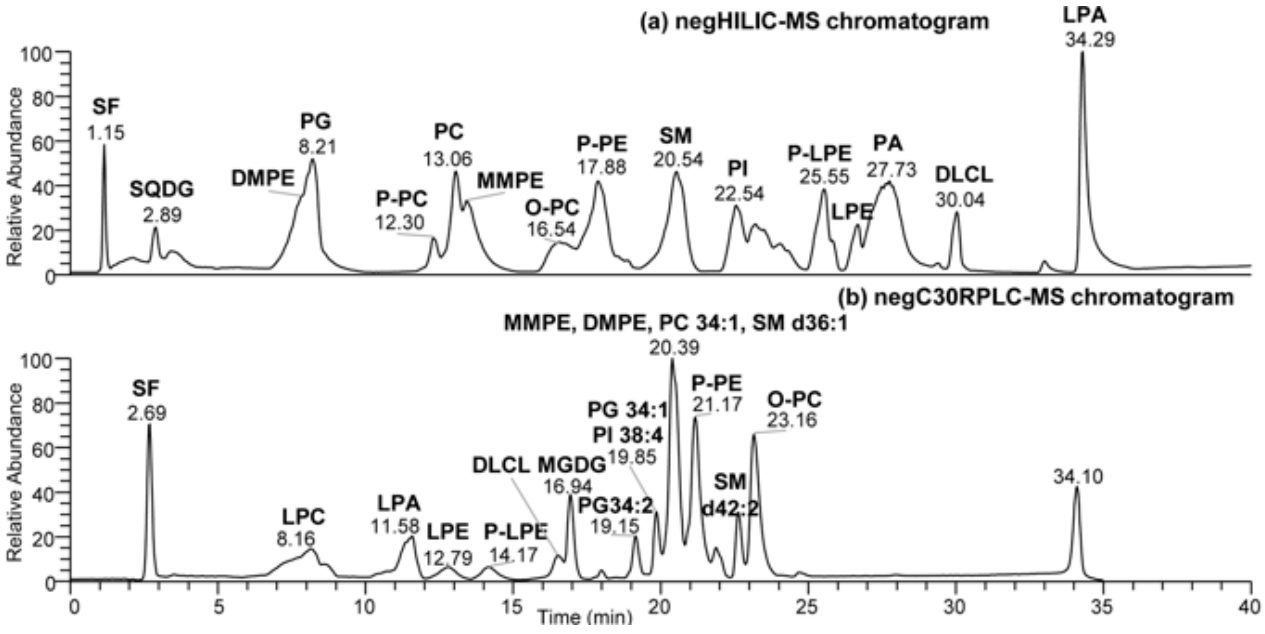

Figure 15. Chromatograms of a HILIC and a C30 HPLC/MS separation in negative mode.
Reprinted from **ref 124 © 2019, Springer Nature**
SF: N/A (steroidogenic factor?), **SQDG**: sulfoquinovosyl diacylglycerol, **MMPE**: monomethyl phosphatidylethanolamine, **DLCL**: dilysocardiolipin, **MGDG**: monogalactosyldiacylglycerol

As representative UHPLC/MS chromatograms and their lipid distributions, *Figure 16* shows EICs of multiple lipids in both positive and negative mode. Some programs combine EICs to improve peak shape and identification.

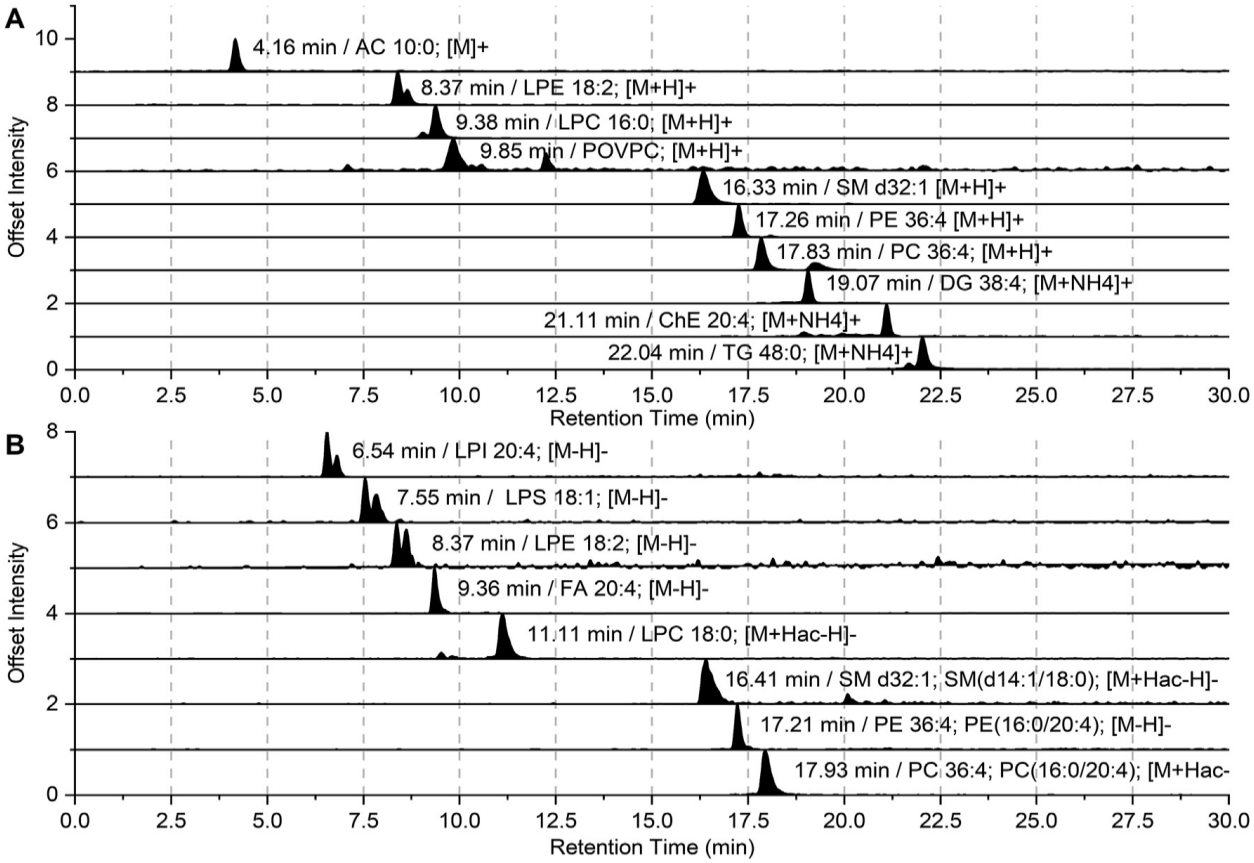

Figure 16. EICs for ***A***: positive and ***B***: negative mode UHPLC ESI with a C8 column, solvents H_2O and 50:40:5 ACN:IPA:H_2O (10 mM AmAc). Reprinted from **ref 119 © 2018 Elsevier B.V. All rights reserved AC**: acyl carnitine, **POVPC**: 1-palmitoyl-2-(5-oxovaleroyl)-sn-glycero-3-phosphatidylcholine

Nano-LC seemed to have even more capacity for analyte identification than UHPLC, since it has both an extremely broad lipid range[52] and a sensitivity in the low fmol scale.[103] Moreover, a lipid standard C18-filled capillary separation in both positive and negative mode ESI takes approximately as long as a HPLC/MS analysis (*Figure 17*).

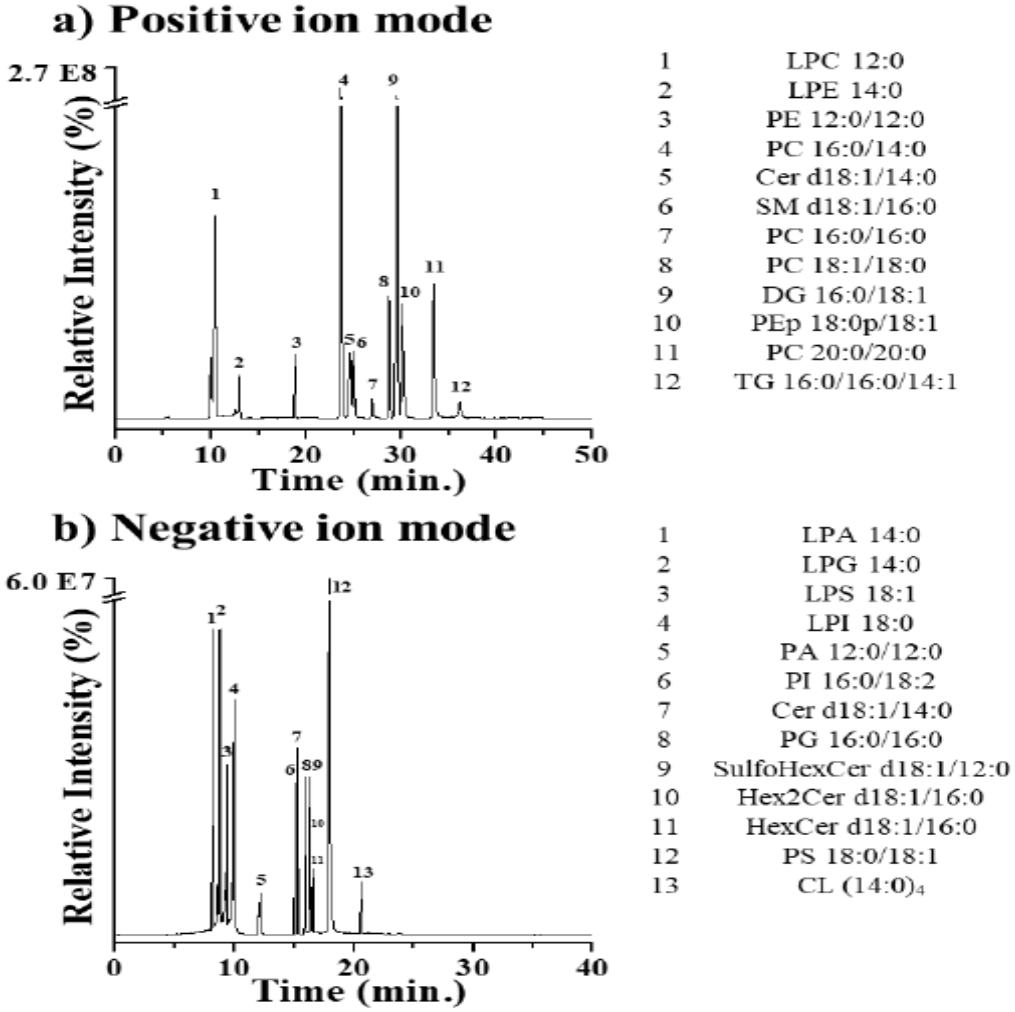

Figure 17. Positive and negative ion mode chromatograms for nanoLC MS/MS with a C18 column, with the solvents 90:10 H_2O:ACN and 20:20:60 MeOH:ACN:IPA (5 mM AmFo, 0.05% FoA). Reprinted from **ref 103 © 2018 Elsevier B.V. All rights reserved**.

Lipidomic profiles differ a lot from sample to sample, though some consistencies remain: in most mammalian cells, ~60% of lipids are usually GPs and ~10% SPs, PCs and PEs usually rank highest in GP and SMs in SPs by concentration in a given sample. To demonstrate the difference in the lipidome of a medium, *Figure 18* demonstrates this by comparing kidney and serum chromatograms acquired through the same method and treatment of samples. The functionality between the occurring variety of lipidomes in fluids and solids (even by their individual cell organelles) is yet to be uncovered, as is the connection between lipidome structure and functionality in the first place.

Researchers like van Meer et al.[13] have attempted to find and describe poorly understood aspects of lipidomes. This includes functions such as inter- and intracellular signalling, in-cell

lipid transport (especially non-vesicular mechanisms) and macromolecular assemblies including lipids (e.g. lipid rafts, liquid-ordered and liquid-disordered systems).[13]

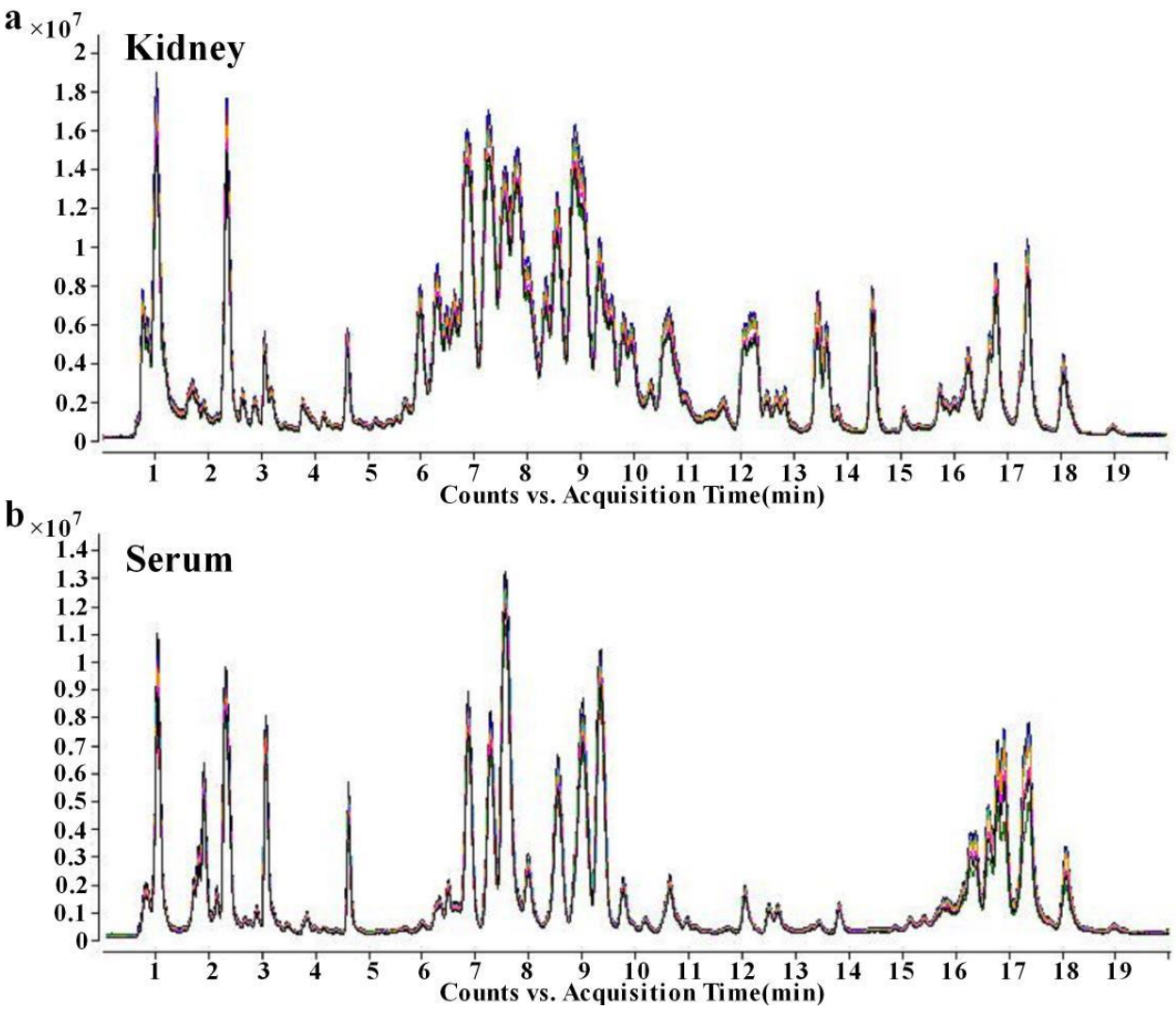

Figure 18. Kidney (**a**) and serum (**b**) profile chromatograms in positive mode UHPLC ESI with a C18 column separation, solvents 60:40 ACN:H_2O and 81:10:9 IPA:ACN:H_2O (10 mM AmFo, 0.1% FoA). Reprinted from **ref 104 © 2018 Elsevier B.V.**

For MS/MS identification, Chao et al.[104] documented product ion spectra for typical species found in mouse serum (*Figure 19*). The spectra acquired served for the manual identification of molecular species (i.e. where FA chain lengths are determined) and lipid class confirmation via fragmentation experiments. The next step would be the determination of the stereochemical sn-position, which may be possible with a datalibrary comparison of known spectra.

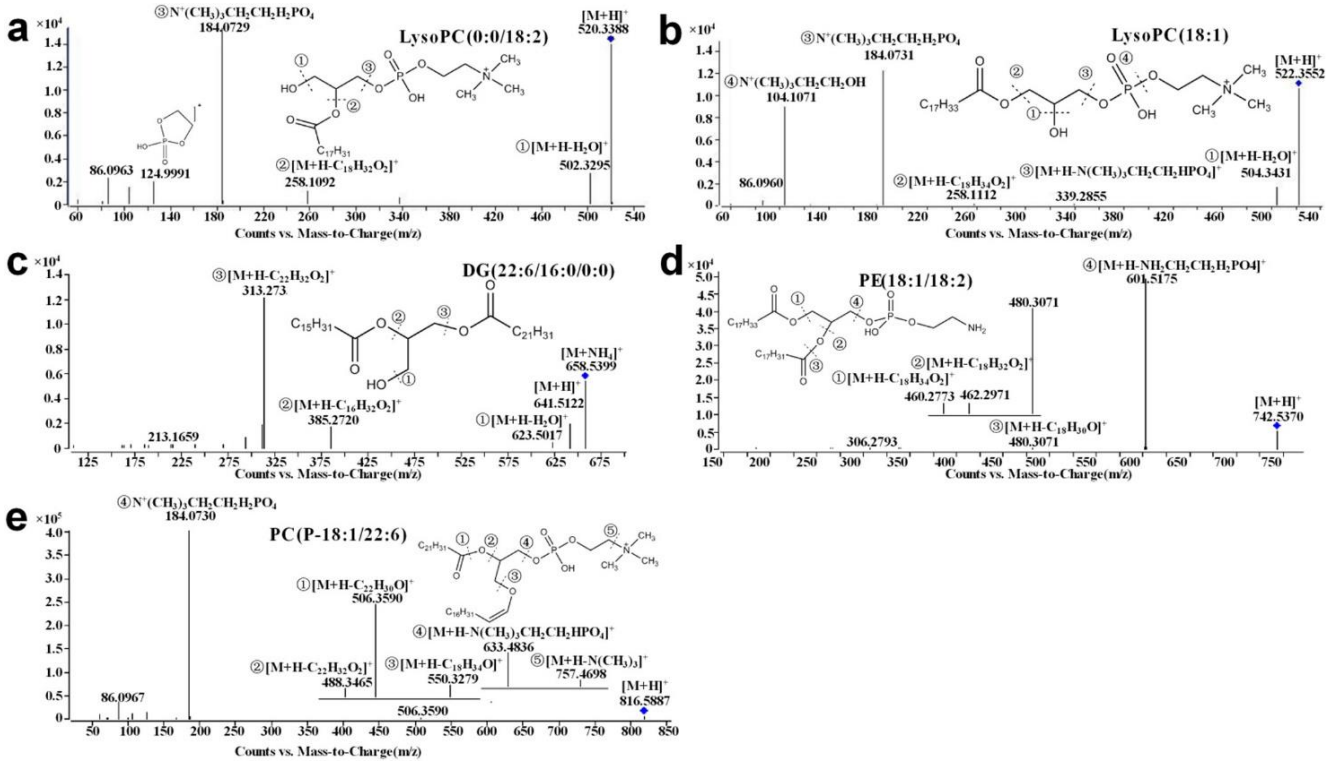

Figure 19. Fragmentation patterns for multiple species (molecular ion is marked with a dot). Positive ESI mass spectra acquired via product ion scans with a QTOF. Reprinted from **ref 104 © 2018 Elsevier B.V.**

As for negative mode ESI, *Figure 20* depicts a product ion scan of the same PI-species in two different separations. As observed, the fragmentation patterns deviate slightly, possibly due to different matrix effects. Similarly, *Figure 21* displays negative ion patterns typical to multiple lipid classes (i.e. headgroups) respectively.

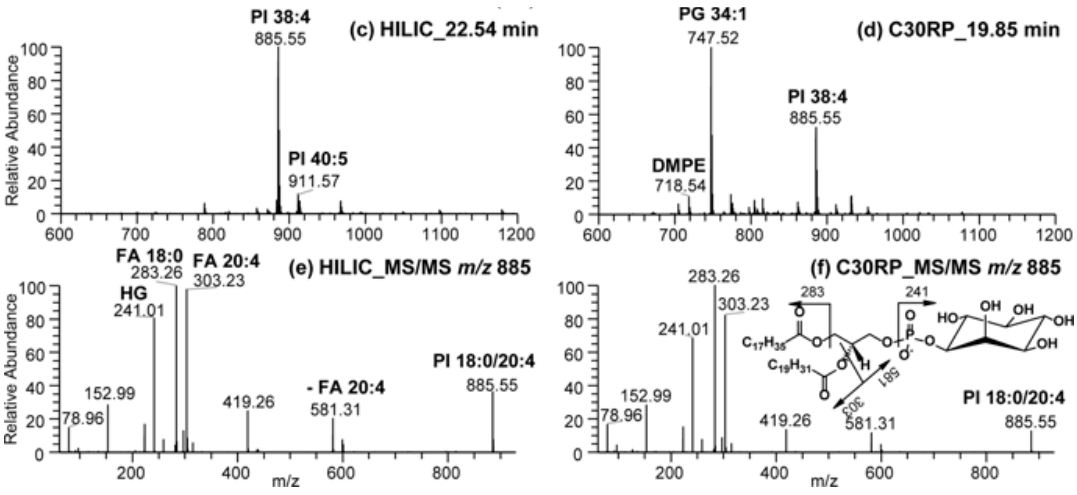

Figure 20. Product ion mass spectra of PI(38:4) in negative mode, one HILIC-, one C30-separation. **(c)** and **(d)** are scans before, **(e)** and **(f)** scans after the fragmentation of the m/z species 885. Reprinted from **ref 124 © 2019, Springer Nature**

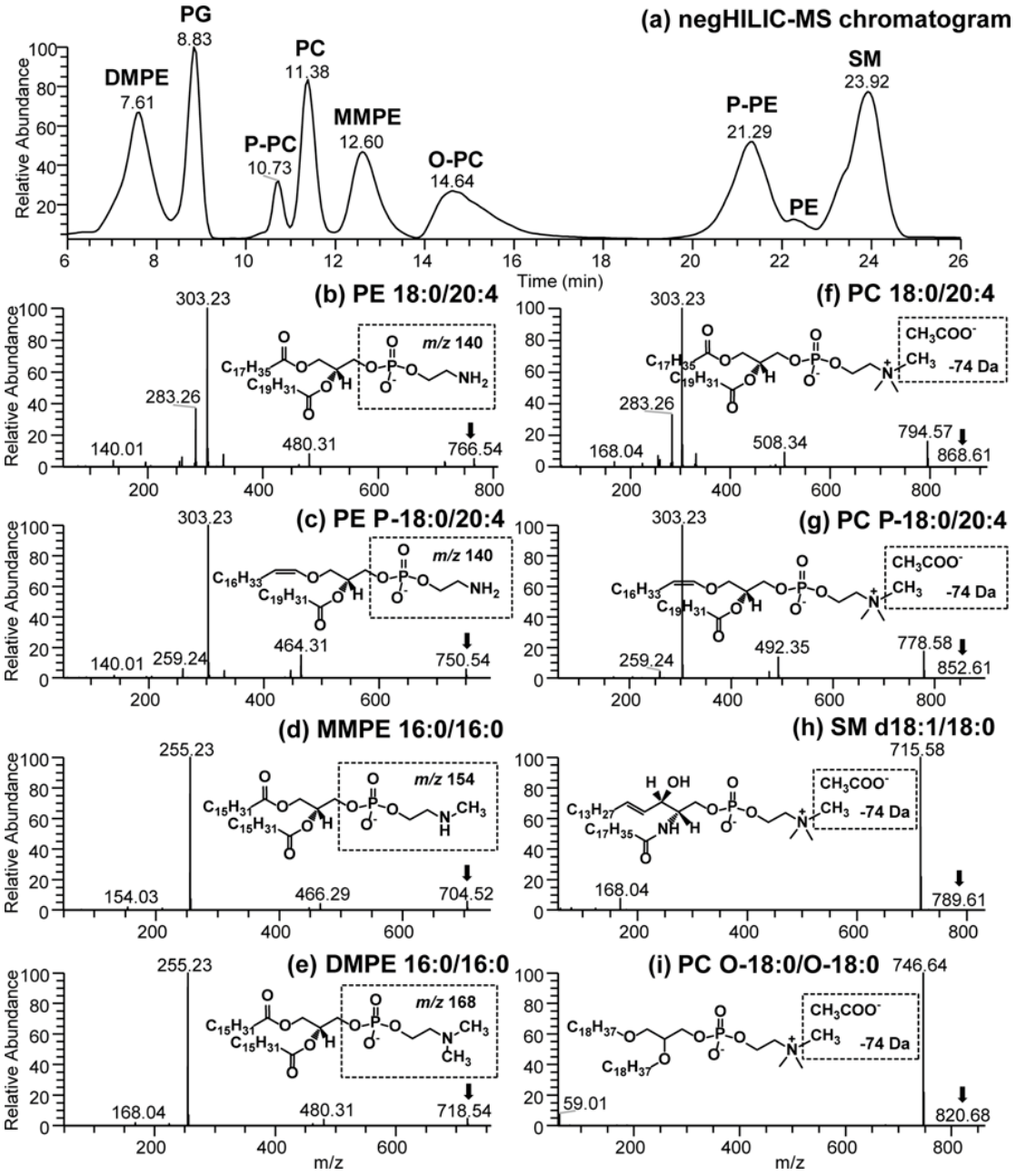

Figure 21. Product ion scans of negative mode HILIC-separated lipids from a standard mix (molecular ion is marked with an arrow). Reprinted from **ref 124 © 2019, Springer Nature**
MMPE: monomethyl-phosphatidylethanolamine,
DMPE: dimethyl-phosphatidylethanolamine

9 Discussion

According to lipidomic research, some lipids are only observable in the column domain with particle size less than 2 µm compared to a conventional HPLC separation,[52] making UHPLC the best method for repeatable and rather comprehensive lipid identification[96, 106] and pathway analysis.[109] However, UHPLC is a relatively new method with expensive instrumentation and maintenance. This may also explain the smaller amount of UHPLC article publications compared to HPLC research.

In 57 out of 58 studies -with 5 reviews subtracted from the total 63 articles- with an average runtime range of 18-23 minutes used mainly RP UHPLC techniques (C18: n=52). A minority of pre-columns was used in UHPLC experiments, presumably to avoid risk of void volume and preserve reproducibility among lipidomic UHPLC-studies. As for the mobile phase consistency, variations of ACN:H_2O and IPA:ACN gradients (n=27) were used. The most typical additives in buffer solutions are ammonium formate and formic acid (n=25). The trend of overwhelming RPLC over NPLC in UHPLC research may be due to the effective separation of nonpolar structures (i.e. by fatty acid chain lengths) between lipid species. Since Monnin et al.[48] used additives to increase sensitivity and improve peak shape for certain adducts, it could be stipulated that additive introduction (i.e. addition of source chemical for achieving specific ligand formation) could bring greater uniformity among lipid polarity if the complex affinity is strong enough.

46 out of 58 studies focused specifically on identification of GPs, out of which 29 included LPLs and 12 PLs. 42 articles on GLs were especially interested in DGs and TGs, and out of 39 articles on SPs, 7 included reports on SP hexosyl metabolites. On average, 3 lipid classes were included per a paper, though the maximum of lipid classes analysed in one study included 7 groups. Lipids were reported from a range of 5-700 total lipids and 5-87 potential biomarkers. Apart from the studied lipids (GLs, GPs and SPs), CEs[7, 35, 37,55, 62, 63, 66, 91, 101, 106, 108, 114, 115] and FAs[7, 28, 36, 45, 46, 64, 79, 89, 99, 104, 105, 110, 111, 117, 119, 121] were often reported.

Conventional biological material topics i.e. research on routine *in vivo* analysis samples included six (6) categories of matrices: primarily blood derivatives (plasma, serum, erythrocytes and blood platelets), faecal matter, and urine. One paper even proposed a multimatrix analysis by pooling plasma, faecal matter, and urine in one sample to increase

method repeatability and lipid coverage.[102] Unconventional biological materials, i.e. harder-to-get *in vivo* samples, consisted of 18 different biofluid and tissue types, of which the most frequent topic of interest being liver tissue.[15, 30, 63, 82, 92, 98] In addition, experiments with 18 different cell lines were found to be cultured *in vitro*, and more exotic samples like plant, entire organism and food product analyses were occasionaly conducted in the set of articles.

Not only have new applications emerged due to improved computer algorithms, but also the amount of commercial, open-source and in-house software platforms and data libraries for automated identification. Out of the 59 articles, approximately half of the studies used automation platforms for identification. Current improvements in identification have been found at the dawn of higher computing power and software development for lipidomic analysis. This has given way to machine learning for *in silico*-based analyses, a boom in lipidomic and metabolomic tools and MS/MS methods such as parallel reaction monitoring-data-dependent acquisition PRM (DDA)[42, 52, 61] and all ions in data-independent acquisition in MS^E mode (MSE-mode, DIA)[30, 41, 42, 82, 92, 94, 97, 105, 108, 111, 115, 118]. Furthermore, recent DIA research has used sequential window acquisition of all theoretical fragment ion spectra in mass spectrometry (SWATH MS). The PRM-like consecutive fragmentation of all precursors has an improved detection rate, broader analyte range, and specifity in any given fragmentation frame compared to DDA methods.[37, 61, 119] Similar though not yet observed in the UHPLC-lipidomics articles, sliding window adduct removal method (SWARM), i.e. adduct signal overlap correction for low-to moderate resolution mass spectra has also appeared. Introduced by Kitov et al.[125] for proteomics, SWARM is based on the statistical basis of ESI adduct formation, which produces systematic noise patterns that can be corrected.

Due to the inherent delocalization of analytes and the slow pace of chromatographic methods, imaging techniques have diverted towards alternative methods. Alongside rather standardized DIMS, MALDI-MS and DESI and other MSI methods,[3, 53, 81, 82] more experimental approaches like probe,[81] CRS,[86, 87] and LESA[52] techniques have started to be the trend. Further outside of lipidomics research, the iKnife, an "intelligent" scalpel using rapid evaporative ionization mass spectrometry (REIMS, i.e. ionization with electrically burning tissue) had reached surgical environment testing in 2018.[127] In 2017, LESA-type analyses with a MS-linked "pen" was tested and proposed by Zhang et al. as a non-destructive alternative for histopathologic tissue diagnosis.[128] Though a high resolution is obtained in MS, the small

probe is impractical for moving. However, the surgical *in situ* MSI technology may help for cutting corners in metabolomic and lipidomic "shotgun"-research. In my opinion, however, an in-depth understanding of the biochemical properties, as well as of the physiological/metabolic network, is needed to understand lipidomic or metabolomic pathways in a complex matrix. Moreover, a new way for improved identification and quantitation in lipidomic studies has been found: The utilization of the lipidome isotope labelling of yeast (LILY) standard.[126] To achieve a labelled array of standard analytes, yeast is fed with 99% $^{13}C_6$ D-glucose.[126]

Moreover, an interdisciplinary analysis on multifunctional and computational methods in lipidomic analytics will be crucial for effectively improving the practice and understanding of available tools. Multifunctional methods include statistical and chemometric analyses, whereas computational methods include algorithms, data-processing interfaces, specific software, and machine learning strategies. Both method categories have been attempted to refine with tailored software platforms for necessary data pre-processing, pattern recognition and analysis of large datasets, resulting in an immense amount of data-processing interfaces to choose from. On average, the sample sizes were rather small, most probably due to the scarce availability of subjects or organisms to analyse. Student t-tests and ANOVA were used for null hypothesis testing, and an increase of Mann-Whitney U-tests and false discovery rate corrections with Benjamini-Hochberg FDR[77] could be observed. For chemometric methods, the routine boxplots and heatmaps, HCA, PCA, PLS-DA and occasional VIP corrections for PLS-DA analyses were accompanied with an increased usage of volcano plots and OPLS-DA, where an orthogonal plane of principal components is sought for.

High resolution UHPLC-MS is a highly sensitive separation method currently most suitably used for complex biomarker analysis and pathway identification. This information is important for metabolism-acquainted clinicians tackling highly complex metabolic systems, e.g. cancer and other metabolic disorders. Alas, the complexity of metabolism and its multiple aspects are rather inaccessible to health professionals unacquainted with the field. As diagnosing of diseases is desired as robust and exact as possible in the future, complex program-assisted lipidomics with direct, chromatographic and desorption-based methods show promises for comprehensive in-depth groundwork of the lipidomics area.

II Experimental part: Lipidomic profiling of Ascites -
Method development for the identification and quantitation of lipids

Master's Thesis/ Pro Gradu
BSc Henri Avela
Johannes-Kepler Universität Linz
Technical chemistry Dept.

Supervisors:
Prof. Christian Klampfl
MSc Bernd Reichl
10/2018-03/2019

10 Introduction

Ovary or ovarial cancer (OC) is "cancer originating in the cells of ovaries or fallopian tubes".[129] It is at present the most deadly gynecological disease globally[129, 130] and, according to a global report by the World Cancer Research Fund (WCRF), the 18th most occurring cancer overall with a yearly diagnosis count of 250 000-300 000 each year.[131] Only occurring in the female reproductive system, it is "the [7th-8th] most commonly occurring cancer in women",[129, 131] not to mention the 6th most deadly cancer on the global scale according to the European Institute of Women's Health. Furthermore, Europe has the highest rates of ovarial cancer occurrences continentally: with near to 43 000 deaths per year and over 65 000 diagnoses in 2012.[129]

With no effective screening programs yet proven,[132] pathological research around metabolomic processes of ovarial cancer is on-going in the year of 2019. The suffix "-omics", derived from the word "genomics", indicates a form of totality. It is mostly associated with the Human Genome Project (HGP), which mapped out the entire genome (i.e. all deoxy-ribonucleic acid-sequences of all chromosomes) of the human species, proposed in 1984 and funded between 1988-2003. Though found surprisingly complex, the idea of obtaining a total matrix of a biomolecule-group giving insight to diseases and physiological functions remained. Since the HGP, -omics research of biomolecule groups other than DNA have become an ever-increasing interest of biomolecular and -chemical laboratories globally. Lipidomics, a subgroup of metabolome analysis in the omics cascade, comprises of the mapping out of organic lipids and lipid metabolites, thus hoping to gain more information of the system at hand.

As one alternative, the field of lipidomics has been widely studied for both pathological diagnostics and identification of biomarkers.[4] For ovarial cancer, Perrotti et al's review on multiple large studies (n>40) strongly suggests an increase of LPLs (specifically LPAs, which have been proposed as early-detection plasma biomarkers) and a change in the FA profile. Here, one explanation for LPL was suggested[133] In addition, Zhang et al found potential biomarkers in the groups of TGs (decreased), PCs and LPCs (increased).[138] This would back up the up-regulation of PC 32:3, 34:1 and 36:2, moreover: the increased LPC levels caused by "deregulation of phospholipase A2" mentioned by Perrotti et al. Back in 2008, Qadir and Malik also reported decreases in TG levels as well as HDL-cholesterol, cholesterol and LDL-cholesterol of ovarial cancer patients.[134] Furthermore, Perrotti et al mentions Zhao et al's research on the GP PL-profiling of ovarial cancer patients.[133]

11 Experimental

11.1 Chemicals and Solvents

The reagents and eluents used in the analysis are listed in *Table 20*. The table includes information of the deuterium-labelled and plasma-imitating Splash® Lipidomix® mixture by Avanti Polar Lipids Inc., which contributed as a one-to-ten dilutable standard for method development and an inspiration for the surrogate concentrations used in the clinical sample targeted analysis.

Table 20. Chemicals and solvents used for the analysis

	Standards	Formula	Molar mass [g/mol]	CAS	State	Purity	Provider	
	Acetic Acid	C_2H_4O2	60.052	64-19-7	l	100 %	VWR Chemicals	
	Acetonitrile	C_2H_3N	41.053	75-05-8	l	99.90 %	VWR Chemicals	
	Ammonium Acetate	$C_2H_7NO_2$	77.083	631-61-8	s	98.50 %	VWR Chemicals	
	Ethanol AA*	C_2H_6O	46.069	64-17-5	l	99.89 %	Merck	
	Methanol	CH_4O	32.042	67-56-1	l	99.90 %	VWR Chemicals	
	Milli-Q Water**	H_2O	18.015	7732-18-5	l	18.2 MΩ	Milli-Q	
	2-Propanol	C_3H_8O	60.1	67-63-0	l	≥99.9 %	VWR Chemicals	
Mixture	**Standards**	**Formula**	**Exact mass [g/mol]*** **	**CAS**	**State**	**Purity**	**Provider**	**Concentration [mg/l]**
SPLASH® Lipidomix®	15:0-18:1(d7) PC	$C_{41}H_{73}D_7NO_8P$	752.60612	N/A	l	>99 %****	Avanti®	160
	15:0-18:1(d7) PE	$C_{38}H_{67}D_7NO_8P$	710.55917	2097561-15-2				5
	15:0-18:1(d7) PS	$C_{39}H_{66}D_7NNaO_{10}P$	776.53095	N/A				5
	15:0-18:1(d7) PG	$C_{39}H_{67}D_7NaO_{10}P$	763.53571	N/A				30
	15:0-18:1(d7) PI	$C_{42}H_{75}D_7NO_{13}P$	846.59636	N/A				10
	15:0-18:1(d7) PA	$C_{36}H_{61}D_7NaO8P$	689.49892	N/A				7
	18:1(d7) LPC	$C_{26}H_{45}D_7NO_7P$	528.3921	2097561-13-0				25
	18:1(d7) LPE	$C_{23}H_{39}D_7NO_7P$	486.34515	N/A				5
	18:1(d7) Chol Ester	$C_{45}H_{71}D_7O_2$	657.64412	1416275-35-8				350
	18:1(d7) MG	$C_{21}H_{33}D_7O_4$	363.3366	N/A				2
	15:0-18:1(d7) DG	$C_{36}H_{61}D_7O_5$	587.55063	2097561-14-1				10
	15:0-18:1(d7) TG	$C_{51}H_{89}D_7O_6$	811.76465	2097561-17-4				55
	18:1(d9) SM	$C_{41}H_{72}D_9N_2O_6P$	737.63973	N/A				30
	Cholesterol (d7)	$C_{27}H_{39}OD_7$	393.3988	83199-47-7				100
	Cer2(d9)	$C_{34}H_{58}D_9NO_3$	546.56858	N/A	s	>99%	Avanti®	Pure

*** AA:** absolute analytical grade

****** Produced directly with Milli-Q Elix 3, Milli-Q Reference A+ and Q-POD

******* Exact mass calculated with chemical formulas via the SIS Isotope Distribution Calculator: https://www.sisweb.com/mstools/isotope.htm

******** Each individual standard sold separately had the purity of >99%, the Splash® Lipidomix® (however) had the marking N/A

11.2 Sample overview and ethics statement

The Ethics Committee of the Federal State Upper Austria agreed upon the plausibility of the lipid analyses in blood, amniotic fluid and ascites. The decision can be found with the EK Nr. 1163/2018. The prepared and analyzed clinical samples were obtained from the Kepler University Hospital Department of Gynecology, Obsterics and Gynaecological Endocrinology, where both sampling and pre-preparation took place.

First, *in vitro* CMs from three different cancer cell lines and two in vivo amniotic fluid samples were prepared and analyzed. These samples were analyzed for both sample preparation training and method development, but first and foremost to attain information about adduct formation of all lipid classes to be investigated. Having a better understanding of class-specific adducts, a lipid extract from EDTA-plasma was injected and analyzed. Plasma, a commonly studied medium in lipid biomarker research,[135] was chosen as a basis for the generation of an in-house database.

Finally, ascites samples were prepared with two different preparation techniques and analyzed predominantly with the Agilent in-house database (personal compound database library, PCDL) created during the preceding plasma analysis. In addition, a Douglas lavage fluid (DLF) sample collected from an endometriosis patient was included. Not being present in healthy individuals, control samples like these were typically acquired from "nonmalignant patients" (e.g. patients with liver failure).[136] As such, the DLF collected from the rectouteral pouch of Douglas – the lowest part of a female's peritoneal cavity – was assumed to be an ideal control sample for ascites.

11.3 Sample preparation

Samples were taken in the operating room of the Kepler University Hospital, transferred and stored in their pathology department. At the Department of Gynecology, samples were pre-prepared by a collaborating scientist using the following protocol: the samples were immediately placed on ice, centrifuged at 4 ˚C with 500 rpm in ten minutes (500'10), phase-separated into supernatant and cell pellet, after which the supernatant was further centrifuged at 4 ˚C with 2500 rpm for 30 minutes (2500'30), filtered through a 0.22 µm filter, snap-frozen and finally stored at -80 ˚C before shipment on dry ice to the JKU, Institute of Analytical Chemistry, to be once again stored in a -80 ˚C freezer prior to analysis.

Acquired sample fluids were obtained at the Institute of Analytical Chemistry in Eppendorf tubes, aliquoted, then put to -80 ˚C and possibly sampled after only one freeze-thaw-cycle. To avoid enzymatic activity, oxidation, hydrolyzation and other degradation, the storage was performed at -80 ˚C.[8]

Two sample preparation methods -BUME and Folch- were compared through analysis of ascites and Douglas fluid. For the amniotic fluid and CM samples during pre-experiments, only the Folch-method was applied: a 100 µl volume of each respective sample was pipetted into a 15 ml Falcon tube and mixed with 2 ml of a 1:2 methanol/chloroform (MeOH/Chloroform) mixture. The mixture was vortexed and shaken for one hour at 1500 rpm (1500'60) in a Thermal Shake Lite thermoshaker by VWR (Radnor, Pennysylvania, USA). After shaking, 400 µl H_2O was added and the two immiscible phases vortexed together. The resulting emulsion was centrifuged with 4700 rpm at 10 ˚C for 8 minutes (4700'8) to separate the water/MeOH phase from the organic chloroform phase. The lower organic phase was collected under the denaturated protein plug formed between the two phases. Special care was taken not to include any solids in the resulting isolate, thus the plug was pushed aside by keeping the tip of the pipette towards the Eppendorf tube wall and far enough from the solid phase. A second extraction was performed with an addition of 400 µl 1:1 MeOH/chloroform mixture, vortexing, centrifugation and organic phase recovery. Finally, the combined isolate was dried under an inert nitrogen gas flow and dissolved into 1 ml of MeOH. The resulting samples were divided into five aliquots with 200 µl each. The samples that were not immediately analyzed were stored at -80 ˚C.[118] In the course of the study, the Folch method was scaled down to half the volume for a 50 µl plasma sample, which allowed the sample to be prepared in a 1.5 ml Eppendorf tube.

Instead of scaling the sample preparation down to 50 µl (as was done with ascites), 100 µl of DLF and ascites were prepared with the BUME method: the sample was mixed with 150 µl of a 3:1 BUME mixture and shaken for 10 minutes. 75 µl of 3:1 heptane/ethylacetate was added and the mixture further mixed for 5 minutes. 150 µl of 1% acetic acid (AcA) was added, followed by another shaking period of 5 minutes. Finally, the sample was centrifuged at 1000G for 5 minutes, after which the upper organic phase was collected. The second extraction consisted of another mixing of 125 µl 3:1 heptane/ethylacetate with the polar phase, 5 minutes mixing and centrifugation at 1000G and organic phase recovery. As before with the Folch procedure, the organic solvent was evaporated, the sample reconstituted into 1.0 ml of MeOH and finally aliquoted.

11.4 Instruments and Analysis

Basic laboratory equipment such as an AT261 balance by the former Mettler (now Mettler Toledo. Columbus, Ohio, USA), a VV3 vortex (VWR), a Thermal Shake Lite thermoshaker (VWR) for one hour shaking, Eppendorf Reference and Research microliter pipettes (Hamburg, Germany) and a temperature-adjustable Megastar 1.6R centrifuge (VWR) were used for sample preparation. For method optimization and biological sample analysis, a 1260 series HPLC system and a 6560 QTOF interfaced with a Dual AJS ESI-source, all by *Agilent Technologies* (Santa Clara, CA, USA), was used. Because the QTOF included an IMS section, ion mobility measurements could be included into the analysis for improved analyte identification.

Final analysis parameters used after method development are listed I *Table 21*. In summary: column type, compartment temperature, flow rate, injection volume and gradient were optimized for analysis. Subsequently, the included ESI-parameters were optimized due to problems addressed during method development in negative mode. Bad ionization efficiency with the stated parameters lead to the complete exclusion of negative mode data.

Table 21. Analysis parameters. Quat=quaternary, Iso=isocratic

Parameter	Value
Autosampler temperature [°C]	6
Hyphenation	Dual AJS ESI, Electrospray ionization
Polarity Mode	Positive
-sheath gas flow [l/min] **-drying gas flow [l/min]** **-nebulizer pressure [psi]** **-gas temperature [°C]** **-capillary voltage [V]** **-nozzle voltage**	12 11 30 350 3800 700
Guard column	Security C18, Phenomenex
- dimensions [mm]	*4 * 3*
Column	Eclipse Plus C8, Agilent
- dimensions [mm] **- particle size [um]**	3.0 * 150 3.5
Compartment temperature [°C]	50
Eluent A (pump 1) **Eluent B (pump 2)**	**H_2O:ACN (60:40)**, 10 mM AmAc 1 mM acetic acid **IPA:ACN (90:10)**
- flow rate Quat pump [ml/min] **- flow rate Iso pump [ml/min]** **- gradient**	0.7 *1.0* *Table X3*
Injection volume [µl]	20

ACN: acetonitrile, AmAc: ammonium acetate, IPA: isopropanol, 2-propanol

The HPLC instrumentation included two pumps: a quaternary pump for the conventional HPLC instrument and an isocratic pump that continuously fed the ESI with a standard mix of instrument reference masses. The reference masses increased the mass accuracy of the instrument and allowed a post-acquisition mass calibration with the *IM-MS Reprocessor* tool (Agilent).

11.4.1.1 Data processing

All data-analysis of the spectra was conducted with the software solutions belonging to the *Agilent MassHunter*-family. *Workstation Data Acquisition* was used for the management and data collection of the HPLC/IMQTOF-instrument.

The aim for the *IM-MS Reprocessor* was the post-acquisition mass calibration of IM-MS data files against defined reference masses. These data files were then further processed with the single-field tune information by using the *IM-MS Browser B.08.00*. This step was done to calibrate measured flight times against CCS values of the Agilent tune mix. Through this, CCS values could be determined for all unknown compounds afterwards. After these calibrations, data were further processed using Mass Profiler software. This separate software finds in a first step features based on chromatographic peak shape, m/z, RT and CCSs that fulfil the requirements of the filtering (e.g. minimum signal intensity, limitation to first n hits etc.). The hits found by the program were then compared to the PCDL in assistance of *ID Browser B.08.00.* Information of the final PCDL is available in *Attachment 7*, the experimentally attained CCS values and species in *Attachment 8.* All IMS-measurements were conducted with nitrogen gas (N_2).

Fitting of theoretical spectra, available CCSs and RTs with measured values contributed to scores (0-100%) for each compound hit. Thus, the data accumulated in the PCDL directly affected the results of further identifications, be it collected theoretically (e.g. *in silico* m/z species) or experimentally (e.g. RTs and identified compound name). Indeed, false positives are a major issue when accumulating in-house databases.

Quantification of the lipids was conducted via a single point calibration with a surrogate mix mimicking one-to-ten diluted Avanti's Splash Lipidomix® dissolved in methanol (i.e. a

concentration of lipids comparable to plasma), created from single deuterated standards. Surrogate mix composition and concentrations were compounded in *Table 22.*

Table 22. Surrogate mix composition

Name	c(mg/l)
PC(15:0/18:1(d7))	15.6
PE(15:0/18:1(d7))	0.53
PS(15:0/18:1(d7))	0.39
LPC(18:1(d9))	2.5
LPE(18:1(d9))	0.5

Name	c(mg/l)
DG(15:0/18:1(d7))	0.88
TG(15:0/15:0/18:1(d7))	5.28
SM(18:1(d9))	3
Cer2(d9)	0.2

12 Results and Discussion

12.1 Optimization of the method, pre-experiments

12.1.1 Liquid chromatography

Multiple mixtures of H_2O and one or two organic solvents (MeOH, ethanol [EtOH], IPA, ACN) in multiple proportions were tried to no avail. The idea was to decrease or even substitute the use of IPA, which is known as a solvent with moderate matrix effect and high backpressure. For the separation of lipids, ACN as an organic phase was too weak. EtOH showed promising separation efficiency, but a full-fledged method would have taken too long to produce. Hence, the initial solvent mixtures A and B were used (A[60:40] H_2O:ACN and B[90:10] IPA:ACN).

For pre-optimization of the method, 7 ul of Splash mix was injected with a flow rate of 1 ml/min. The gradient was as follows: for the C18 column, the initial plateau of 60% B was kept between 0 and 8 minutes of detection, a ramp towards 97% B between 8 and 25 minutes established, and a 97% B plateau between 25 to 40 minutes held, followed by a post-time phase between 40 to 55 minutes; for the C8 column, the initial plateau of 40% B was kept between 0 and 8 minutes of detection, a ramp towards 70% between 8 and 9 minutes established, a 70% B plateau between 9 to 16 minutes held, another ramp towards 90% B conducted between 16 and 17 minutes, and finally a 90% B plateau kept between 17 to 25 minutes, followed by a post-time phase between 25 to 35 minutes. The comparison was done to test the suitability for both high-throughput and reasonable resolution analysis. When deciding on the column and method to use, the separation efficiency of the representative lipid group standards with the C8 column (*Figure 22*) was considered better for its shorter runtime and comparable peak shapes with the C18 column in exchange of lower and broader signals (*Figure 23*).

For a more simplified analysis, ranges where analytes retained at once were classified as bulks (**Bulk 1**: 11-16 minutes, **Bulk 2**: 18-21 minutes). In addition, potential bulks between 3-5 minutes (LPC, LPE) and around 12 minutes (PI, PG, very close to **Bulk 1**) was present.

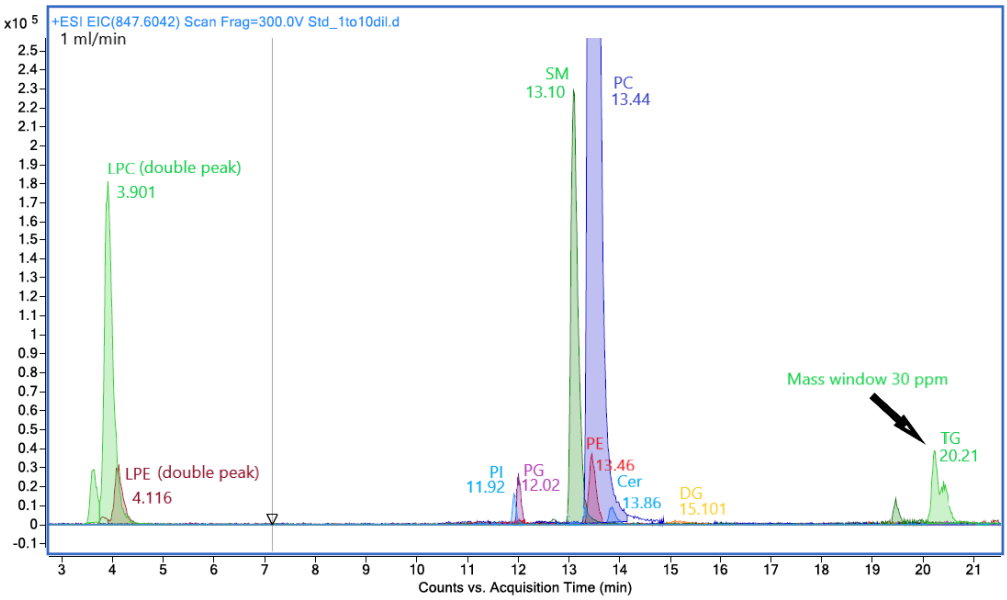

Figure 22. The initial HPLC method with a C8-column. Representative deuterated standard extracted ion chromatograms (EICs) are displayed.

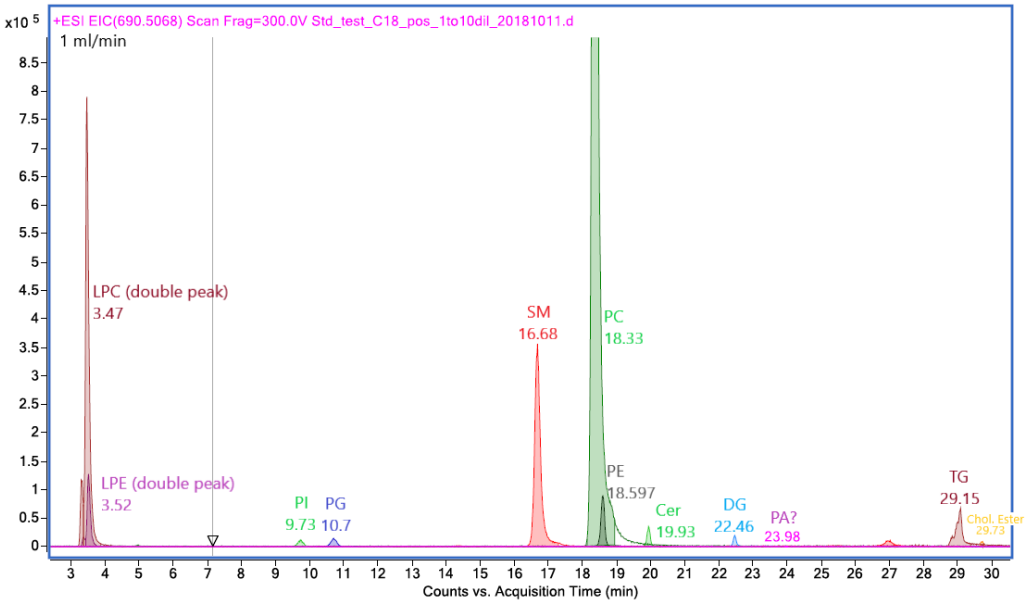

Figure 23. The initial lipid extraction method with a C18-column.
Representative deuterated standard EICs are displayed.

Next, a three-stepped gradient was chosen and improved experimentally to separate analytes more efficiently in the first five minutes of the runtime (*Table 23*).

Table 23. The optimized gradient

Time (min)	Solution A (%)	Solution B (%)
0	55 %	**45 %**
8	55 %	**45 %**
9	30 %	**70 %**
20	30 %	**70 %**
21	10 %	**90 %**
30	10 %	**90 %**
40	**← Posttime**	

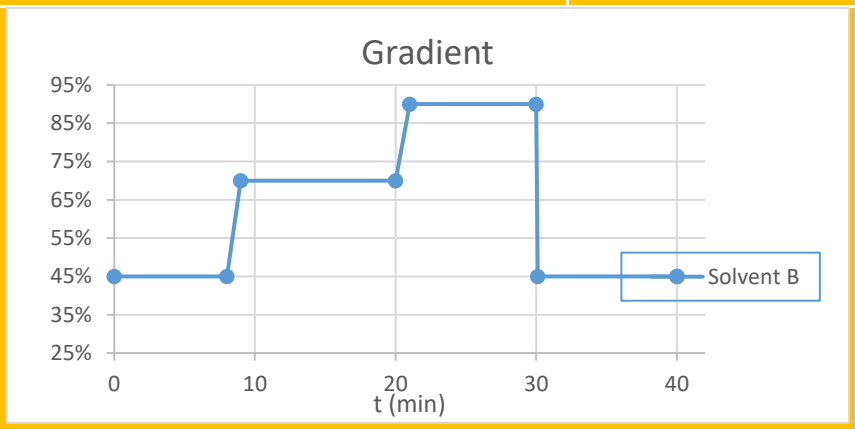

The flow rate's effect on the resolving power was inspected at 0.5, 0.7 and 1.0 ml/min (*Figure 24*). According to visual comparison of the three total ion chromatograms (TICs), a flow rate of 0.7 ml/min was chosen. As flow rate was increased, peaks after 10 minutes experienced only a slight shift in their retention times. This could point out to strong interaction between the column and the analytes, as the analytes after 10 minutes must have reached equilibrium with the packing material even at double the flow rate.

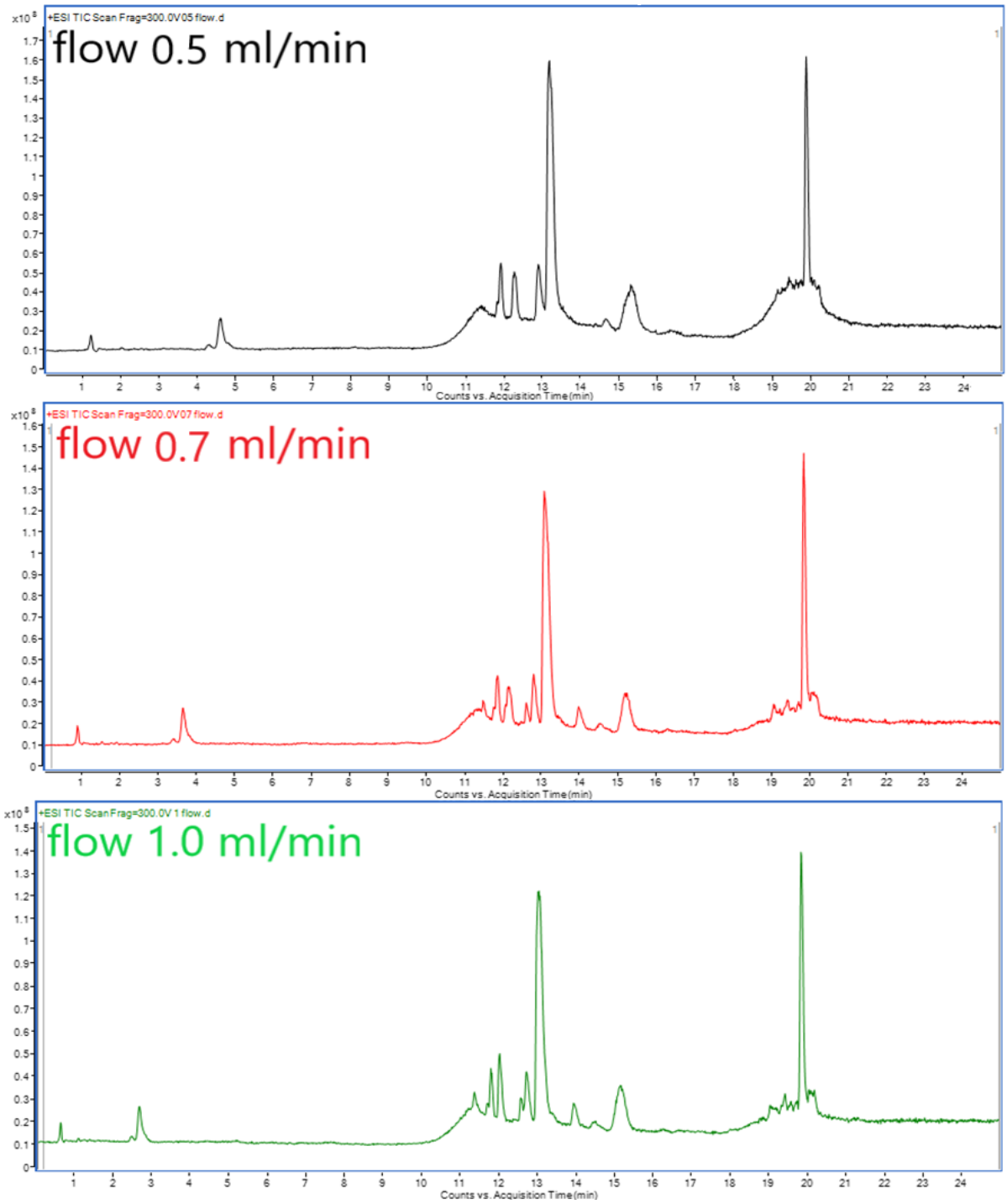

Figure 24. Chromatograms for flow rate optimization

After defining the flow to be used during analysis, the temperature was tuned manually with the help of separate runs (*Figure 25*). Not only were the RTs shifted to the left with increasing temperature and the background during the second "bulk" (**Bulk 1**: 11-16 minutes, **Bulk 2**: 18-21 minutes) substantially reduced, but peak broadening of the broadest peak at around 15.5 minutes was suppressed. Though some peaks were separated better than others, some peaks merged with each other or lost intensity.

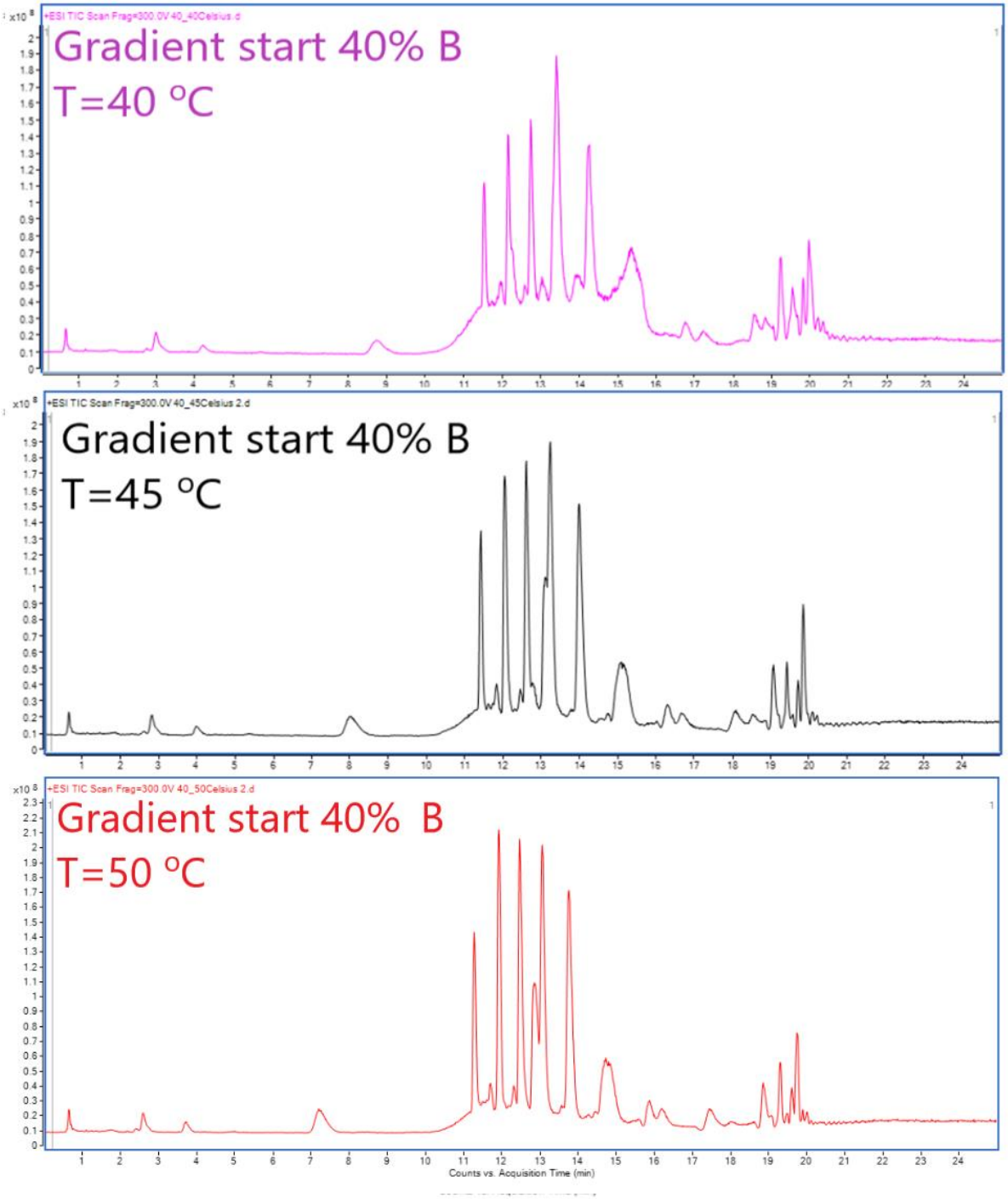

Figure 25. Chromatograms for temperature optimization

By only changing the starting conditions of the gradient from 40% B to 45% B, the separation of the second "bulk" of peaks were resolved in an improved manner (*Figure 26*). However, as the temperature was increased from 50 ˚C to 55 ˚C, a sharp up to three-fold decrease in signal sensitivity was observed. This could be explained with lipid degradation in high temperatures.

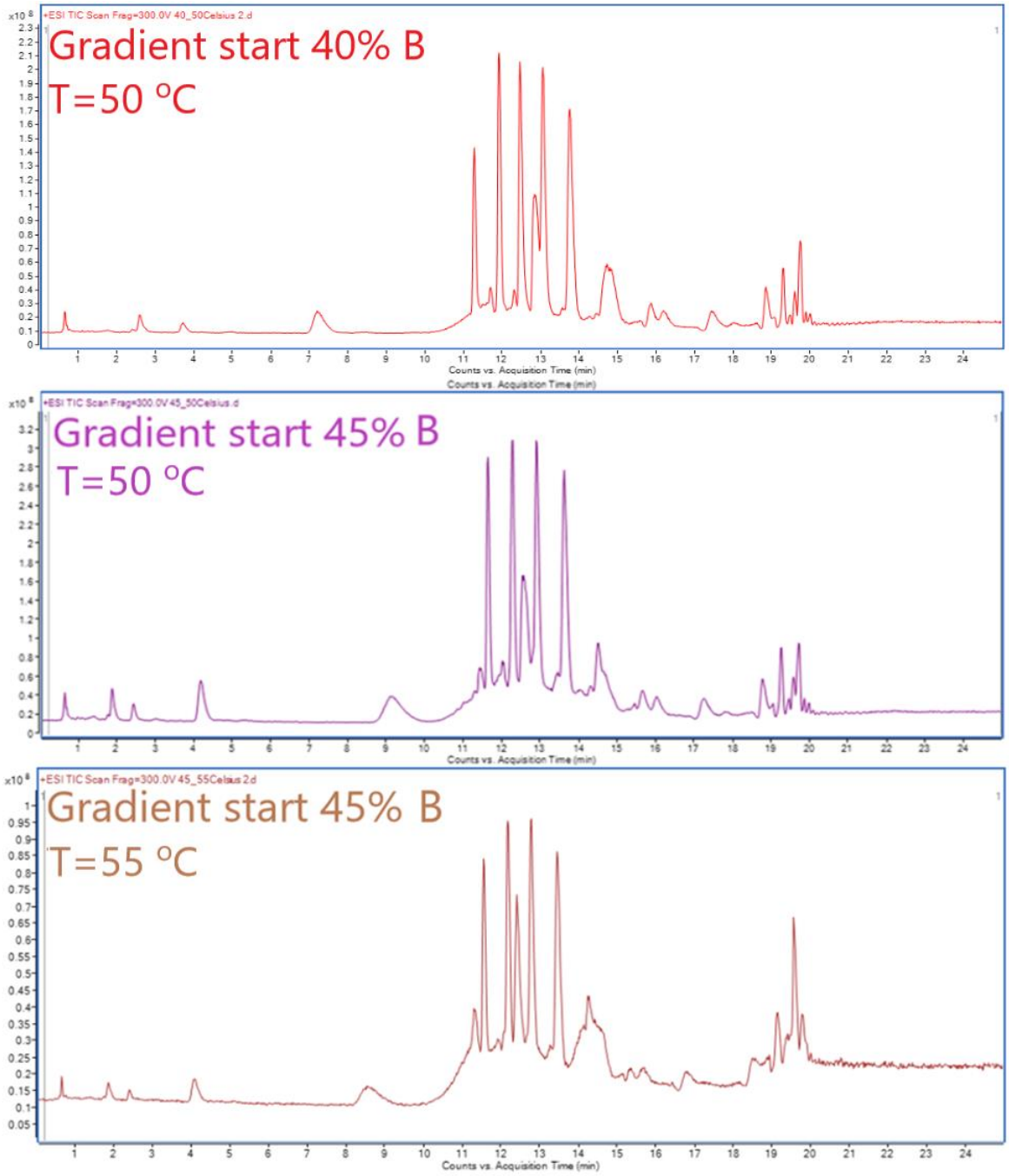

Figure 26. Modifications in gradient starting conditions and temperature
(final method in the middle)

In summary, the chromatograms with deviating run parameters were compared with each other visually in *Table 24* and *Table 25*. Thereby many factors could be considered at once in a more analytic manner. Improving separation and peak intensity I of simultaneously retained peak "bulks" were considered (**Bulk 1**: 11-16 minutes, **Bulk 2**: 18-21 minutes).

A shorter retention time, higher intensity or better separation efficiency was considered an improvement if other parameters stood the same or improved as well. However, as stated before, the flow rate was compromised because of the back pressure.

Table 24. Visual analysis of runs with different flow rates and gradients. Grey indicates the parameter staying the same, red as the parameter worsening from the perspective of performance and green as improving the chromatography (RT=retention time, I=intensity, STD=method that is compared)

Name	Description	Gradient	Bulk 1 (RT, I)	Bulk 2 (RT,I)	Separation
40%_45C 0.5	lower flow (ml/min)	Step	later, lower	later, higher	Same
40%_45C 0.7	middle flow (ml/min)	Step	later, same	later, higher	Same
40%_45C 1.0	max flow (ml/min)	Step	**STD**	**STD**	**STD**
35%_45C 1.0	Middle	Step	later, lower	later, lower	same/worse
30%_45C 1.0	Lower	Step	later, lower	later, lower	Worse
30%_45C 1.0 lin1	linear to 17	Linear	later, lower	earlier,lower	Worse
30%_45C 1.0 lin2	Linear to 22	Linear	later, lower	later, lower	worse

Table 25. Visual analysis of runs with different starting conditions and temperature (RT=retention time, I=intensity, STD=method that is compared)

Name	Description	Gradient	Bulk 1 (RT, I)	Bulk 2 (RT, I)	Separation
40%_45C 1.0	**STD**	Step	**STD**	**STD**	**STD**
40%_50C 1.0	higher temp	Step	earlier,higher	earlier,higher	same
40%_55C 1.0	higher temp	Step	earlier,higher	earlier,higher	better?
45%_45C 1.0	B 40%->45%	Step	earlier,higher	earlier,higher	better
45%_50C 1.0	**Final method**	Step	**earlier,higher**	**earlier,higher**	**better**
45%_55C		Step	earlier,lower	earlier,lower	same

12.1.2 Ion mobility and Mass spectrometry

The instrument was calibrated for a m/z range of under 3200 via a IM-QTOF tune before running the sequence. Mass spectrometer resolution for the calibration masses had to be >10,000 with IMS-QTOF and >20,000 for QTOF only, with a relative standard deviation of less than 1%. These criteria were met with a great margin to the limits mentioned above.

Collision energy experiments were executed in the form of *autoMSMS*. After some RTs and precursors were attained, the search for more fragmentation patterns was refined with a targeted MSMS approach: proper lipid adducts for each respective lipid class were established via a pre-optimization analysis (*Attachment 6*). Then, these precursors were added to the exclude-list at a discrete RT-range, including the rest of the lipids on the PCDL in the targets to be analyzed at their own RT.

A ramped CE profile between collision energies of 10, 15, 20 and 25 was evaluated to obtain the best fragmentation spectrum of the target analytes. These collision energies with arbitrary units of the instrument were tested in *autoMS*-mode and listed in *Table 26*. An optimal collision energy was determined so that the analyte was fragmented formidably, as long as the precursor ion was still separable from the background noise

Table 26. Optimized collision energies for lipid analytes. Bolded m/z fragments were verified via the Lipidmaps® mass-spectral Database

Name	Adduct	m/z	RT (min)	CE ()	Characteristic fragments
LPC(16:0) 1	H	496.3403	2.373	25	
LPC(18:0) 2	Na	546.3536	2.43	20	104.1068, 184.0744
LPC(18:1) 2	H	522.356	2.749	20	**104.1066**, **184.0733**, **504.3408***
LPE(20:0)	H	510.356	2.951	25	
LPC(18:0) 3	Na	546.3536	3.281	20	
DG(34:1) 1	Na-H2O	599.5015	10.504	25	
DG(34:0)	Na-H2O	601.5172	10.721	25	
DG(36:2) 1	Na	643.5277	10.933	20	
PS(34:1)	H	704.5594	11.6	20	**184.0733**, **124.9995**
PE(34:1) 1	H	718.5387	11.872	25	
PC(34:2) 1	H	758.57	12.055	25	
PC(34:0)	Na	784.5832	12.186	15	
SM(d36:1)	H	731.6067	12.318	25	
PE(34:0)	Na-H2O	724.5257	12.365	20	
PI(34:0)	H-H2O	829.5571	12.637	25	
PE(38:1) 2	H	774.6013	12.863	25	
PS(38:1)	H	818.5911	13	25	184.0743, 283.2609, 650.0833
SM(d40:0)	H	785.6537	13.291	25	
SM(d40:2)	H	789.685	13.308	25	
DG(34:1) 3	H	595.5302	13.77	25	577.5, 339.3
SM(d40:1)	H	787.6693	13.968	20	104.1066, **184.073**, 439.2024, 495.2649, 551.3269
DG(36:2) 1	Na	643.5277	13.971	20	
TG(50:1) 2	NH4	850.7864	23.203	20	**265.2515**, **239.2358**, **551.5013**, **577.5191**

*characteristic fragment is observed before fragmentation operation => water neutral loss?
RT=retention time, CE=collision energy (Agilent arbitrary units)

12.1.3 Data-analysis

12.1.3.1 Generation of an in-house database

Around 3000 GLs, GPs and SLs were extracted from the LIPID MAPS Structure Database (LMSD).[14] The extraction was performed by first choosing and downloading classes via the classification-based search of the LMSD, then limiting the possible lipids by removing deuterated and uneven fatty acyl chain species manually. Because the data analysis was intended to be performed mainly manually, the amount of analytes had to be decreased drastically. Further filtering of the lipid list was done by removing exact mass duplicates with Excel; this achieved lists with only one representative structural isomer for any possible variation of a subgroup's species' chemical formula. However, some overlap and thus removal of lipid class species with same exact masses may have taken place.

As the number of analytes was still impractical for the analysis at hand (~800 species), GL- and GPL-species were skimmed by their combined FA-carbon atom and double bond count. The filtering was done by excluding remaining lipids from a discrete molar mass range: for DGs this range included the species 30:0-40:6, for TGs 46:0-60:9, for PCs/PSs/PEs/PGs/PIs/PAs 30:0-40:2 and for the lyso-forms of PEs and PCs 14:0-22:6. The methoxy-forms of GPs (06 suffix of GP) was cut out entirely. From start to end, *Figure 27* illustrates the filtering process of PCDL formulas.

FAs were entirely cut out of the list, since no reliable signals were found during analysis. This is backed up by Tumanov et al, who claim the column and solvent combination not to be suited for FA separation. Instead, a more polar mobile phase is needed for a FAs as well as PAs.[21]

Creation and management of the PCDL was performed with the *Agilent MassHunter PCDL Manager B.08.00*, starting at first with only the name and the chemical formula of a compound. With the remaining 834 lipids (includes FAs), a test PCDL for adduct analysis was produced containing 102 manually picked lipids. The choice which lipids to include was a rough sketch of probable lipids. Again, this information can be retrieved from *Attachment 8.* Multiple adducts were documented for the upcoming quantitation, as the less abundant adduct was under the limit of saturation at times. Non-saturated signals were preferred, if the calibration and its respective peak area could be determined.

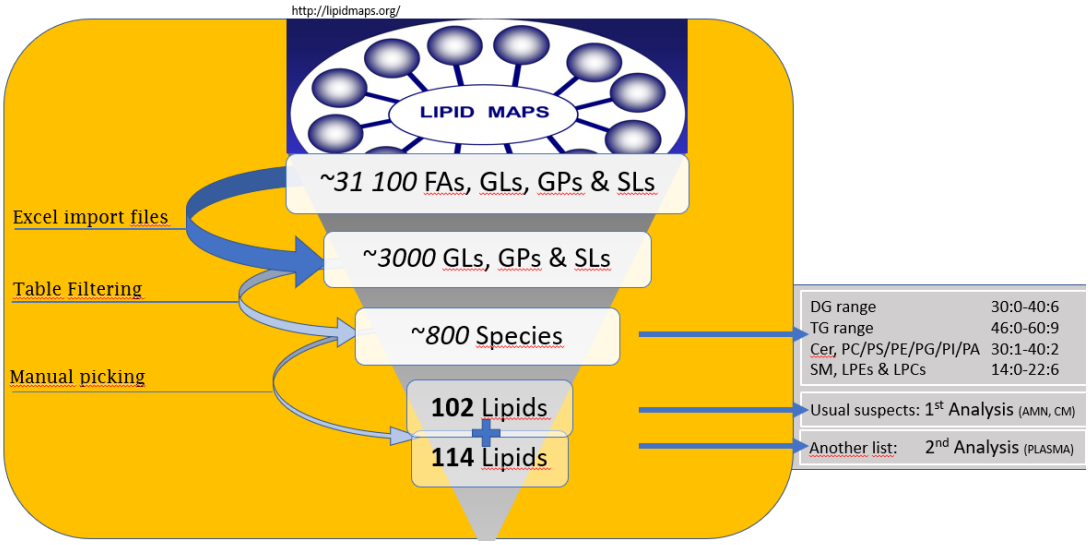

Figure 27. Selection of analytes and their formulas.
1st analysis: analysis conducted with CMs and amniotic fluid
2nd analysis: analysis conducted with plasma sample (overlap with 1st analysis)

As our perception of important common lipids improved, another 114 new and around 18 previously identified lipids were chosen to fill out various gaps in RTs and CCS values. The list included a handful of representatives of the groups MG, DG, TG, PC, PE, LPC, LPE, PS, PG, PI, Cer, SM CerPC and SM CerPE; now with more naturally abundant choices. The widely studied biomarker sphingosine-1-phosphate (S1P) and sphinganine-1-phosphate (SA1P) was also included in the PCDL.

12.2 Method optimization with plasma

The Folch-prepared plasma sample was used as the basis for the in-house built database for targeted lipidomic analysis in ascites. Having around 130 lipids with their respective formulas included in the PCDL, 70 RTs were spotted via Feature finding of *Qualitative Workflows B.08.00*. Furthermore, 36 CCS values were found for different lipid species via the *Mass Profiler* tool. The final PCDL used in the analysis can be further inspected in *Attachment 8. Qualitative Navigator B.08.00* was used for double checking deuterated standards that were not directly found via the exact masses included in the PCDL; some standards present in the surrogate mix were only found via separate inspection of the exact masses and their known retention times from earlier pre-experiments. In addition, 24 collision energies were optimized for potential MS/MS fragmentation analyses in the future.

12.2.1 Matrix effect analysis

Before identifying and quantitating lipids, matrix effects of all sample analytes in addition to pre-preparation added surrogates, were studied with the chromatographic method optimized for analysis. Samples included both the pooled QC sample, which included all control DLF and ascites samples in equal proportions by volume, and the control and prior samples separately. In hindsight though, this analysis only applied for the suppression of the ceramide peak area and its RT proximity (12.44 min). As different analytes are retained at a different RT, so is the case with matrix components, which varies the matrix effects along the runtime of a chromatogram. However, this can be circumvented in relative quantitation with an ISTD or surrogate.[19] Also, positive and negative mode are not directly comparable with each other as there are no complementary ions to be ionized.

The ISTD peak area included in ascites and DLF samples (~33 ppm) was retrieved from the *all ions* data and plotted as a function of time in *Figure 28* positive and *Figure 29* negative mode. As can be observed, a four- to near tenfold peak area was found for the surrogate in comparison to the clinical samples and their QC pools in positive ESI-mode. Thus, rather strong matrix-based ion suppression can be suggested during the analysis of these samples. However, it must be noted that the suppression of the pooled QC sample was greater than that of the individual samples. Speculatively, it could be a specific sample's contamination or the fact that a mixed sample degrades faster.

The DLF in both extractions showed a comparable matrix effect as in ascites, which pointed to at least similar suppression in both fluids. Both BUME and Folch showed a similar pattern, as all four samples were measured in the same order in sequence. In conclusion, the QC sample's three measurements before, in between and after the actual samples were evaluated as rather stable compared to each other, hence showing good instrumental stability and justifying the decision to only normalize the samples with the representative surrogates. DLF samples had ISTD peak areas in the same range as ascites samples, insinuating towards similar matrix effects occurring in both media.

In negative mode, even for the ISTD of the surrogate mix blank a three-fold suppression was observed. This is backed by Monnin et al, who observed in negative mode a "2- to 1000-fold signal suppression of all lipid classes" with ammonium hydroxide additive in comparison to acetic acid additive only, which in turn had an "2- to 19-fold" increase in intensity for all other

lipid subclasses except for the decreased signals for Cers and PCs. Apparently, even the lipid coverage increased by 21-50% by using only acetic acid instead of ammonium acetate, by direct consequence of the ionization efficiency improvement.[48]

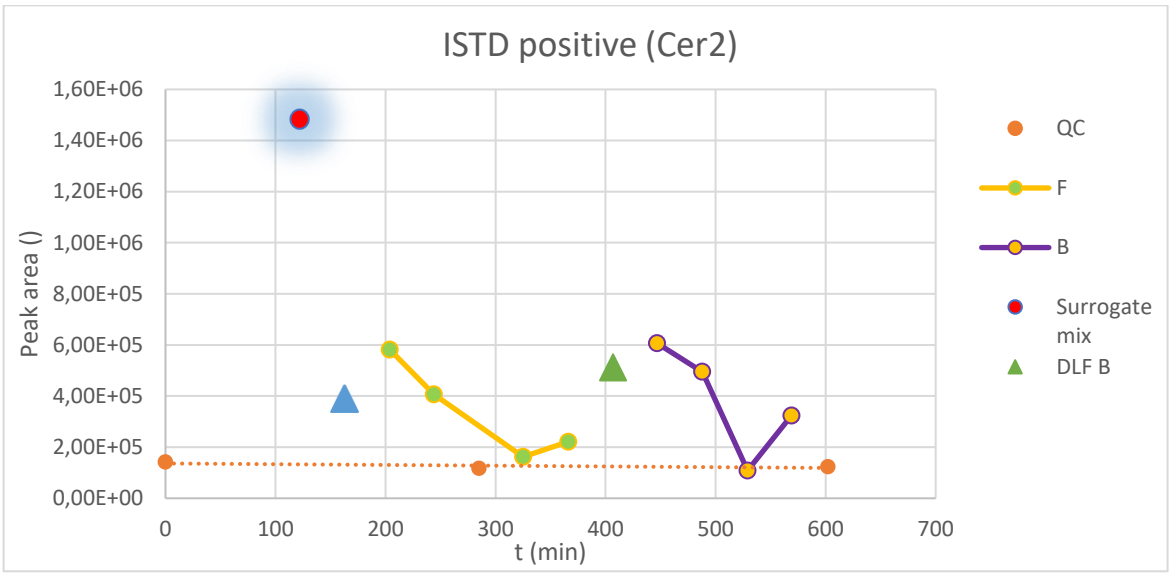

Figure 28. Peak areas of the deuterated internal standard (ceramide) in positive mode, as a function of time. The two line-graphs depict a set of four ascites samples extracted by either Folch (F) or BUME (B) to compare individual matrix effects among themselves, juxtapose their combined shape among the extraction methods or to set the samples against control sample (triangles) or the blank (surrogate).

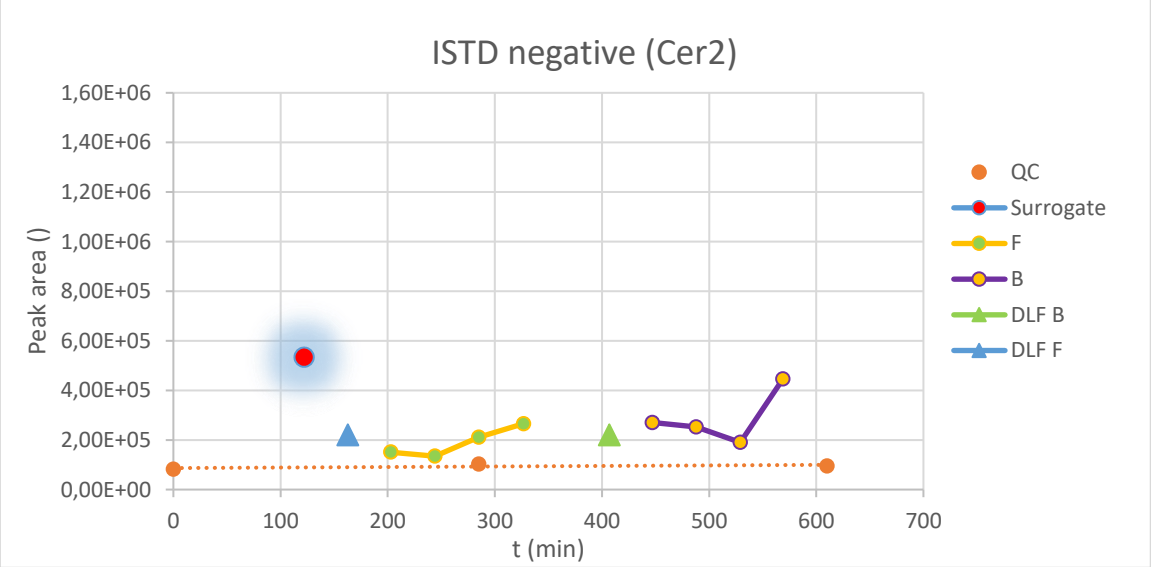

Figure 29. Peak areas of the deuterated internal standard in negative mode as a function of time, scaled to compare it more easily with positive mode.

12.2.2 Ascites and DLF samples

Increased injection volumes (from 10 µl plasma to 20 µl ascites) were used in the hope of finding low-abundance species. This combined with other factors (e.g. surprisingly high-abundance concentrations of lipids in aqueous solutions, co-elution) lead to frequent saturation of the detector. Though this was an expected hindrance to the accurate quantitation of lipids, it did work as a compromise to qualitatively detect both low-abundance and mid- to high-abundance species in the biological sample.

As stated in the experimental chapter, four ascites samples in addition to a DLF control sample were analyzed with a PCDL compounded from plasma sample analysis. The aim of the study was to profile common lipid species -preferably at least one of each lipid class of interest- in the ascites microenvironment. Chromatograms of the plasma sample, surrogate mix blank, DLF control samples and ascites samples were collected in *Attachment 9.*

After the preparative analysis and compounding of the PCDL the lipid groups DG, TG, PC, LPC, PE, LPE, PS, SM CerPC and SM CerPE were represented; in plasma, a low score of possible lipid classes PG, PI and Cer was observed; and finally, MG, S1P and sphinganine-1-phosphocholine were never found.

When ascites samples, DLF control samples, QC samples and the tenfold diluted surrogate mix were run with the optimized HPLC-IMS-MS method, a qualitative analysis with the PCDL was conducted to retrieve scored hits from the *all ions* scan data. The chromatographic data were analysed with Mass Profiler's *ID Browser B.08.00*: features with an exact mass window of 10 ppm were searched for, after which found features were identified and scored by comparing the experimental data (RT, CCS, m/z) with the PCDL data.

Table 27 summarizes the identification of lipids with both BUME and Folch as the sample preparation technique of ascites. With BUME, more hits were found for individual lipid species and a slightly greater amount of lipid species was attained.

Table 27. Summary of all lipid species identified with the PCDL: the totality of lipids identified in both analyses with the BUME and Folch extraction (**TOT**), total amount found in "**BUME**" or "**Folch**", the amount of "**SHARED**" and extraction-"**SPECIFIC**" analytes, and single extraction-specific identifications (o.o.w. single). In addition, species pairs with "**2 isomers**" were noted

o.o.w. single / analytes found in only one sample

TOT	SHARED	SPECIFIC	o.o.w. single
38	32	6	1

BUME	o.o.w. single	2 isomers
35	10	7

Folch	o.o.w. single	2 isomers
33	16	6

Moreover, lipid species hits were analyzed in a more detailled fashion to evaluate the plausibility and commonality of analytes (*Table 28*). Again, BUME tallied a higher amount of hits among and within extracted lipid species hits and the four ascites samples. The hits had scores over 79 and were manually controlled.

Table 28. Visualized amount of all hits found in respectively four prepared ascites samples (Folch or BUME). An empty field means no hits were found, full blue field means the analyte was found in all four ascites samples. The red fields show a respective (Σ) and combined (Tot.) total of species found when neglecting their isomers; isomers were denoted with a number at the end of their name.

		Folch	BUME
DG	DG(34:1) 1		
	DG(34:1) 3		
	DG(36:2) 1		
	DG(36:2) 2		
LPC	LPC(16:0) 1		
	LPC(18:0) 1		
	LPC(18:0) 2		
	LPC(18:0) 3		
	LPC(18:1) 1		
	LPC(18:1) 2		
LPE	LPE(16:0)		
	LPE(18:0) 1		
	LPE(18:0) 2		
	LPE(18:1)		
	LPE(20:0)		
PC	PC(34:0)		
	PC(34:1) 1		
	PC(34:1) 2		
	PC(34:2) 1		
	PC(34:2) 2		
	PC(O-34:1) 1		

		Folch	BUME
PE	PE(32:0)		
	PE(34:0)		
	PE(34:1) 1		
	PE(34:1) 2		
	PE(34:2)		
	PE(38:1) 2		
	PE(O-34:1)		
SM	SM(d36:1)		
	SM(d36:2)		
	SM(d40:0)		
	SM(d40:1)		
	SM(d40:2)		
TG	TG(48:0) 2		
	TG(50:1) 1		
	TG(52:1) 3		
	TG(52:2)		
	Σ (no isomers)	25	27
	Tot. (no isomers)	28	

Out of all the found lipids in total, 19 were present in three or all the ascites samples. Thus, these lipids were trusted to be most abundant in the clinical samples. This made them most likely to be relatively quantifiable by normalization and a one-point calibration with their representative deuterated surrogates.

The normalized peak areas were sorted out by lipid subclass and put into a histogram as a function of individual samples in *Figure 30*. After excluding the outlier samples LA-979 and LA-170 from properly stored and prepared ascites samples, the found lipid group concentrations of the ascites samples were in the range of 10-18.5 ppm for SM (DLF: 7 ppm), 0.08-0.7 ppm for DG (DLF: 0.08 ppm), 0.21-1.75 ppm for LPC (DLF: 0.4-1.66 ppm), 0.04-0.21 ppm for LPE (DLF: 0.06-0.15 ppm), 0.08-2.92 ppm for PE (DLF: 0.42 ppm) and 0.08-2.08 ppm for PC (DLF: N/A). Many, though not all, of the DLF lipid concentrations were representatively present compared to the ascites samples. However, the representativeness (i.e. homogeneity) of lipid species and classes should be checked case by case for applications.

After sampling of ascites in the operating room and transfer to the pathology department, some samples experienced deviating states and paths: a coagulation was formed due to processing purposes in LA-979 before centrifugation, leading to a suspicion of blood platelet lipid contamination. The coagulate-mixture was centrifuged along with the cell-pellet and pre-prepared accordingly. As another divergence, though fundamentally the same medium, the LA-170 ascites sample spent its first one week after sampling and centrifugation by protocol under 4 ˚C instead of staying under the safest storing temperature of -80 ˚C. The comparatively high concentrations of PCs in LA-979 and its large deviation at several species could hint towards the possible platelet contamination mentioned before. Similarly, the minimal concentrations observed in LA-170 communicate of a larger degradation of lipids, probably the result of the broken cold-chain before sample preparation. However, LA-827 and LA-833 concentrations stood surprisingly equal throughout lipid species.

Through more visual examination, lipid classes appeared to have distinct characteristics. If most abundant lipids express the most typical FAs (palmitic acid FA(16:N) and stearic acid FA(18:N)), the abundance of mixed DG(34:1) was greater than the isomers of two possible stearic acids in DG(36:1). In contrast, LPCs could have stearic acid chains, which can be further backed up by the concentration trend of the normalized PC graphs (“PC(34:2) 1” and “PC(34:1) 2” have been scaled by dividing by a factor of 10).

Moreover, LPEs and PEs showed a trend of longer FA chain lengths being more common compared with PCs and LPCs. This was observed and confirmed by other research team members in other lipidomics experiments. In conclusion, SM(40:N) had distinctly higher concentrations for double bonds with N=2 than N=1 or 0.

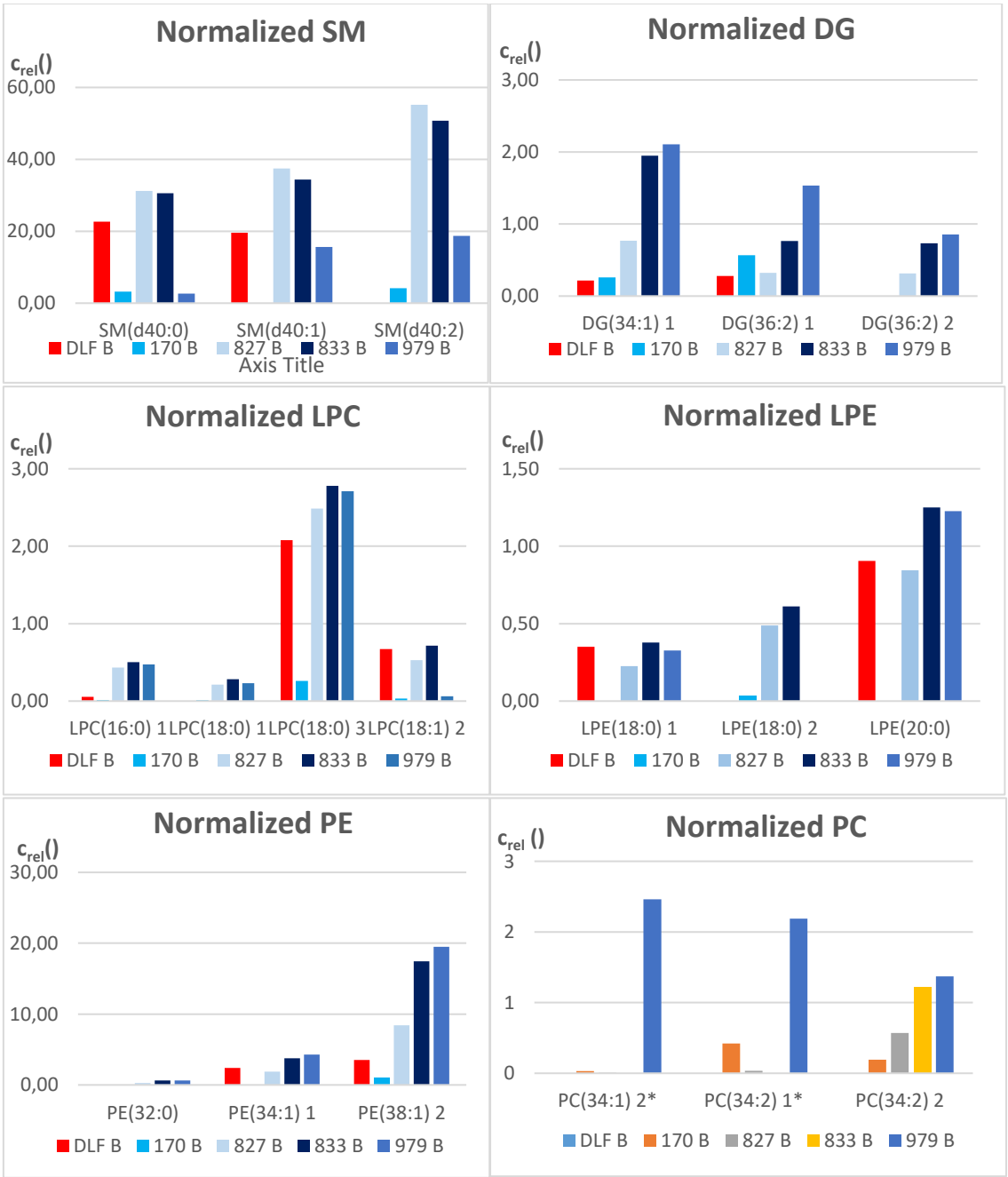

Figure 30. Relative concentration multipliers of normalized lipids. The lipids were sorted out according to their sample ID, lipid group and and lipid classes. The last number insinuates of a possible isomer. *: PC(34:1) 2 and PC(34:2) 1 was scaled to LPE(20:0) by dividing them by 10

13 Conclusions

Chromatographic methods in lipidomics are used to achieve either very selective or all-encompassing analyses for lipid classes, identifying lipid species from their molecular up to stereochemical structure. The review of the literature part studied and compared 63 articles between the years 2017-05/2019 to detect any trends and commonalities for the individual years and full time-frame. Apparently, HPLC/MS is an insufficient method for fully encompassing low-abundance lipids, which is why UHPLC/MS is needed. UHPLC/MS was mostly used for metabolic profiling where its large analyte range due to high sensitivity, separation efficiency and resolution excels in performance compared to other methods.

Sample preparation revolved around methods already established in lipidomics, e.g. Folch, Bligh and Dyer, and Matyash extractions from both biological tissues and fluids. If no ISTD normalization is conducted, special care must be taken to ensure specifity of the extraction for the lipid classes to be analysed: each extraction has their own extraction efficiency profile since lipids range from very nonpolar to polar species. Similarly, chromatographic methods revolved heavily around RPLC (UHPLC, nanoLC, SFC) while imaging techniques are spreading towards newly developed non-chromatographic methods (e.g. CRS, LESA) alongside DIMS and desorption techniques. RPLC was probably preferred due to easy lipid head group MS/MS identification and separation according to FAs and other nonpolar structures, but not vice versa like in NPLC.

According to my findings, the field of lipidomics is divided between studies using isotope-labeled standards or fully standardless algorithm-based analyses. Since computational methods alongside chemometric and statistical methods have increased in both importance and usage for cross-validation and data-analysis, lipidomics needs interdisciplinary studies to reach its full potential with big and complex datasets.

In the experimental part, a HPLC-MS method enhanced with IMS data was optimized for lipidomic analysis. Main glycero-, glycerophospho- and sphingolipids found in ascites samples were extracted and identified via a three-dimensional feature finding and identification analysis (including chromatographic separation, ion mobilities, and mass-to-charge ratios) in an *all ions* scan. An *all ions* scan was conducted for potential MS/MS fragmentation behaviour post-analysis, in addition to the conventional m/z- and CCS-values gathering for identification. The targeted analysis of the lipids was conducted with the assistance of a PCDL-list including common lipids in plasma, which in turn was created at the beginning of the study by accumulating information of supposed lipids in a single plasma sample. The initial set of plasma lipids was narrowed down from the vast LIPID MAPS Database into around 130 potential lipids including all lipid subgroups of interest.

During analysis, 70 RTs and 36 CCS values were found and added to the PCDL, leading to a total of 36 identified lipids found in ascites with a *Mass Profiler* library search score of over 79%. The score was determined by the fit of the theoretically (exact mass, formula of the compound) or experimentally (RTs, CCS values) claimed values in the PCDL compared to the instrumentally observed properties.

Possible errors and fields to improve are various: special care should be taken to keep the cold-chain uninterrupted and freeze-thaw cycles should be minimized. Furthermore, supportive research should be increased prior to choosing the right lipid analytes to be studied: some research representative clinical samples among the irrelevant ones. Limitations of this study could be addressed with research concentrating specifically on low-abundant lipids and the methods surrounding the topic (e.g. SPE, affinity chromatography and other concentration or depletion methods), studies on in-source fragmentation and fragmentation behaviour in MS/MS for identification purposes and optimization of sample dilution and injection volume to avoid unnecessary detector saturation. Saturation leads to the broadening of peaks, thus, to higher uncertainty in quantitation. Furthermore, the analysis in negative mode was left out entirely due to unfitting ESI-parameters and signal suppression proposedly caused by the ammonium additive. Lowest limit of detection (LOD) was observed when analysing the twentyfold dilution of the Splash mix: added deuterated Cer2 had a concentration of 0.1 mg/l, LPE, PE and PS a concentration of 0.25 mg/l. As the calibration of

representative samples included only one point and the samples were injected only once, no linearity or repeatability could be evaluated.

In hindsight, by using plasma as a feature-finding base we could only observe commonalities between this medium and the clinical samples. As there is wide heterogeneity between lipid arrangements of biological systems such as ascites and plasma, it may have been merely a snippet of the ascites lipidome that was observed.

14 Appendix List

Attachment 1.

Collected identification accuracy extremes (Acc. min/max) for UHPLC-MS lipidomic techniques

Attachment 2.

Further information about the columns and additives in the literature part

Attachment 3.

Standards for identification and quantitation

Attachment 4.

Method parameters for UHPLC/MS methods 2017, 2018 and 2019.

Attachment 5.

Extension of lipid classes analyzed in different research articles (2017-05/2019)

Attachment 6.

Potential ion species table of two amniotic fluid samples and three cell culture CMs.

Attachment 7.

The final PCDL

Attachment 8.

CCS values for attained adduct ion species

Attachment 9.

Chromatograms of the blank (surrogate mix), control samples (DLF F&B) and ascites samples (F&B)

15 Citations

[1] Fahy, E., Subramaniam, S., Brown, H. A., Glass, C. K., Merrill Jr, A. H., Murphy, R. C., Raetz, C. R. H., Russell, D.W., Seyama, Y., Shaw, W., Shimizu, T., Spener, F., van Meer, G., van Nieuwenhze, M. S., White, S. H., Witztum, J. L., & Shimizu, T. (2005). A comprehensive classification system for lipids. *European journal of lipid science and technology*, *107*(5), 337-364.

[2] Gross, R. W. (2017). The evolution of lipidomics through space and time. *Biochimica et Biophysica Acta (BBA)-Molecular and Cell Biology of Lipids*, *1862*(8), 731-739.

[3] Holcapek, M., Liebisch, G., & Ekroos, K. (2018). Lipidomic Analysis.

[4] LIPID MAPS: Tutorials and Lectures on Lipids, Categories of Lipids. 02.10.2018 http://lipidmaps.org/resources/tutorials/lipid_tutorial.php#FA

[5] Lam, S. M., Tian, H., & Shui, G. (2017). Lipidomics, en route to accurate quantitation. *Biochimica et Biophysica Acta (BBA)-Molecular and Cell Biology of Lipids*, *1862*(8), 752-761.

[6] Human Genome Project, history by the National Human Genome Research Institute NIH: https://www.genome.gov/human-genome-project/What, checked 01.01.2019

[7] Ghosh, A., & Nishtala, K. (2017). Biofluid lipidome: a source for potential diagnostic biomarkers. *Clinical and translational medicine*, *6*(1), 22.

[8] Fahy, E., Subramaniam, S., Murphy, R. C., Nishijima, M., Raetz, C. R., Shimizu, T., Spener, F., van Meer, G. , Wakelam, M. J. O., & Dennis, E. A. (2009). Update of the LIPID MAPS comprehensive classification system for lipids. *Journal of lipid research*, *50*(Supplement), 9-14.

[9] LIPID MAPS: Classification, nomenclature and structure drawing. 20.11.2018 https://www.lipidmaps.org/resources/tutorials/lipid_cns.html

[10] Dennis, EA: “LIPID MAPS Lipid Metabolics Tutorial, Fatty Acid Biosynthesis”, Powerpoint, 2010, University of California, San Diego

[11] Wakil, S. J., Stoops, J. K., & Joshi, V. C. (1983). Fatty acid synthesis and its regulation. *Annual review of biochemistry*, *52*(1), 537-579.

[12] Nelson DL, Cox MM (2005), Lehninger Principles of Biochemistry, 4th ed., W.H. Freeman & Co.

[13] Van Meer, G., Voelker, D. R., & Feigenson, G. W. (2008). Membrane lipids: where they are and how they behave. *Nature reviews Molecular cell biology*, *9*(2), 112.

[14] LIPID MAPS, Databases: "Classification-based search", Lipid Categories, 22.11.2018, http://lipidmaps.org/resources/databases/index.php

[15] Manni, M. M., Sot, J., Arretxe, E., Gil-Redondo, R., Falcón-Pérez, J. M., Balgoma, D., Alonso, C., Goñi, F. M., & Alonso, A. (2018). The fatty acids of sphingomyelins and ceramides in mammalian tissues and cultured cells: Biophysical and physiological implications. *Chemistry and physics of lipids*, *217*, 29-34.

[16] Kothari, C. R. (2004). *Research methodology: Methods and techniques*. New Age International, s.14

[17] Patterson, R. E., Ducrocq, A. J., McDougall, D. J., Garrett, T. J., & Yost, R. A. (2015). Comparison of blood plasma sample preparation methods for combined LC–MS lipidomics and metabolomics. *Journal of Chromatography B*, *1002*, 260-266.

[18] Jurowski, K., Kochan, K., Walczak, J., Barańska, M., Piekoszewski, W., & Buszewski, B. (2017). Comprehensive review of trends and analytical strategies applied for biological samples preparation and storage in modern medical lipidomics: State of the art. *TrAC Trends in Analytical Chemistry*, *86*, 276-289.

[19] Hyötyläinen, T., & Orešič, M. (2015). Optimizing the lipidomics workflow for clinical studies—practical considerations. *Analytical and bioanalytical chemistry*, *407*(17), 4973-4993.

[20] C.A. Zien, C.Wang, X.Wang, R. Welti, In vivo substrates and the contribution of the common phospholipase D, PLDalpha, to wound-induced metabolism of lipids in Arabidopsis, Biochim. Biophys. Acta 1530 (2001) 236–248.

[21] Tumanov, S., & Kamphorst, J. J. (2017). Recent advances in expanding the coverage of the lipidome. *Current opinion in biotechnology*, *43*, 127-133.

[22] Folch, J., Lees, M., & Sloane Stanley, G. H. (1957). A simple method for the isolation and purification of total lipides from animal tissues. *J biol Chem*, *226*(1), 497-509.

[23] Löfgren, L., Ståhlman, M., Forsberg, G. B., Saarinen, S., Nilsson, R., & Hansson, G. I. (2012). The BUME method: a novel automated chloroform-free 96-well total lipid extraction method for blood plasma. *Journal of lipid research*, *53*(8), 1690-1700.

[24] Lofgren, L., Stahlman, M., Forsberg, G. B., Saarinen, S., Nilsson, R., & Hansson, G. I. (2012). The BUME method: a novel automated chloroform-free 96-well total lipid extraction method for blood plasma. *Journal of lipid research*, jlr-D023036.

[26] Reis, A., Rudnitskaya et al. 2013 A comparison of five lipid extraction solvent systems for lipidomic studies of human LDL. *J Lipid Res*. 2013 Jul; 54(7): 1812–1824.

[27] Cruz, M., Wang, M., Frisch-Daiello, J., & Han, X. (2016). Improved Butanol–Methanol (BUME) Method by Replacing Acetic Acid for Lipid Extraction of Biological Samples. *Lipids*, *51*(7), 887-896.

[28] Yuan, Z. X., Majchrzak-Hong, S., Keyes, G. S., Iadarola, M. J., Mannes, A. J., & Ramsden, C. E. (2018). Lipidomic profiling of targeted oxylipins with ultra-performance liquid chromatography-tandem mass spectrometry. *Analytical and bioanalytical chemistry*, *410*(23), 6009-6029.

[29] Teo, C. C., Chong, W. P. K., Tan, E., Basri, N. B., Low, Z. J., & Ho, Y. S. (2015). Advances in sample preparation and analytical techniques for lipidomics study of clinical samples. *TrAC Trends in Analytical Chemistry*, *66*, 1-18.

[30] Bang, G., Kim, Y. H., Yoon, J., Yu, Y. J., Chung, S., & Kim, J. A. (2017). On-Chip Lipid Extraction Using Superabsorbent Polymers for Mass Spectrometry. *Analytical chemistry*, *89*(24), 13365-13373.

[31] Rainville, P. D., Stumpf, C. L., Shockcor, J. P., Plumb, R. S., Nicholson, J. K. J. Proteome Res. 6 (2007) 552.

[32] Onorato, J. M., Shipkova, P., Minnich, A., Aubry, A. F., Easter, J., & Tymiak, A. (2014). Challenges in accurate quantitation of lysophosphatidic acids in human biofluids. *Journal of lipid research*, *55*(8), 1784-1796. 1194/jlr.D050070

[33] Bligh, E. G., & Dyer, W. J. (1959). A rapid method of total lipid extraction and purification. Canadian journal of biochemistry and physiology, 37(8), 911-917

[34] Pöhö, P. (2013). Lipid profiling from biological samples.

[35] Zhang, H., Gao, Y., Sun, J., Fan, S., Yao, X., Ran, X., Zheng, C., Huang, M. & Bi, H. (2017). Optimization of lipid extraction and analytical protocols for UHPLC-ESI-HRMS-based lipidomic analysis of adherent mammalian cancer cells. *Analytical and bioanalytical chemistry*, *409*(22), 5349-5358.

[36] Ulmer, C. Z., Jones, C. M., Yost, R. A., Garrett, T. J., & Bowden, J. A. (2018). Optimization of Folch, Bligh-Dyer, and Matyash sample-to-extraction solvent ratios for human plasma-based lipidomics studies. *Analytica chimica acta*, *1037*, 351-357.

[37] Calderón, C., Sanwald, C., Schlotterbeck, J., Drotleff, B., & Lämmerhofer, M. (2019). Comparison of simple monophasic versus classical biphasic extraction protocols for comprehensive UHPLC-MS/MS lipidomic analysis of Hela cells. *Analytica chimica acta*, *1048*, 66-74.

[38] Lee, G. B., Lee, J. C., & Moon, M. H. (2019). Plasma lipid profile comparison of five different cancers by nanoflow ultrahigh performance liquid chromatography-tandem mass spectrometry. *Analytica Chimica Acta*.

[39] Ferchaud-Roucher, V., Croyal, M., Moyon, T., Zair, Y., Krempf, M., & Ouguerram, K. (2017). Plasma lipidome analysis by liquid chromatography-high resolution mass spectrometry and ion mobility of hypertriglyceridemic patients on extended-release nicotinic acid: a pilot study. *Cardiovascular drugs and therapy*, *31*(3), 269-279.

[40] Lemke, A., Castillo-Sánchez, J. C., Prodinger, F., Ceranic, A., Hennerbichler-Lugscheider, S., Pérez-Gil, J., Redl, H. & Wolbank, S. (2017). Human amniotic membrane as newly identified source of amniotic fluid pulmonary surfactant. *Scientific reports*, *7*(1), 6406.

[41] Ribeiro, M. A., Murgu, M., de Moraes Silva, V., Sawaya, A. C., Ribeiro, L. F., Justi, A., & Meurer, E. C. (2017). The screening of organic matter in mineral and tap water by UHPLC-HRMS. *Talanta*, *174*, 581-586.

[42] Castro-Gómez, P., Montero, O., & Fontecha, J. (2017). In-depth lipidomic analysis of molecular species of triacylglycerides, diacylglycerides, glycerophospholipids, and sphingolipids of buttermilk by GC-MS/FID, HPLC-ELSD, and UPLC-QToF-MS. *International journal of molecular sciences*, *18*(3), 605.

[43] Capriotti, A. L., Cavaliere, C., & Piovesana, S. (2019). Liposome protein corona characterization as a new approach in nanomedicine. *Analytical and bioanalytical chemistry*, 1-14.

[44] Rudralingam, Velauthan et al. "Ascites matters" Ultrasound (Leeds, England) vol. 25,2 (2016): 69-79.

[45] Van Meulebroek, L., De Paepe, E., Vercruysse, V., Pomian, B., Bos, S., Lapauw, B., & Vanhaecke, L. (2017). Holistic lipidomics of the human gut phenotype using validated ultra-high-performance liquid chromatography coupled to hybrid orbitrap mass spectrometry. *Analytical chemistry*, *89*(22), 12502-12510.

[46] Jeucken, A., & Brouwers, J. F. (2019). High-Throughput Screening of Lipidomic Adaptations in Cultured Cells. *Biomolecules*, *9*(2), 42.

[47] Erngren, I., Haglöf, J., Engskog, M. K., Nestor, M., Hedeland, M., Arvidsson, T., & Pettersson, C. (2019). Adduct formation in electrospray ionisation-mass spectrometry with hydrophilic interaction liquid chromatography is strongly affected by the inorganic ion concentration of the samples. *Journal of Chromatography A*, *1600*, 174-182.

[48] Monnin, C., Ramrup, P., Daigle-Young, C., & Vuckovic, D. (2018). Improving negative liquid chromatography/electrospray ionization mass spectrometry lipidomic analysis of human plasma using acetic acid as a mobile-phase additive. *Rapid Communications in Mass Spectrometry*, *32*(3), 201-211.

[49] Merrill Jr, A. H., Sullards, M. C., Allegood, J. C., Kelly, S., & Wang, E. (2005). Sphingolipidomics: high-throughput, structure-specific, and quantitative analysis of sphingolipids by liquid chromatography tandem mass spectrometry. *Methods*, *36*(2), 207-224.

[50] Fekete, S., Schappler, J., Veuthey, J. L., & Guillarme, D. (2014). Current and future trends in UHPLC. *TrAC Trends in Analytical Chemistry*, *63*, 2-13.

[51] Witting, M., Ruttkies, C., Neumann, S., & Schmitt-Kopplin, P. (2017). LipidFrag: Improving reliability of in silico fragmentation of lipids and application to the Caenorhabditis elegans lipidome. *PloS one*, *12*(3), e0172311.

[52] Danne-Rasche, N., Coman, C., & Ahrends, R. (2018). Nano-LC/NSI MS refines lipidomics by enhancing lipid coverage, measurement sensitivity, and linear dynamic range. *Analytical chemistry*, *90*(13), 8093-8101.

[53] Yang, K., & Han, X. (2016). Lipidomics: techniques, applications, and outcomes related to biomedical sciences. *Trends in biochemical sciences*, *41*(11), 954-969.

[54] Sethi, S., & Brietzke, E. (2017). Recent advances in lipidomics: Analytical and clinical perspectives. *Prostaglandins & other lipid mediators*, *128*, 8-16.

[55] Lísa, M., Cífková, E., Khalikova, M., Ovčačíková, M., & Holčapek, M. (2017). Lipidomic analysis of biological samples: comparison of liquid chromatography, supercritical fluid chromatography and direct infusion mass spectrometry methods. *Journal of Chromatography A*, *1525*, 96-108.

[56] Gross, Jürgen H. *Mass spectrometry: a textbook*. Springer Science & Business Media, 2006.

[57] Robinson, J. W., Frame, E. S., & Frame II, G. M. (2014). *Undergraduate instrumental analysis*. CRC press.

[58] Siu, K. W. M., Guevremont, R., Le Blanc, J. C. Y., O'brien, R. T., & Berman, S. S. (1993). Is droplet evaporation crucial in the mechanism of electrospray mass spectrometry?. *Organic mass spectrometry*, *28*(5), 579-584.

[59] Hogan Jr, C. J., Carroll, J. A., Rohrs, H. W., Biswas, P., & Gross, M. L. (2008). Combined charged residue-field emission model of macromolecular electrospray ionization. Analytical chemistry, 81(1), 369-377.

[60] Cech, N. B., & Enke, C. G. (2001). Practical implications of some recent studies in electrospray ionization fundamentals. *Mass spectrometry reviews*, *20*(6), 362-387.

[61] Drotleff, B., Hallschmid, M., & Lämmerhofer, M. (2018). Quantification of steroid hormones in plasma using a surrogate calibrant approach and UHPLC-ESI-QTOF-MS/MS with SWATH-acquisition combined with untargeted profiling. *Analytica chimica acta*, *1022*, 70-80.

[62] Beccaria, M., Inferrera, V., Rigano, F., Gorynski, K., Purcaro, G., Pawliszyn, J., Dugo, P., & Mondello, L. (2017). Highly informative multiclass profiling of lipids by ultra-high performance liquid chromatography–Low resolution (quadrupole) mass spectrometry by

using electrospray ionization and atmospheric pressure chemical ionization interfaces. *Journal of Chromatography A*, *1509*, 69-82.

[63] Xuan, Q., Hu, C., Yu, D., Wang, L., Zhou, Y., Zhao, X., Li, Q, Hou, X. & Xu, G. (2018). Development of a High Coverage Pseudotargeted Lipidomics Method Based on Ultra-High Performance Liquid Chromatography–Mass Spectrometry. *Analytical chemistry*, *90*(12), 7608-7616.

[64] Gobo, L. A., de Carvalho, L. M., Temp, F., Viana, C., & Mello, C. F. (2018). A rapid method for identification and quantification of prostaglandins in cerebral tissues by UHPLC-ESI-MS/MS for the lipidomic in vivo studies. *Analytical biochemistry*, *545*, 98-103.

[65] Chao, H. C., Chen, G. Y., Hsu, L. C., Liao, H. W., Yang, S. Y., Wang, S. Y., Li, Y. L., Tang, S. C., Tseng, Y. J., & Kuo, C. H. (2017). Using precursor ion scan of 184 with liquid chromatography-electrospray ionization-tandem mass spectrometry for concentration normalization in cellular lipidomic studies. *Analytica chimica acta*, *971*, 68-77.

[66] Lee, J. W., Mok, H. J., Lee, D. Y., Park, S. C., Kim, G. S., Lee, S. E., Lee, Y.S., Kim, K. P., & Kim, H. D. (2017). UPLC-QqQ/MS-based lipidomics approach to characterize lipid alterations in inflammatory macrophages. *Journal of proteome research*, *16*(4), 1460-1469.

[67] Kurulugama, R., Imatani, K., & Taylor, L. (2013). The Agilent Ion Mobility Q-TOF Mass Spectrometer System. *Technical overview by Agilent Technologies*.

[68] Riekkola, M. L., & Hyötyläinen, T. (2000). *Kolonnikromatografia ja kapillaarielektromigraatiotekniikat*. Helsingin yliopisto, analyyttisen kemian laboratorio.

[69] Taylor, N., White, T., & Viant, M. (2017). Defining the baseline and oxidant perturbed lipidomic profiles of daphnia magna. *Metabolites*, *7*(1), 11.

[70] Hu, A., Noble, W. S., & Wolf-Yadlin, A. (2016). Technical advances in proteomics: new developments in data-independent acquisition. *F1000Research*, *5*.

[71] Khouri, Hania, “IM-QTOF Training”, Agilent Technologies, 12.-18.01.2019 at the Department of Technical chemistry (Johannes-Kepler University Linz)

[72] Gorrochategui, E., Jaumot, J., Lacorte, S., & Tauler, R. (2016). Data analysis strategies for targeted and untargeted LC-MS metabolomic studies: Overview and workflow. *TrAC Trends in Analytical Chemistry*, *82*, 425-442.

[73] Koelmel, J. P., Kroeger, N. M., Ulmer, C. Z., Bowden, J. A., Patterson, R. E., Cochran, J. A., Beecher, C. W. W., Garrett, T. J.& Yost, R. A. (2017). LipidMatch: an automated workflow for rule-based lipid identification using untargeted high-resolution tandem mass spectrometry data. *BMC bioinformatics*, *18*(1), 331.

[74] Youtube-user "StatQuest with Josh Starmer": "*Principal Component Analysis (PCA) clearly explained (2015)*" https://www.youtube.com/watch?v=_UVHneBUBW0
Web-page checked 8.7.2019

[75] Youtube-user "Camo Analytics": "*PLS Basics*" https://www.youtube.com/watch?v=0xFdu5okHkw, Web-page checked 8.7.2019

[76] Youtube-user "StatQuest with Josh Starmer": "*StatQuest: Hierarchical Clustering*" https://www.youtube.com/watch?v=7xHsRkOdVwo, Web-page checked 8.7.2019

[77] Youtube user 'StatQuest with Josh Starmer': "StatQuest: FDR and the Benjamini-Hochberg Method clearly explained", https://www.youtube.com/watch?v=K8LQSvtjcEo, Web-page checked 18.07.2019

[78] Youtube-user "zedstatistics": Non-parametric tests - Sign test, Wilcoxon signed rank, Mann-Whitney https://www.youtube.com/watch?v=IcLSKko2tsg, Web-page checked 8.7.2019

[79] Law, T. H., Volk, H. A., Pan, Y., Zanghi, B., & Want, E. J. (2018). Metabolic perturbations associated with the consumption of a ketogenic medium-chain TAG diet in dogs with idiopathic epilepsy. *British Journal of Nutrition*, *120*(5), 484-490.

[80] Tietz-Bogert, P., Kim, M., Cheung, A., Tabibian, J., Heimbach, J., Rosen, C., Nandakumar, M., Lazaridis, K. N., LaRusso, N. F., Sung, J. & O'Hara, S. (2018). Metabolomic Profiling of Portal Blood and Bile Reveals Metabolic Signatures of Primary Sclerosing Cholangitis. *International journal of molecular sciences*, *19*(10), 3188.

[81] Calderón, C., Sanwald, C., Schlotterbeck, J., Drotleff, B., & Lämmerhofer, M. (2019). Comparison of simple monophasic versus classical biphasic extraction protocols for comprehensive UHPLC-MS/MS lipidomic analysis of Hela cells. *Analytica chimica acta*, *1048*, 66-74.

[82] Li, Z., Guan, M., Lin, Y., Cui, X., Zhang, Y., Zhao, Z., & Zhu, J. (2017). Aberrant lipid metabolism in hepatocellular carcinoma revealed by liver lipidomics. *International journal of molecular sciences*, *18*(12), 2550.

[83] Lee, D. Y., Kind, T., Yoon, Y. R., Fiehn, O., & Liu, K. H. (2014). Comparative evaluation of extraction methods for simultaneous mass-spectrometric analysis of complex lipids and primary metabolites from human blood plasma. *Analytical and bioanalytical chemistry*, *406*(28), 7275-7286.

[84] Sokol, E., Almeida, R., Hannibal-Bach, H. K., Kotowska, D., Vogt, J., Baumgart, J., Kristiansen, K., Nitsch, R, Knudsen, J., & Ejsing, C. S. (2013). Profiling of lipid species by normal-phase liquid chromatography, nanoelectrospray ionization, and ion trap–orbitrap mass spectrometry. *Analytical biochemistry*, *443*(1), 88-96.

[85] Zong, L., Pi, Z., Liu, S., Xing, J., Liu, Z., & Song, F. (2018). Liquid extraction surface analysis nanospray electrospray ionization based lipidomics for in situ analysis of tumor cells with multidrug resistance. *Rapid Communications in Mass Spectrometry*, *32*(19), 1683-1692.

[86] Kim, H. S., Waqued, S. C., Nodurft, D. T., Devarenne, T. P., Yakovlev, V. V., & Han, A. (2017). Raman spectroscopy compatible PDMS droplet microfluidic culture and analysis platform towards on-chip lipidomics. *Analyst*, *142*(7), 1054-1060.

[87] Gupta, A., Dorlhiac, G. F., & Streets, A. M. (2019). Quantitative imaging of lipid droplets in single cells. *Analyst*, *144*(3), 753-765. nanoflow liquid chromatography-tandem mass spectrometry. *Analytical chemistry*, *89*(4), 2488-2496.

[88] Blaženović, I., Shen, T., Mehta, S. S., Kind, T., Ji, J., Piparo, M., Cacciola, F., Mondello, L., & Fiehn, O. (2018). Increasing Compound Identification Rates in Untargeted Lipidomics Research with Liquid Chromatography Drift Time–Ion Mobility Mass Spectrometry. *Analytical chemistry*, *90*(18), 10758-10764.

[89] Lin, M., Wang, Z., Wang, D., Chen, X., & Zhang, J. (2019). A mathematical model-assisted UHPLC-MS/MS method for global profiling and quantification of cholesteryl esters in hyperlipidemic golden hamsters. *Analytical chemistry*.

[90] Dong, S., Zhang, R., Liang, Y., Shi, J., Li, J., Shang, F., Mao, X., & Sun, J. (2017). Changes of myocardial lipidomics profiling in a rat model of diabetic cardiomyopathy using UPLC/Q-TOF/MS analysis. *Diabetology & metabolic syndrome*, *9*(1), 56.

[91] Yang, J. S., Lee, J. C., Byeon, S. K., Rha, K. H., & Moon, M. H. (2017). Size dependent lipidomic analysis of urinary exosomes from patients with prostate cancer by flow field-flow fractionation and nanoflow liquid chromatography-tandem mass spectrometry. Analytical chemistry, 89(4), 2488-2496.

[92] Triebl, A., Trötzmüller, M., Hartler, J., Stojakovic, T., & Köfeler, H. C. (2017). Lipidomics by ultrahigh performance liquid chromatography-high resolution mass spectrometry and its application to complex biological samples. *Journal of Chromatography B*, *1053*, 72-80.

[93] Lloyd, A. J., Beckmann, M., Wilson, T., Tailliart, K., Allaway, D., & Draper, J. (2017). Ultra high performance liquid chromatography–high resolution mass spectrometry plasma lipidomics can distinguish between canine breeds despite uncontrolled environmental variability and non-standardized diets. *Metabolomics*, *13*(2), 15.

[94] Cheema, A., Mehta, K., Fatanmi, O., Wise, S., Hinzman, C., Wolff, J., & Singh, V. (2017). A Metabolomic and lipidomic serum signature from nonhuman primates administered with a promising radiation countermeasure, gamma-tocotrienol. *International journal of molecular sciences*, *19*(1), 79.

[95] Liu, M. Y., Burgos, A., Ma, L., Zhang, Q., Tang, D., & Ruan, J. (2017). Lipidomics analysis unravels the effect of nitrogen fertilization on lipid metabolism in tea plant (Camellia sinensis L.). *BMC plant biology*, *17*(1), 165.

[96] Wu, J., Wu, Q., Wang, D., Kong, J., Dai, W., Wang, X., & Yu, X. (2017). Common lipid features of lethal ventricular tarchyarrhythmias (LVTAs) induced by myocardial infarction and myocardial ion channel diseases. *Scientific reports*, *7*(1), 4220.

[97] Chen, Y., Wen, S., Jiang, M., Zhu, Y., Ding, L., Shi, H., Dong, P., Yang, J., & Yang, Y. (2017). Atherosclerotic dyslipidemia revealed by plasma lipidomics on ApoE−/− mice fed a high-fat diet. *Atherosclerosis*, *262*, 78-86.

[98] Patterson, R. E., Kirpich, A. S., Koelmel, J. P., Kalavalapalli, S., Morse, A. M., Cusi, K., Sunny, K., McIntyre, L. M., Garrett, T. J., & Yost, R. A. (2017). Improved experimental data processing for UHPLC–HRMS/MS lipidomics applied to nonalcoholic fatty liver disease. *Metabolomics*, *13*(11), 142.

[99] Li, Q., Liang, X., Zhao, L., Zhang, Z., Xue, X., Wang, K., & Wu, L. (2017). UPLC-Q-exactive orbitrap/MS-based lipidomics approach to characterize lipid extracts from bee pollen and their in vitro anti-inflammatory properties. *Journal of agricultural and food chemistry*, *65*(32), 6848-6860.

[100]Lee, J. H., Yang, J. S., Lee, S. H., & Moon, M. H. (2018). Analysis of lipoprotein-specific lipids in patients with acute coronary syndrome by asymmetrical flow field-flow fractionation and nanoflow liquid chromatography-tandem mass spectrometry. *Journal of Chromatography B*, *1099*, 56-63.

[101] Yan, B., Chu, H., Yang, D., Sze, K. H., Lai, P. M., Yuan, S., Shuai, H., Wang, Y., Kao, R. Y. T., Chan, J. F. W., & Yuen, K. Y. (2019). Characterization of the Lipidomic Profile of Human Coronavirus-Infected Cells: Implications for Lipid Metabolism Remodeling upon Coronavirus Replication. *Viruses*, *11*(1), 73.

[102] De Paepe, E., Van Meulebroek, L., Rombouts, C., Huysman, S., Verplanken, K., Lapauw, B., Wauters, J., Hemeryck, L. Y., Vanhaecke, L., & Vanhaecke, L. (2018). A validated multi-matrix platform for metabolomic fingerprinting of human urine, feces and plasma using ultra-high performance liquid-chromatography coupled to hybrid orbitrap high-resolution mass spectrometry. *Analytica chimica acta*, *1033*, 108-118.

[103] Kim, S. H., Yang, J. S., Lee, J. C., Lee, J. Y., Lee, J. Y., Kim, E., & Moon, M. H. (2018). Lipidomic alterations in lipoproteins of patients with mild cognitive impairment and Alzheimer's disease by asymmetrical flow field-flow fractionation and nanoflow ultrahigh performance liquid chromatography-tandem mass spectrometry. *Journal of Chromatography A*, *1568*, 91-100.

[104] Chao, Y., Gao, S., Wang, X., Li, N., Zhao, H., Wen, X., Kou, Z., & Dong, X. (2018). Untargeted lipidomics based on UPLC-QTOF-MS/MS and structural characterization reveals dramatic compositional changes in serum and renal lipids in mice with glyoxylate-induced nephrolithiasis. *Journal of Chromatography B*, *1095*, 258-266.

[105] Cheema, A., Hinzman, C., Mehta, K., Hanlon, B., Garcia, M., Fatanmi, O., & Singh, V. (2018). Plasma Derived Exosomal Biomarkers of Exposure to Ionizing Radiation in Nonhuman Primates. *International journal of molecular sciences*, *19*(11), 3427.

[106] Wu, J., Wu, Q., Dai, W., Kong, J., Lv, J., Yu, X., Wang, X., & Wang, D. (2018). Serum lipid feature and potential biomarkers of lethal ventricular tachyarrhythmia (LVTA) induced by myocardial ion channel diseases: a rat model study. *International journal of legal medicine*, *132*(2), 439-448.

[107] He, Z., Wang, Y., Zhang, Y., Cheng, H., & Liu, X. (2018). Stereoselective bioaccumulation of chiral PCB 91 in earthworm and its metabolomic and lipidomic responses. *Environmental pollution*, *238*, 421-430.

[108] Chen, Y., Ma, Z., Shen, X., Li, L., Zhong, J., Min, L. S., Xu, L., Li, H., Zhang, J., & Dai, L. (2018). Serum lipidomics profiling to identify biomarkers for non-small cell lung cancer. *BioMed research international*, *2018*.

[109] Gao, X., Luo, J., Lü, L., Zhang, L., Zhang, S., & Cui, J. (2018). RNA-Seq and UHPLC-Q-TOF/MS Based Lipidomics Study in Lysiphlebia japonica. *Scientific reports*, *8*(1), 7802.

[110] Shan, J., Qian, W., Shen, C., Lin, L., Xie, T., Peng, L., Xu, J., Yang, R., Ji, J., & Zhao, X. (2018). High-resolution lipidomics reveals dysregulation of lipid metabolism in respiratory syncytial virus pneumonia mice. *RSC Advances*, *8*(51), 29368-29377.

[111] Lee, H., Choi, J. M., Cho, J. Y., Kim, T. E., Lee, H. J., & Jung, B. H. (2018). Regulation of endogenic metabolites by rosuvastatin in hyperlipidemia patients: An integration of metabolomics and lipidomics. *Chemistry and physics of lipids*, *214*, 69-83.

[112] Rombouts, C., De Spiegeleer, M., Van Meulebroek, L., De Vos, W. H., & Vanhaecke, L. (2019). Validated comprehensive metabolomics and lipidomics analysis of colon tissue and cell lines. *Analytica Chimica Acta*.

[113] Shan, J., Qian, W., Kang, A., Peng, L., Xie, T., Lin, L., Di, L., Xiao, P., & Zhou, W. (2019). Lipid profile perturbations in the plasma and lungs of mice with LPS-induced acute lung injury

revealed by UHPLC-ESI-Q Exactive HF MS analysis. *Journal of pharmaceutical and biomedical analysis*, *162*, 242-248.

[114] Wang, J., Zhang, L., Xiao, R., Li, Y., Liao, S., Zhang, Z., Yang, W., & Liang, B. (2019). Plasma lipidomic signatures of spontaneous obese rhesus monkeys. *Lipids in health and disease*, *18*(1), 8.

[115] Zalloua, P., Kadar, H., Hariri, E., Farraj, L. A., Brial, F., Hedjazi, L., Lay, A. L., Colleum A., Dubus, J., Touboul, D., Matsuda, F., Lathrop, M., Nicholson, J. K.,Dumas, M. E. & Matsuda, F. (2019). Untargeted Mass Spectrometry Lipidomics identifies correlation between serum sphingomyelins and plasma cholesterol. *Lipids in health and disease*, *18*(1), 38.

[116] Wang, X., Xu, Y., Song, X., Jia, Q., Zhang, X., Qian, Y., & Qiu, J. (2019). Analysis of glycerophospholipid metabolism after exposure to PCB153 in PC12 cells through targeted lipidomics by UHPLC-MS/MS. *Ecotoxicology and environmental safety*, *169*, 120-127.

[117] Chamberlain, C. A., Hatch, M., & Garrett, T. J. (2019). Metabolomic and lipidomic characterization of Oxalobacter formigenes strains HC1 and OxWR by UHPLC-HRMS. *Analytical and bioanalytical chemistry*, 1-12.

[118] Creydt, M., Vuralhan-Eckert, J., Fromm, J., & Fischer, M. (2019). Effects of elevated CO2 concentration on leaves and berries of black elder (Sambucus nigra) using UHPLC-ESI-QTOF-MS/MS and gas exchange measurements. *Journal of plant physiology*, *234*, 71-79.

[119] Schlotterbeck, J., Chatterjee, M., Gawaz, M., & Lämmerhofer, M. (2019). Comprehensive MS/MS profiling by UHPLC-ESI-QTOF-MS/MS using SWATH data-independent acquisition for the study of platelet lipidomes in coronary artery disease. *Analytica chimica acta*, *1046*, 1-15.

[120] Byeon, S. K., Kim, J. Y., Lee, J. Y., Chung, B. C., Seo, H. S., & Moon, M. H. (2015). Top-down and bottom-up lipidomic analysis of rabbit lipoproteins under different metabolic conditions using flow field-flow fractionation, nanoflow liquid chromatography and mass spectrometry. *Journal of Chromatography A*, *1405*, 140-148.

[121] Chang, W. Q., Zhou, J. L., Li, Y., Shi, Z. Q., Wang, L., Yang, J., Li, P., Liu, L. F., & Xin, G. Z. (2017). An in vitro approach for lipolysis measurement using high-resolution mass spectrometry and partial least squares based analysis. *Analytica chimica acta*, *950*, 138-146.

[122] Hyötyläinen, T., & Orešič, M. (2014). Systems biology strategies to study lipidomes in health and disease. *Progress in lipid research*, *55*, 43-60.

[123] Criscuolo, A., Zeller, M., Cook, K., Angelidou, G., & Fedorova, M. (2019). Rational selection of reverse phase columns for high throughput LC–MS lipidomics. *Chemistry and physics of lipids*, *221*, 120-127.

[124] Pham, T. H., Zaeem, M., Fillier, T. A., Nadeem, M., Vidal, N. P., Manful, C., Cheema, S., Cheema, M., & Thomas, R. H. (2019). Targeting Modified Lipids during Routine Lipidomics Analysis using HILIC and C30 Reverse Phase Liquid Chromatography coupled to Mass Spectrometry. *Scientific reports*, *9*(1), 5048.

[125] Kitov, P. I., Han, L., Kitova, E. N., & Klassen, J. S. (2019). Sliding Window Adduct Removal Method (SWARM) for Enhanced Electrospray Ionization Mass Spectrometry Binding Data. *Journal of The American Society for Mass Spectrometry*, 1-9.

[126] Rampler, E., Coman, C., Hermann, G., Sickmann, A., Ahrends, R., & Koellensperger, G. (2017). LILY-lipidome isotope labeling of yeast: in vivo synthesis of 13 C labeled reference lipids for quantification by mass spectrometry. *Analyst*, *142*(11), 1891-1899.

[127] Phelps, D. L., Balog, J., Gildea, L. F., Bodai, Z., Savage, A., El-Bahrawy, M. A., Speller, A. V. M., Rosini, F., Kudo, H., McKenzie, J. S., Brown, R., Takáts, Z., & Brown, R. (2018). The surgical intelligent knife distinguishes normal, borderline and malignant gynaecological tissues using rapid evaporative ionisation mass spectrometry (REIMS). *British journal of cancer*, *118*(10), 1349.

[128] Zhang, J., Rector, J., Lin, J. Q., Young, J. H., Sans, M., Katta, N., Giese, N., Yu, W., Nagi, C., Suliburk, J., Liu, J., Bensussan, A.m DeHoog, R. J., Garza, K. Y., Ludolph, B., Sorace, A. G.,, Syed, A., Zahedivash, A., Milner, T. E., & Eberlin, L. S. (2017). Nondestructive tissue analysis for ex vivo and in vivo cancer diagnosis using a handheld mass spectrometry system. *Science translational medicine*, *9*(406), eaan3968.

[129] European Institute of Women's Health Eurohealth, "Women and ovarian cancer in the EU", 25.05.2018: https://eurohealth.ie/policy-brief-women-and-ovarian-cancer-in-the-eu-2018/

[130] Xu, Y. (2018). Lysophospholipid signaling in the epithelial ovarian cancer tumor microenvironment. Cancers, 10(7), 227.

[131] World cancer research fund, "Ovarian cancer statistics", page visited 22.11.2018: https://www.wcrf.org/dietandcancer/cancer-trends/ovarian-cancer-statistics

[132] European Network of Gynaecological Cancer Advocacy Groups. 2018. Ovarian Cancer Factsheet. https://engage.esgo.org/media/2017/08/ENGAGe_What_is_ovarian_cancer_en_FINAL-2018.pdf

[133] Perrotti, F., Rosa, C., Cicalini, I., Sacchetta, P., Del Boccio, P., Genovesi, D., & Pieragostino, D. (2016). Advances in lipidomics for cancer biomarkers discovery. *International journal of molecular sciences*, *17*(12), 1992.

[134] Qadir, M. I., & Malik, S. A. (2008). Plasma lipid profile in gynecologic cancers. *European journal of gynaecological oncology*, *29*(2), 158.

[135] Quehenberger, O., Armando, A. M., Brown, A. H., Milne, S. B., Myers, D. S., Merrill, A. H., Bandyopadhyay, S., Jones, K. N., Kelly, S., Shaner, R. L., Sullards, C. M., Wang, E., Murphy, R. C., Barkley, R. M., LEiker, T. J., Raetz, C. R. H., Guan, Z., Laird, G. M., Six, D. A., Russell, D. W., McDonald, J. G., Subramaniam, S., Fahy, E., & Dennis, E. A. (2010). Lipidomics reveals a remarkable diversity of lipids in human plasma. Journal of lipid research, jlr-M009449.

[136] Xiao, Y.J.; Schwartz, B.; Washington, M.; Kennedy, A.; Webster, K.; Belinson, J.; Xu, Y. Electrospray ionization mass spectrometry analysis of lysophospholipids in human ascitic fluids: Comparison of the lysophospholipid contents in malignant vs. nonmalignant ascitic fluids. Anal. Biochem. 2001, 290, 302–313.

[137] Lennart Eriksson, Sartorius Stedim Biotech, Umetrics Suite blog - "OPLS vs PCA: Explaining differences or grouping data? " https://blog.umetrics.com/explaining-differences-or-grouping-data-opls-da-vs-pca-data-analysis, page checked 24.06.2019

[138] Zhang, Y., Liu, Y., Li, L., Wei, J., Xiong, S., & Zhao, Z. (2016). High resolution mass spectrometry coupled with multivariate data analysis revealing plasma lipidomic alteration in ovarian cancer in Asian women. *Talanta*, *150*, 88-96.

16 Appendix

Attachment 1. Collected identification accuracy extremes (Acc. min/max) for UHPLC-MS lipidomic techniques

Citation	Acc. min	Acc. max
88	0.892	0.927
28	0.99	0.999
89	0.949	1.051
64	0.706	1.226
65	0.889	1.051
AVERAGE	89 %	105 %
SD	10 %	10 %

Attachment 2. Further information about the columns and additives in the literature part

Year	Citation	Precolumn	Column	Particle size (um)	Additives
2017	42	VanGuard 10x2.1 mm	Acquity HSS T3 100x2.1 mm	1.8	A&B: 5 mM AmFo, 0.5% FoA
2017	66		Hypersil GOLD 100x2.1	1.9	A&B: 20 mM AmFo, 0.1% FoA
2017	42	VanGuard 10x2.1 mm	Acquity HSS T3 100x2.1 mm	1.8	A&B: 0.1% NH4OH
2017	121		Acquity BEH C18 100x2.1 mm	1.7	-
2017	93		N/A	1.7	A&B: 10 mM AmAc
2017	35		Ascentis Express C18 100x2.1 mm	2.7	A&B: 5 mM, 0.1 FoA
2017	97		CORTECS™ C18 100x2.1 mm	1.6	B: 10 mM AmFo; 0.01% FoA
2017	65		Eclipse Plus C18 100x2.1	1.8	A: 10 mM AmAc 0.2% AcA
2017	99		CORTECS C18 100x2.1 mm	2.7	A&B: 10 mM AmAc
2017	51		Waters Cortecs C18 150x2.1 mm	1.6	A&B: 10 mM AmFo, 0.1% FoA
2017	90		Acquity CSH C18 50x2.1 mm	1.7	-
2017	39		Acquity CSH C18	1.7	A&B: 10 mM AmAc;0.1% FoA
2017	99		XSelect CSH C18 100x2.1 mm	2.5	A&B: 10 mM AmAc
2017	30		Acquity CSH C18 100x2.1 mm	2.1	A&B: 10 mM AmFo, 0.1% FoA
2017	96		hypersil GOLD C18 100x2.1 mm	1.9	A&B: 10 mM AmFo
2017	98		BEH C18 50x2.1 mm	1.7	A&B: 10 mM AmFo, 0.1% FoA
2017	91		BEH C18 70x0.1 mm	1.7	A&B: 5 mM AmFo, 0.05% FoA
2017	82		HSS T3 100x2.1 mm	1.7	A&B: 10 mM AmFo
2017	55		BEH HILIC 150x2.1 mm	1.7	A&B: 7 mM AmAc
2017	92		Waters BEH C8 100x1 mm	1.7	A&B: 10 mM AmFo, 0.1% FoA
2017	121		Acquity BEH C18 100x2.1 mm	1.7	A: 10 mM AmAc, 0.1% FoA
2017	62		Titan C18 100x2.1 mm	1.9	A: 20 mM AmFo
2017	95		C8 100x2.1 mm	1.8	A&B: 10 mM AmAc, 0.1% AcA
2017	94		Acquity BEH C18 50x2.1 mm	1.7	0.1% FoA
2017	41		Acquity HSS T3 100x2.1 mm	1.8	A&B: 0.1% FoA
2017	45		Acquity BEH 150x2.1 mm	1.7	3.5 mM AmAc

Year	Citation	Precolumn	Column	Particle size (um)	Additives
2018	110		CSH C18 100x2.1 mm	2.6	A&B: 5 mM AmFo, 0.1% FoA
2018	64		Poroshell 120EC C18 50x3.0 mm	2.7	0.02% AcA
2018	104		Xbridge™ BEH C18 100x2.1 mm	2.5	A&B: 10 mM AmFo 0.1% FoA
2018	79		Acquity C18 CSH 100x2.1 mm	1.7	0.1% FoA, 10 mM AmFo
2018	108		Kinetex C18 100x2.1 mm	1.7	A&B: 10 mM AmFo
2018	107		Kinetex C18 100x2.1 mm	2.6	A: 5 mM AmAc
2018	88	UPLC CSH C18 VanGuard 5x2.1 mm	Waters Acquity UPLC CSH C18 100x2.1 mm	1.7	A&B: 10 mM AmFo, 0.1% FoA
2018	106		hypersil GOLD C18 100x2.1 mm	1.9	A&B: 10 mM AmFo
2018	52	Supelco guard cartage 5x2.1 mm	Nanobore + Ascentis Express C18 150x2.1 mm	2.7	A&B: 10 mM AmFo, 0.1% FoA
2018	52	Supelco guard cartage 5x2.1 mm	Nanobore + Ascentis Express C18 150x2.1 mm	2.7	
2018	63		BEH C8 100x2.1 mm	1.7	A&B: 10 mM AmAc
2018	63		BEH C8 100x2.1 mm	1.7	A&B: 10 mM AmAc
2018	63		BEH C8 100x2.1 mm	1.7	A&B: 10 mM AmAc
2018	15		Acquity BEH C18 100x2.1 mm	3.5	A&B: 10 mM AmFo
2018	36		BEH C18 100x2.1 mm	N/A	A&B: 10 mM AmFo, 0.1% FoA
2018	100	ODS-P Watchers® C18 5x0.1 3 um*	Xbridge® BEH C18 70x0.1 mm**	1.7	A&B: 5 mM AmFo, 0.05% FoA
2018	103	ODS-P Watchers® C18 5x0.1 3 um*	Xbridge® BEH C18 70x0.1 mm**	1.7	A&B: 5 mM AmFo, 0.05% FoA
2018	28		ZorBAX RRHD Eclipse Plus C18 100x4.6 mm	1.8	A&B: 12 mM AmAc, A: +0.02% AcA
2018	61		Kinetex C18 50x2.1 mm	2.6	A&B: 0.1% FoA
2018	105	-	Acquity BEH C18 50x2.1 mm	1.7	A&B: 0.1% FoA
2018	101	-	Acquity BEH C18 100x2.1 mm	1.7	A: 0.1% AcA
2018	102		Acquity HSS T3 C18 150x2.1 mm	1.7	A&B: 0.1% FoA
2018	80		Waters BEH Amide 150x2.1 mm	1.7	6.5 mM AmHCO3
2018	80		Waters BEH Amide 150x2.1 mm	1.7	10 mM AmFo
2018	80		Waters BEH C18 100x2.1 mm	1.7	0.05% PFPA, 0.1%FoA
2018	80		Waters BEH C18 100x2.1 mm	1.7	0.05% PFPA, 0.01%FoA
2018	111		BEH C18 100x2.1 mm	1.7	A&B: 0.1% FoA
2018	79		Acquity C18 HSS 100x2.1 mm	1.8	0.1% FoA

Year	Citation	Precolumn	Column	Particle size (um)	Additives
2019	38		Xbridge® BEH C18 70x0.02 mm**	1.7	A&B: 5 mM AmFo, 0.05% NH4OH
2019	113		CSH C18 100x2.1 mm	1.7	A&B: 5 mM FoA, 0.1% FoA
2019	116		Xbridge C18 100x2.1 mm	1.7	A&B: 5 mM AmAc
2019	115	Acquity CSH	Acquity CSH C18	1.7	A&B: 0.1% AmFo 0.1% FoA
2019	37	CSH C18 VanGuard 5x2.1 mm	Acquity CSH C18 100x2.1 mm	1.7	A&B: 10 mM FoA, 0.1% FoA
2019	117	BEH C18 VanGuard	Acquity BEH C18 50x2.1 mm	1.7	A&B: 10 mM AmFo, 0.1% FoA
2019	46		HILIC 50x4.6 mm	1.7	B: 10 mM AmFo, A&B: 0.1% FoA
2019	46		HILIC 50x4.6 mm	1.7	B: 10 mM AmFo, A&B: 0.1% FoA
2019	119	C8 Security guard Ultra 2.1 um	Kinetex C8 150x2.1	1.7	A&B: 10 mM AmAc
2019	118		C18 150x2.1 mm	1.7	positive: A&B: 10 mM AmFo
2019	118		C18 150x2.1 mm	1.7	negative: A&B: 10 mM AmAc
2019	114	-	ZORBAX Eclipse Plus C18 100x2.1 mm	1.8	B: 10 mM AmAc, 0.01% FoA
2019	114		ZORBAX Eclipse Plus C18 100x2.1 mm	1.8	B: 10 mM AmAc, 0.01% FoA
2019	112	Hypersil GOLD 50x2.1 mm	Acquity BEH Phenyl 150x2.1 mm	1.7	3.5 AmAc
2019	89		BEH C18 100x2.1 mm	2.6	A&B: 10 mM AmAc, 0.1% FoA

Attachment 3. Standards for identification and quantitation. Surrogates and internal standards not included

Citation	Standards for identification/calibration	T/PT/UT	Quantitation? ISTD? Surrogate?
88	Representative standards	UT	no, no, no
51	Reference lipid matrix (e.g. chicken egg PC, e. coli extract, PS porcine brain…)	PT	no, no, no
92	Single representative standards	UT	Yes, no, yes (odd carb)
52	6 representative standards	UT	yes, no, yes (deuterated)
45	127 representative standards	T/UT	yes, no, yes (deuterated)
28	50 single standards	T	yes, no, yes
42	Single standards, reference matrix (butterBCR-519)	T	yes, no, yes
94	None	UT	no, yes, no
79	None	UT	relative, no, yes
107	None	UT	relative, no, yes
115	None	UT	relative, no, yes
39	None	UT	relative, no, yes
101	4 FAs, LPC and LPE respective representative standards	UT	relative, no, yes
114	N/A	UT	yes, no, yes
80	N/A	UT	yes, no, yes
106	19 representative standards	UT	no, no, yes
90	None	UT	(yes), no, no
104	None	UT	no, no, yes
96	None	UT	relative, no, yes
97	None	UT	no, no, yes
100	32 representative standards	UT	relative, yes, no
91	14+15 representative standards	UT	relative?, yes, no
103	12+13 representative standards	UT	relative?, yes, no
112	28 from 6 classes	T/UT	no, no, yes
82	N/A	UT	no, no, no
38	38 standards	T/UT	yes, no, yes
95	N/A	UT	no, no, no
105	None	UT	relative, no, yes
117	None	UT	relative, no, yes
102	291 target analytes	T/UT	no, no, yes
30	Reference lipid matrix, SPLASH, pseudo-plasma premixed standard solution	T/UT	yes, no, yes
86	None		
120	19 representative standards	UT	yes, no, yes?
46	None	UT	relative, no, no
89	17 CEs	PT/T	yes, no, yes
118	None	UT	no, no, no
108	PC, PE (both deuterated)	T/UT	yes, yes?, no?

Citation	Standards for identification/calibration	T/PT/UT	Quantitation? ISTD? Surrogate?
116	22 standards	T	relative, no, yes
15	SPLASH?	T	yes, no, yes
37	SPLASH	UT	no, no, yes
113	None	UT	relative, no, yes
109	None	UT	relative, no, no
119	N/A	UT	yes, yes, no
36	standard reference material	T	no, no, yes
110	None	UT	relative, no, yes
111	Representative standards	UT	yes, no, yes
63	7 representative standards	PT	relative, no, yes
61	12 standard reference steroids	UT	relative, no, yes
64	5 standard reference prostaglandins	T	yes*, no, yes
55	Representative standards	T/UT	yes, no, yes
98	Representative standards	UT	yes, no, yes
99	N/A	UT	relative, no, yes
35	N/A	UT	no, no, yes
41	None	UT	no, no, yes
62	56 representative standards	UT	no, no, yes
65	N/A	UT	relative, no, no
66	24 representative standards	UT	yes, no, yes
93	None	UT	no, no, no
121	1 representative standard	UT	relative, no, yes

SPLASH= deuterium-labelled, plasma-imitating Splash® Lipidomix® mixture, Avanti Polar Lipids Inc.

*quantification with standard addition

Attachment 4. Method parameters for UHPLC/MS methods 2017, 2018 and 2019. Column compartment temperatures marked with yellow are assumed to have a standard room temperature.

Mass analyser	t (min)	Flow (ml/min)	T[column] (˚C)	Ø (um)	Year	Citation
IM-QTOF	10	0.4	40	1.7	2017	55
Orbitrap	15.5	0.4	25	1.7	2017	93
Orbitrap	20	0.3	40	1.7	2017	45
Orbitrap	22	0.4	60	1.7	2017	95
Orbitrap	25	0.2	55	1.7	2017	121
Orbitrap	31	0.2	55	1.7	2017	121
Orbitrap	40	0.15	50	1.7	2017	92
QOrbitrap	20	0.35	45	1.9	2017	96
QOrbitrap	23	N/A	50	1.7	2017	98
QOrbitrap	25	N/A	25	2.7	2017	35
QOrbitrap	27	0.25	25	2.7	2017	99
QOrbitrap	28	0.25	25	2.5	2017	99
QqQ	18.1	0.3	40	1.8	2017	65
QqQ	25	0.4	40	1.9	2017	62
QqQ	30	0.25	40	1.9	2017	66
QTOF	4.6	0.5	45	1.8	2017	41
QTOF	12	0.4	25	1.8	2017	42
QTOF	12	4.00E-01	55	1.8	2017	82
QTOF	13	0.5	60	1.7	2017	94
QTOF	18	0.4	25	1.8	2017	42
QTOF	20	0.3	55	1.7	2017	90
QTOF	20	0.4	25	1.7	2017	30
QTOF	22	0.4	55	1.7	2017	39
QTOF	45	0.3	50	1.6	2017	97
UHR-QTOF	N/A	0.25	50	1.6	2017	51

Mass analyser	t (min)	Flow (ml/min)	T[column] (˚C)	Ø (um)	Year	Citation
IM-QTOF	15	0.6	65	1.7	2018	88
LTQ-Orbitrap	8	0.4	50	1.7	2018	111
LTQ-Orbitrap	20	0.26	55	1.7	2018	63
N/A	15	0.15	60	1.7	2018	15
Orbitrap	110	0.6	60	2.7	2018	52
Orbitrap	110	0.6	60	2.7	2018	52
QOrbitrap	18	0.4	45	2.1	2018	102
QOrbitrap	20	0.26	55	1.7	2018	63
QOrbitrap	20	0.35	45	1.9	2018	106
QOrbitrap	22	0.35	60	1.7	2018	36
QOrbitrap	30	0.3	60	1.7	2018	110
QOrbitrap		N/A	25	1.7	2018	80
QOrbitrap		N/A	25	1.7	2018	80
QOrbitrap		N/A	25	1.7	2018	80
QOrbitrap		N/A	25	1.7	2018	80
QQQ	3	0.4	23	2.7	2018	64
QTOF	5	0.3	30	2.6	2018	61
QTOF	13	0.5	60	1.7	2018	105
QTOF	13.5	0.3	25	1.7	2018	108
QTOF	15	0.3	50	2.6	2018	107
QTOF	20	0.5	55	1.7	2018	79
QTOF	20	0.3	45	2.5	2018	104
QTOF	28	0.5	55	1.8	2018	79
QTOF	N/A	N/A	25	N/A	2018	109
Qtrap	20	0.26	55	1.7	2018	63
Qtrap	30	0.4	45	1.7	2018	101
Qtrap	35	0.5	30	1.8	2018	28
LTQ	4	1	25	2.6	2019	46
Orbitrap Fusion	4	1	25	2.6	2019	46
QOrbitrap	15	0.4	60	1.7	2019	113
QOrbitrap	20	0.4	40	1.7	2019	112
QOrbitrap	23	0.5	25	1.7	2019	117
QOrbitrap	24	0.4	55	1.7	2019	115
QTOF	13	0.5	40	1.8	2019	114
QTOF	13	0.5	50	1.8	2019	114
QTOF	15	0.6	65	1.7	2019	37
QTOF	21	0.3	40	1.7	2019	89
QTOF	27	0.3	50	1.7	2019	118
QTOF	27	0.3	50	1.7	2019	118
QTOF	34	0.4	50	2.6	2019	119
Qtrap	15	0.45	40	3.5	2019	116
AVERAGE	**22**	**0.38**	**48**	**1.9**		
SD	**14**	**0.13**	**11**	**0.4**		

LTQ=linear trap quadrupole**/**linear ion trap (LIT)**, Qtrap=**quadrupole ion trap (QIT)**,**

UHR-QTOF=ultra-high resolution QTOF

Attachment 5. Extension of lipid classes analyzed in different research articles (2017-05/2019)

Citation	Theme	T/relT /UT/PT	FAcyls	CEs	SLs	STs	PRs	PKs	HDLs	LDLs	VLDLs	Identified lipids	Bio-markers
88	Method development	UT										429	
51	Method development	relT											
92	Method development	UT											
92	Method development	UT											
92	Method development	UT											
52	Method development	UT										436	
30	Method development	T/UT			*	*						207	
37	Method development	UT		*								292+206	
36	Method development	T	1									22	
63	Method development	PT		*								515+630+640 [D]	
62	Method development	UT		*								104	
121	Method development	UT	*									403	
35	Method development / cancer research	UT		*								226-414	
98	Method development / Metabolics	UT			*							83	8
55	Method development /cancer research	T/UT		*								132	
91	Cancer research	UT		*								286	34
82	Cancer research	UT											50
108	Cancer research	T/UT		*								493	14+10+2 [B]
101	Diseases	UT										24	
114	Diseases	UT										129	
106	Diseases	UT		*	*							749	16
90	Diseases	UT							1			12	9
104	Diseases	UT	*		*	*	*					179	
104	Diseases		*		*	*	*					196	

Citation	Theme	T/relT /UT/PT	FAcyls	CEs	SLs	STs	PRs	PKs	HDLs	LDLs	VLDLs	Identified lipids	Bio-markers
96	Diseases	UT										746	11
96	Diseases												
97	Diseases	UT				*						261+39	7
100	Diseases	UT				*						365	19
103	Diseases	UT										363	28
105	Diseases	UT	1									Features	Features
7	Diseases		1	*									>25
89	Diseases	relT/T	1						*	*	*	81 [A]	17 [A]
113	Diseases	UT			*								77
119	Diseases	UT	2										77
110	Diseases	UT	2		*							188+62	87
111	Diseases	UT	1									188 [C]	
111	Diseases		1										
39	Drug-testing	UT										155	
42	Foodstuff profiling	T										81	
79	Metabolomics	UT	*									61	
107	Metabolomics	UT											
115	Metabolomics	UT		*									
95	Metabolomics	UT			3							178	
117	Metabolomics	UT	1				1					97	
117	Metabolomics		1				1						
120	Metabolomics	UT							*	*		226	
46	Metabolomics	UT	1									249+451	
118	Metabolomics	UT				1						7	
116	Metabolomics	T										22	5
66	Metabolomics	UT		*								523	
45	Physiology	T/UT	*			*	*	*				Features	
28	Physiology	T	*										
15	Physiology	T										45	
109	Physiology	UT			1							283	
61	Physiology	UT				**						12	
64	Physiology	T	***									5	
99	Physiology	UT	2									184+150	
93	Physiology	UT											35

*Lipid classes not counted

**15 steroids

***5 prostaglandins

[A] for hyperlipidemia: plasma(74, 57 biomarkers), VLDL(74, 52 biomarkers), LDL(76, 42 biomarkers), HDL(73, 41 biomarkers)
[B] non-small cell lung cancer+lung benign disease+healthy controls
[C] metabolites

Attachment 6. Potential ion species table of two amniotic fluid samples and three cell culture CMs.

Attachment 7. Final PCDL

Name	Mass	Retention Time	NumSpectra	CCS Count
15:0-18:1(d7) DG	587.5506	10.89	0	1
15:0-18:1(d7) PA	667.5169		0	0
15:0-18:1(d7) PC	752.6061	12.212	0	1
15:0-18:1(d7) PE	710.5591	12.024	0	2
15:0-18:1(d7) PI	829.5698		0	0
15:0-18:1(d7) PS	754.549	10.954	0	1
15:0-18:1(d7) TG	811.7646	23.001	0	2
18:1(d7) LPC	528.3921	2.817	0	4
18:1(d7) LPE	486.3451	2.8	0	3
18:1(d7) MG	363.3366		0	0
18:1(d9) SM	737.6397	11.816	0	4
Cer(d34:0)	539.5277		0	0
Cer(d36:0)	567.559	22.774	0	0
Cer(d36:0) 2	495.3325		1	0
Cer(d36:1)	565.5434		0	0
Cer(d42:0(2OH))	683.6428	22.837	0	0
Cer(d46:0)	707.7156	16.573	0	0
Cer2(d9)	546.5686	12.435	0	6
DG(34:0)	596.538	10.721	0	1
DG(34:1) 1	594.5223	10.504	0	1
DG(34:1) 2	594.5223	10.851	0	0
DG(34:1) 3	594.5223	13.77	0	2
DG(36:2) 1	620.538	10.933	1	1
DG(36:2) 2	620.538	13.971	1	1
LPC(16:0) 1	495.3325	2.373	1	1
LPC(18:0) 1	523.3638	3.528	1	0
LPC(18:0) 2	523.3638	2.43	1	1
LPC(18:0) 3	523.3638	3.281	1	1
LPC(18:1) 1	521.3481	2.147	6	0
LPC(18:1) 2	521.3481	2.749	6	2
LPE(16:0)	453.2855	2.571	0	0
LPE(18:0) 1	481.3168	2.183	2	1
LPE(18:0) 2	481.3168	3.627	2	0
LPE(18:1)	479.3012	2.799	0	0
LPE(20:0)	509.3481	2.951	1	2
MG(16:0)	330.277	3.988	0	0
MG(18:1)	356.2927	4.413	0	0
PC(32:0)	733.5622		0	0
PC(34:0)	761.5935	12.186	2	1
PC(34:1) 1	759.5778	11.671	1	0
PC(34:1) 2	759.5778	12.52	1	2
PC(34:2) 1	757.5622	11.873	0	2
PC(34:2) 2	757.5622	12.055	0	1
PC(O-32:0)	719.5829		0	0
PC(O-34:0)	747.6142		0	1
PC(O-34:1) 1	745.5985	12.414	0	0
PC(O-34:1) 2	745.5985	24.968	0	0

Name	Mass	Retention Time	NumSpectra	CCS Count
PE(32:0)	691.5152	11.033	0	0
PE(34:0)	719.5465	12.365	0	1
PE(34:1) 1	717.5309	11.872	0	1
PE(34:1) 2	717.5309	12.298	0	0
PE(34:2)	715.5152	11.441	0	0
PE(38:1) 1	773.5935	12.236	1	0
PE(38:1) 2	773.5935	12.863	1	1
PE(O-32:0)	677.5359	12.83	0	0
PE(O-34:0)	705.5672	11.847	0	0
PE(O-34:1)	703.5516	11.6	0	1
PG(32:0)	722.5098	11.6	0	0
PG(34:0)	750.5411		0	0
PG(34:1)	748.5254		0	0
PG(38:1)	804.588	13.341	0	0
PG(38:2) 1	802.5724	12.615	0	0
PG(38:2) 2	802.5724	12.895	0	0
PG(38:3)	800.5567	12.12	0	0
PI(32:0)	810.5258		0	0
PI(34:0)	824.5779	12.637	0	1
PI(34:1)	822.5622	11.128	0	1
PS(32:0)	735.505		0	0
PS(34:0)	763.5363		0	0
PS(34:1)	761.5207		0	0
SM(d34:0)	704.5832	11.821	0	0
SM(d36:0)	732.6145		0	0
SM(d36:1)	730.5989	12.318	1	2
SM(d36:2)	728.5832	11.824	0	0
SM(d40:0)	784.6458	13.291	0	2
SM(d40:1)	786.6615	13.968	1	2
SM(d40:2)	788.6771	13.308	1	1
TG(48:0) 1	806.7363	23.17	0	0
TG(48:0) 2	806.7363	23.434	0	0
TG(50:0)	834.7676		0	0
TG(50:1) 1	832.752	22.709	5	0
TG(50:1) 2	832.752	23.203	5	1
TG(52:1) 1	860.7833	22.902	1	0
TG(52:1) 2	860.7833	22.989	1	0
TG(52:1) 3	860.7833	23.402	1	0
TG(52:2)	858.7676	22.791	0	0

Attachment 8. CCS values for attained adduct ion species

Name	Ion Species	CCS	Date_mode	Formula
15:0-18:1(d7) PE	(M-H)-	245.81	20190307_NEG	C38 H67 D7 N O8 P
18:1(d7) LPE	(M-H)-	199.68	20190307_NEG	C23 H39 D7 N O7 P
Cer2(d9)	(M-H)-	229.44	20190307_NEG	C34 H58 D9 N O3
Cer2(d9)	(M+CH3COO)-	239.23	20190307_NEG	C34 H58 D9 N O3
LPE(18:0) 1	(M-H)-	203.21	20190130_NEG	C23 H48 N O7 P
PC(34:1) 2	(M+CH3COO)-	273.31	20190130_NEG	C42 H82 N O8 P
PC(34:2) 1	(M+CH3COO)-	272.16	20190130_NEG	C42 H80 N O8 P
PI(34:1)	(M+CH3COO)-[-H2O]	273.66	20190130_NEG	C43 H83 O12 P

Name	Ion Species	CCS	Date_mode	Formula
15:0-18:1(d7) DG	(M+H)+[-H2O]	238.46	20190307_POS	C36 H61 D7 O5
15:0-18:1(d7) PC	(M+H)+	265.96	20190307_POS	C41 H73 D7 N O8 P
15:0-18:1(d7) PE	(M+H)+	252.95	20190307_POS	C38 H67 D7 N O8 P
15:0-18:1(d7) PS	(M+H)+	260	20190307_POS	C39 H67 D7 N O10 P
15:0-18:1(d7) TG	(M+Na)+	288.69	20190307_POS	C51 H89 D7 O6
15:0-18:1(d7) TG	(M+NH4)+	290.39	20190307_POS	C51 H89 D7 O6
18:1(d7) LPC	(2M+H)+	308.23	20190307_POS	C26 H45 D7 N O7 P
18:1(d7) LPC	(2M+Na)+	311.99	20190307_POS	C26 H45 D7 N O7 P
18:1(d7) LPC	(M+H)+	217.18	20190307_POS	C26 H45 D7 N O7 P
18:1(d7) LPC	(M+Na)+	220	20190307_POS	C26 H45 D7 N O7 P
18:1(d7) LPE	(M+H)+	201.36	20190307_POS	C23 H39 D7 N O7 P
18:1(d7) LPE	(M+H)+[-H2O]	200.82	20190307_POS	C23 H39 D7 N O7 P
18:1(d9) SM	(2M+H)+	385.1	20190307_POS	C41 H72 D9 N2 O6 P
18:1(d9) SM	(M+H)+	267.45	20190307_POS	C41 H72 D9 N2 O6 P
18:1(d9) SM	(M+H)+	273.7	20190307_POS	C41 H72 D9 N2 O6 P
18:1(d9) SM	(M+Na)+	267.98	20190307_POS	C41 H72 D9 N2 O6 P
Cer2(d9)	(2M+Na)+	348.31	20190307_POS	C34 H58 D9 N O3
Cer2(d9)	(M+H)+	238.97	20190307_POS	C34 H58 D9 N O3
Cer2(d9)	(M+H)+[-H2O]	235.62	20190307_POS	C34 H58 D9 N O3
Cer2(d9)	(M+Na)+	233.8	20190307_POS	C34 H58 D9 N O3
DG(34:0)	(M+Na)+[-H2O]	241.27	20190130_POS	C37 H72 O5
DG(34:1) 1	(M+Na)+[-H2O]	240.91	20190130_POS	C37 H70 O5
DG(34:1) 3	(M+Na)+	241.61	20190130_POS	C37 H70 O5
DG(36:2) 1	(M+H)+[-H2O]	243.73	20190130_POS	C39 H72 O5
LPC(16:0) 1	(M+H)+	213.78	20190130_POS	C24 H50 N O7 P
LPC(18:0) 2	(M+Na)+	215.21	20190130_POS	C26 H54 N O7 P
LPC(18:0) 3	(M+H)+	222.46	20190130_POS	C26 H54 N O7 P
LPC(18:1) 2	(M+H)+	216.85	20190130_POS	C26 H52 N O7 P
LPC(18:1) 2	(M+H)+[-H2O]	213.2	20190130_POS	C26 H52 N O7 P
LPC(18:1) 2	(M+H)+	216.85	20190130_POS	C26 H52 N O7 P
LPE(20:0)	(M+H)+	217.42	20190130_POS	C25 H52 N O7 P
LPE(20:0)	(M+H)+	217.42	20190130_POS	C25 H52 N O7 P
PC(34:0)	(M+Na)+	270.82	20190130_POS	C42 H84 N O8 P

Name	Ion Species	CCS	Date_mode	Formula
PC(34:1) 2	(2M+H)+	391.59	20190130_POS	C42 H82 N O8 P
PC(34:1) 2	(2M+H)+	391.59	20190130_POS	C42 H82 N O8 P
PC(34:2) 1	(M+Na)+	212.1	20190130_POS	C42 H80 N O8 P
PC(34:2) 2	(M+H)+	266.15	20190130_POS	C42 H80 N O8 P
PC(O-34:0)	(M+Na)+	271.38	20190130_POS	C42 H86 N O7 P
PE(34:0)	(M+Na)+[-H2O]	260.3	20190130_POS	C39 H78 N O8 P
PE(34:1) 1	(M+H)+	255.94	20190130_POS	C39 H76 N O8 P
PE(38:1) 2	(M+H)+	271.43	20190130_POS	C43 H84 N O8 P
PE(O-34:1)	(M+NH4)+[-H2O]	264.48	20190130_POS	C39 H78 N O7 P
SM(d36:1)	(M+H)+	270.96	20190130_POS	C41 H83 N2 O6 P
SM(d36:1)	(M+Na)+	271.25	20190130_POS	C41 H83 N2 O6 P
SM(d36:1)	(M+H)+	270.96	20190130_POS	C41 H83 N2 O6 P
SM(d40:0)	(M+H)+	279.71	20190130_POS	C45 H89 N2 O6 P
SM(d40:0)	(M+Na)+	278.62	20190130_POS	C45 H89 N2 O6 P
SM(d40:0)	(M+H)+	279.71	20190130_POS	C45 H89 N2 O6 P
SM(d40:1)	(M+H)+	281.86	20190130_POS	C45 H87 N2 O6 P
SM(d40:1)	(M+Na)+	281.87	20190130_POS	C45 H87 N2 O6 P
SM(d40:2)	(M+Na)+	282.86	20190130_POS	C45 H93 N2 O6 P
TG(50:1) 2	(M+NH4)+	297.07	20190130_POS	C53 H100 O6

Attachment 9. From left to right, all ions chromatograms of the plasma sample, blank (surrogate mix), control samples (LA-670 DLF F&B) and ascites samples (LA-170 F&B, LA-827 F&B, LA-833 F&B and LA-979 F&B)

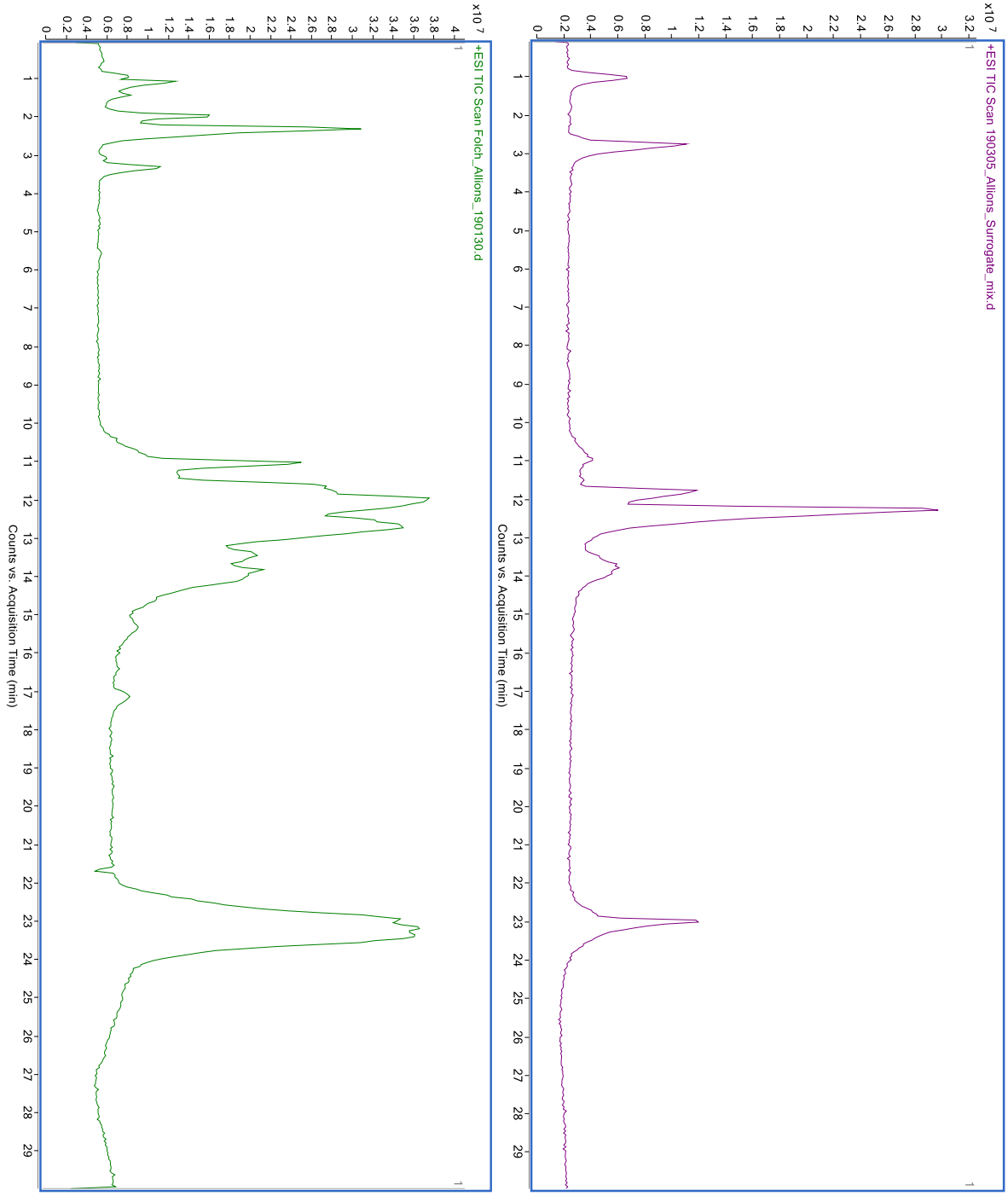

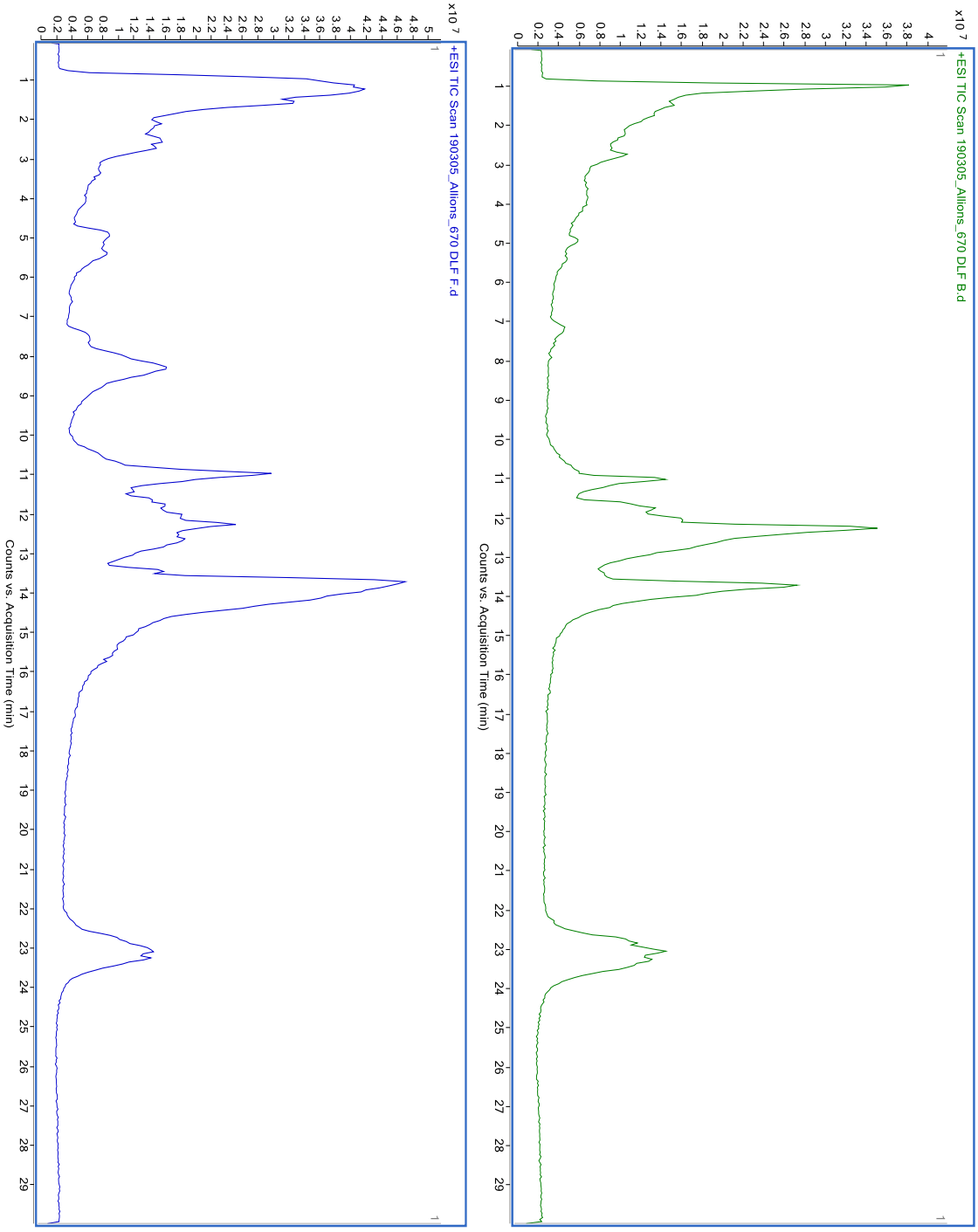
+ESI TIC Scan 190305_Allions_670 DLF B.d
x10 7
Counts vs. Acquisition Time (min)
+ESI TIC Scan 190305_Allions_670 DLF F.d
x10 7
Counts vs. Acquisition Time (min)

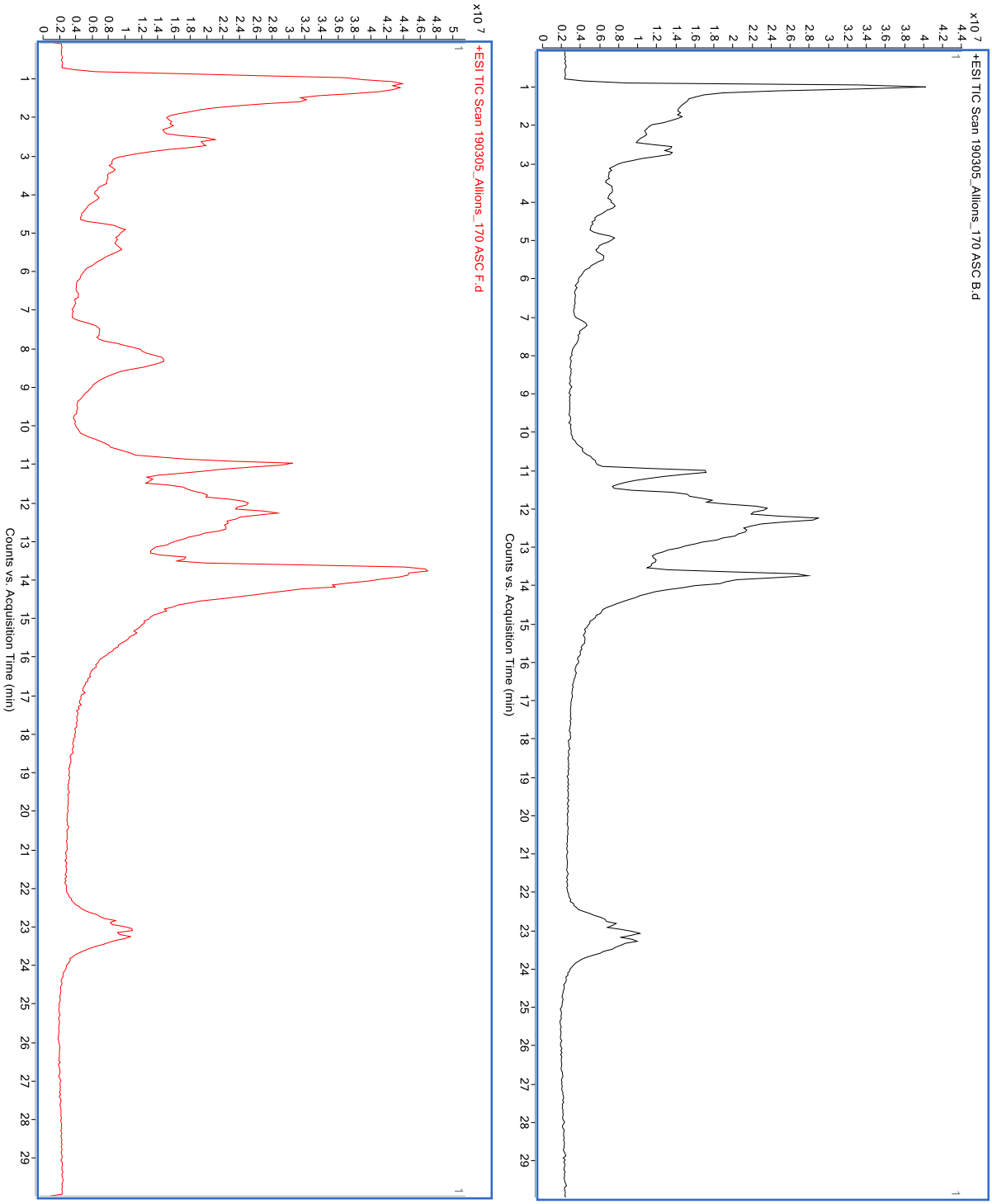
+ESI TIC Scan 190305_Allions_170 ASC B.d
x10 7
Counts vs. Acquisition Time (min)
+ESI TIC Scan 190305_Allions_170 ASC F.d
x10 7
Counts vs. Acquisition Time (min)

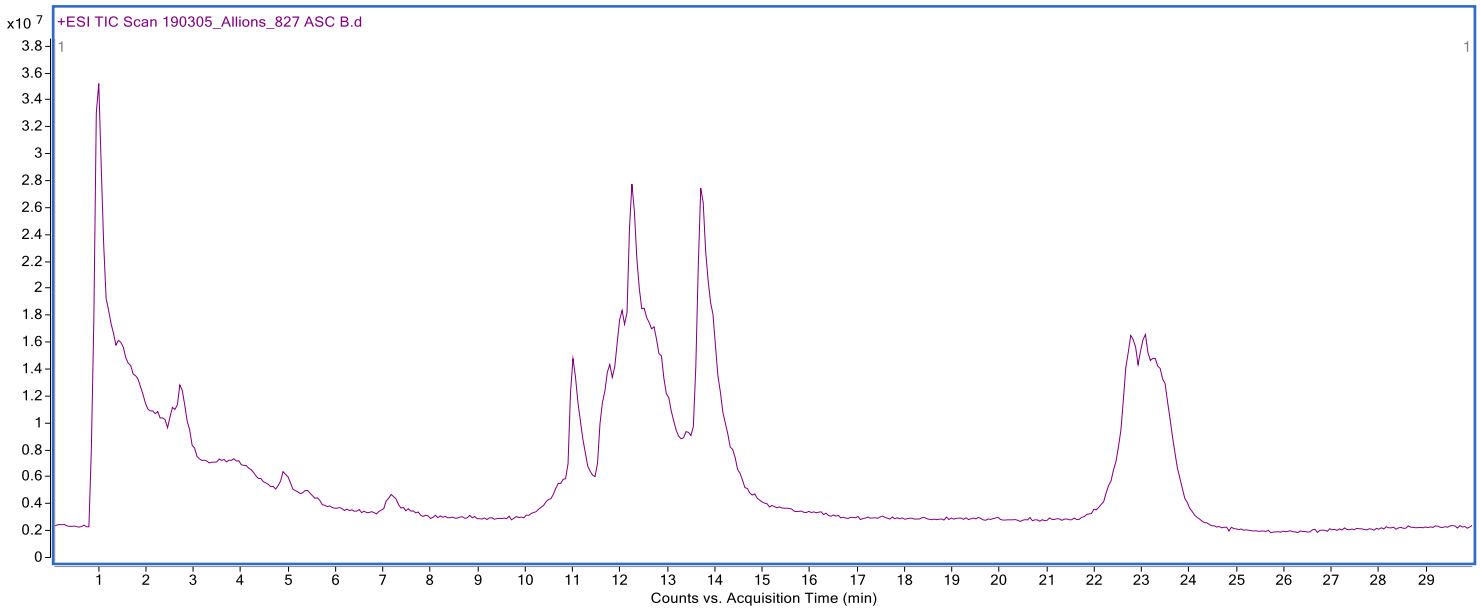
x10 7
+ESI TIC Scan 190305_Allions_827 ASC B.d
Counts vs. Acquisition Time (min)

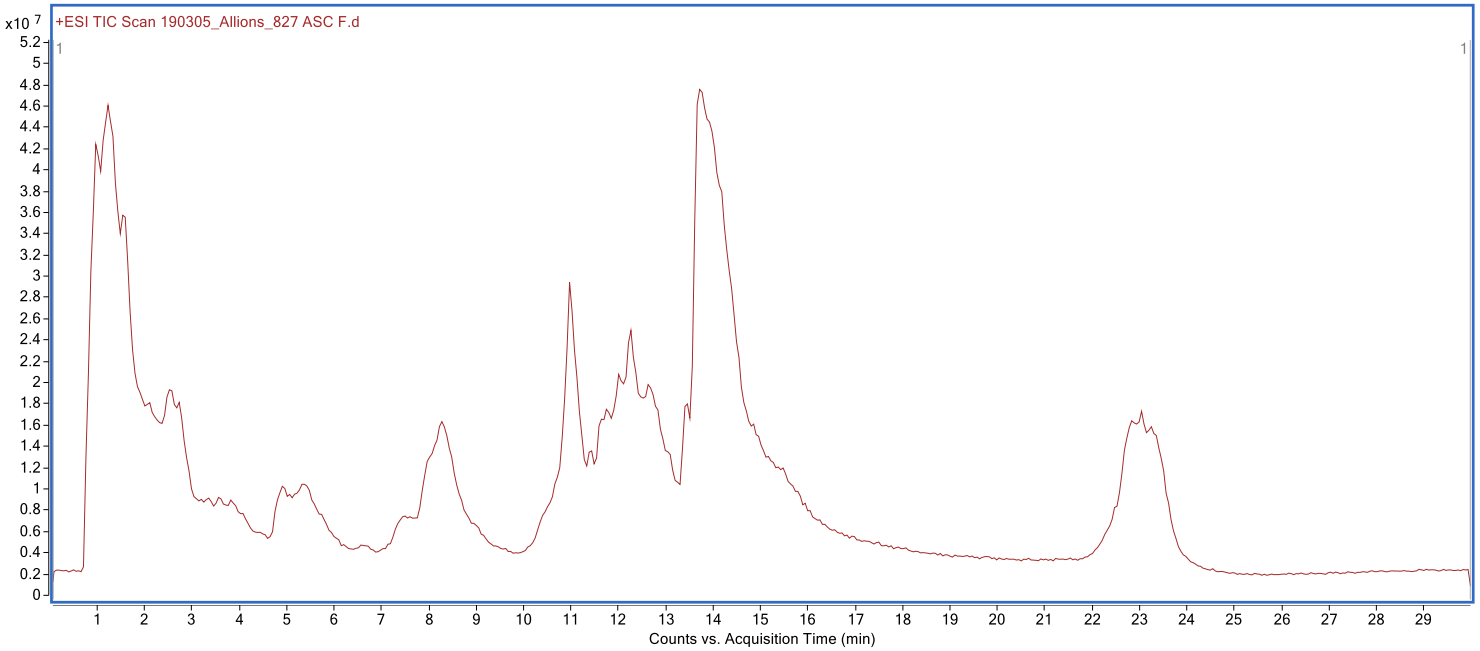
x10 7
+ESI TIC Scan 190305_Allions_827 ASC F.d
Counts vs. Acquisition Time (min)

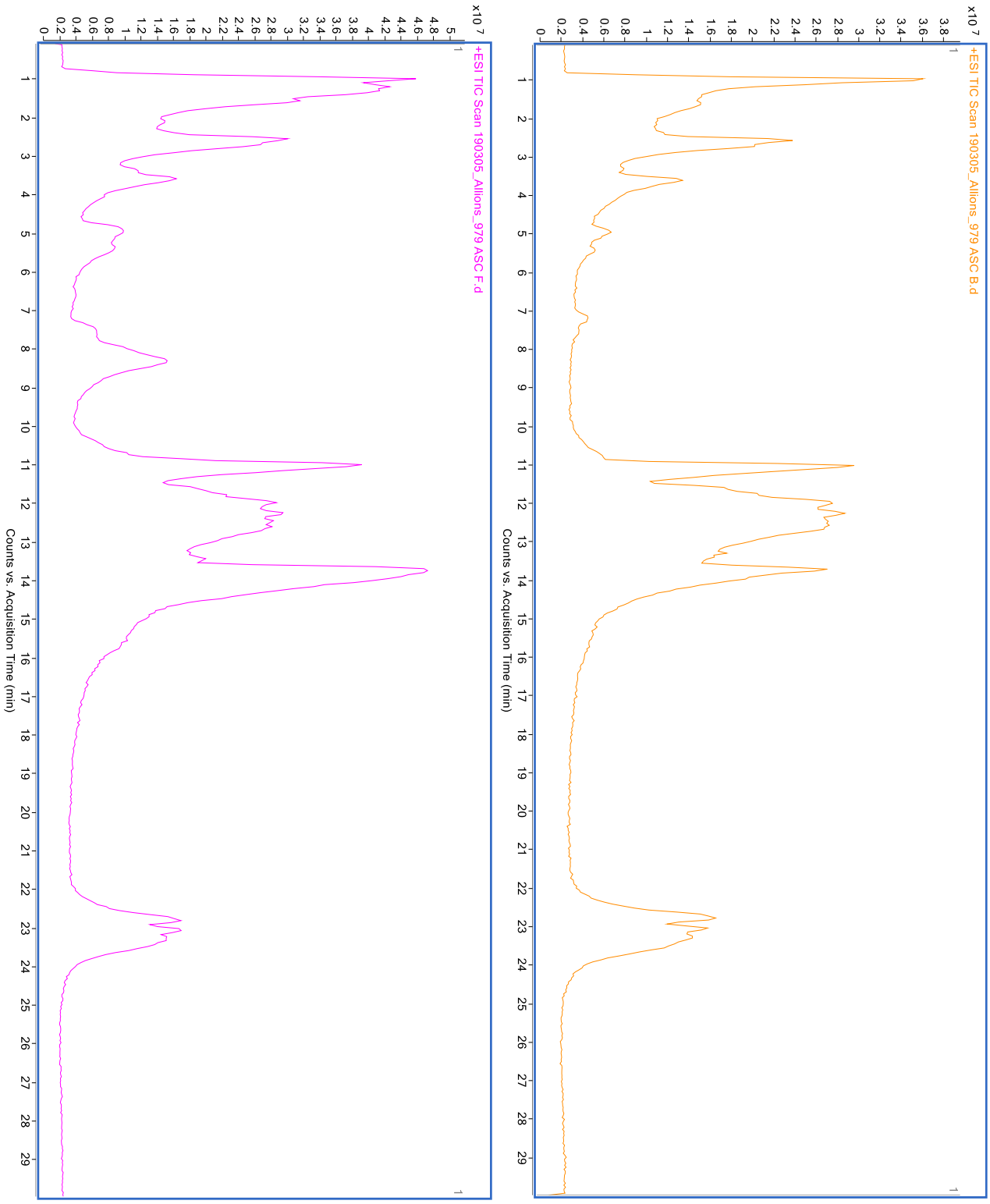
x10 7
+ESI TIC Scan 190305_Allions_979 ASC B.d
Counts vs. Acquisition Time (min)
x10 7
+ESI TIC Scan 190305_Allions_979 ASC F.d
Counts vs. Acquisition Time (min)

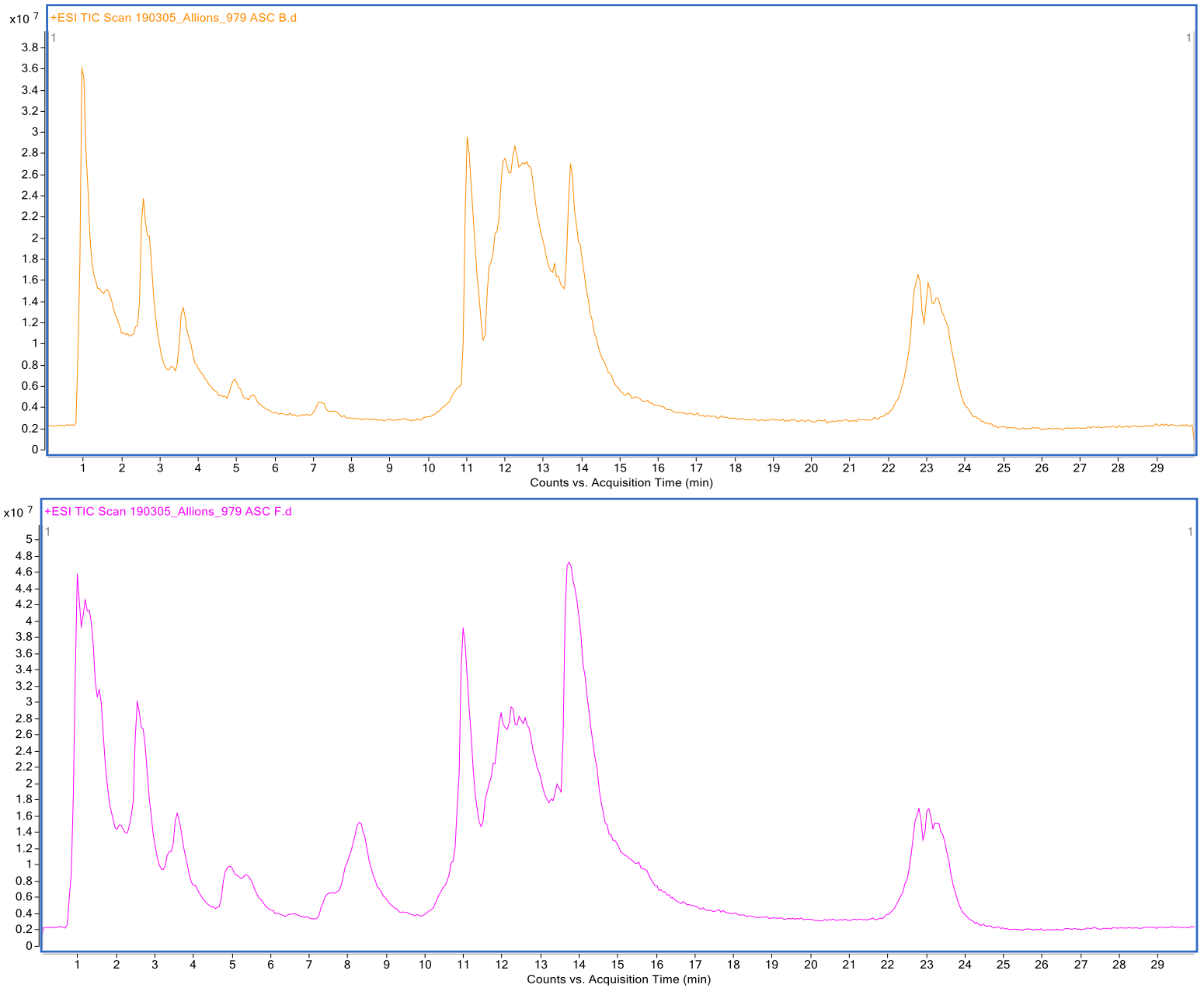
x10 7
+ESI TIC Scan 190305_Allions_979 ASC B.d
Counts vs. Acquisition Time (min)
x10 7
+ESI TIC Scan 190305_Allions_979 ASC F.d
Counts vs. Acquisition Time (min)